Aus der

Universitätsklinik für Thorax-, Herz- und Gefäßchirurgie Tübingen

Sektion Medizinische Werkstoffkunde und Technologie

Establishment of a method for the isolation of monocytes from human whole blood and their differentiation to polarized macrophages to analyze immunomodulatory characteristics of biomaterials

Inaugural-Dissertation
zur Erlangung des Doktorgrades
der Zahnheilkunde

der Medizinischen Fakultät
der Eberhard Karls Universität
zu Tübingen

vorgelegt von

Mangold, Madeline, geb. Fink

2025

Dekan:	Professor Dr. B. Pichler
1. Berichterstatter:	Professorin Dr. S. Krajewski
2. Berichterstatter:	Professorin Dr. S. E. Autenrieth
Tag der Disputation:	26.06.2025

To my family

Table of contents

List of figures

List of tables

List of abbreviations

ANOVA	Analysis of variance
APOL	Apolipoprotein
BCA	Bicinchoninic acid assay
BMdM	Bone marrow-derived macrophages
BMP	Bone morphologic protein
BSA	Bovine serum albumin
CCK	Cell counting kit
CD	Cluster of differentiation
Chap.	Chapter
CLSM	Confocal laser scanning microscopy
CCL	Chemokine C-C motif ligand
CCR	Chemokine C-C motif receptor
CXCL	Chemokine C-X-C motif ligand
DMSO	Dimethyl sulfoxide
DPSS	Diode pumped solid state
DRAQ	Deep red anthraquinone
EDTA	Ethyldiaminetetraacetic acid
EGF	Endothelial growth factor
ELISA	Enzyme-linked immunosorbent assay
FACS	Fluorescence activated cell sorting
FBE	Foreign body reaction equilibrium
FBGC	Foreign body giant cell
FBR	Foreign body reaction
FBS	Fetal bovine serum
FCγR	FCγ receptor
FGF	Fibroblast growth factor
Fig.	Figure
FN	Fibronectin
GM-CSF	Granulocyte macrophage colony stimulating factor
HeNe	Helium-neon
HRP	Horse raddish peroxidase
IDO	Indolamine 2,3-dioxygenase
Ig	Immunoglobulin
IFN	Interferon
IL	Interleukin
iNOS	Indicuble nitric oxide synthase
IRF	Interferon regulatory factor
LPS	Lipopolysaccharide
l	Liter
MCP	Monocyte chemotactic protein
MHC	Major histocompatibility complex
MIP	Macrophage inflammatory protein
M-CSF	Macrophage colony stimulating factor
MdM	Monocyte-derived macrophages
MFI	Mean fluorescence intensity
mg	Milligram
ml	Milliliter
MΦ	Macrophage
NaCl	Sodium chloride

ng	Nanogram
NHS	Normal human serum
NOS	Nitric oxide synthase
ns	Non-significant
PBMC	Peripheral blood mononuclear cells
PBS	Phosphate buffered saline
PDGF	Platelet derived growth factor
PFA	Paraformaldehyde
pg	Picogram
PG	Prostaglandin
PMA	Phorbol-12-myristate-13-acetate
PPAR	Peroxisome proliferator activated receptor
qRT-PCR	Quantitative real-time polymerase chain reaction
R	Receptor
RA	Receptor antagonist
RNase	Ribonuclease
RNS	Reactive nitrogen species
ROS	Reactive Oxygen Species
RPMI	Roswell Park Memorial Institute
SEM	Standard error of the mean
SLA	Sandblasted with large grits and acid-etched
SRB	Scavenger receptor class B
Tab.	Table
TGF	Transforming growth factor
TGM	Transglutaminase
T_h1 cells	Type 1 T helper cells
T_h2 cells	Type 2 T helper cells
TiO	Titanium oxide
TiO_2	Titanium dioxide
Ti_2O_3	Titanium(III) oxide
Ti-Ana	Titanium anatase
Ti-ma	Machined titanium
Ti-SLA	Sandblasted with large grits and acid-etched titanium
TLR	Toll-like receptor
TNF	Tumor necrosis factor
U	Unit
vD	1,25-dihydroxyvitamin D
VEGF	Vascular endothelial growth factor

1 Introduction

The loss of teeth up to total edentulism is a remarkable and globally existent issue [56, 102]. Correspondingly, in Germany adults (35- to 44-year-olds) show 2,1 missing teeth on average [112], while young olds (65- to 74-year-olds) have lost a mean of 11,1 teeth [85] and old olds (75- to 100-year-olds) are even devoid of averagely 17,8 teeth [86] pursuant to the Fifth German Oral Health Study. Furthermore, 12,4 % of the German young olds (65- to 74-year-olds) are completely edentulous whereas even 32,8 % of the German old olds (75- to 100-year-olds) lost their entire dentition [85, 86]. Etiologically, tooth loss can be attributed to caries-related decay, severe periodontitis, traumatic influences as well as, albeit less common, genetic impacts such as amelogenesis imperfecta [56]. Affected patients frequently and, in case of extensive tooth loss, notably suffer from limitations concerning mastication and phonetics as well as constricted aesthetics and psycho-social discomfort [3, 41, 102, 107, 113].

Missing teeth can therapeutically be restored by means of a prosthetic restoration [41, 56, 112]. Depending on, amongst others, the quantity of missing teeth, the dimension and the distribution of tooth gaps as well as the condition of the maxillary and the oral soft tissue, fixed prostheses, such as bridges, or removable dentures are oftentimes employed for treatment [56]. However, these options not only necessitate the preparation of adjacent teeth but also can elicit their successional damage up to further tooth loss [38, 56]. Moreover, due to high functional and aesthetical claims, removable dentures have become less requested by patients and the treatment of anterior tooth gaps is, especially in regard to aesthetics, challenging [38, 56].

On this account, dental implants have evolved into a major alternative within the rehabilitation of tooth loss [25, 38, 41, 56, 85, 110, 112]. Accordingly, an estimated number of 12 million osseointegrated oral implants per annum are inserted throughout the world [8]. Dental implants allow for a reliable and successful therapeutic option as they offer high survival rates as well as longevity besides their functional and aesthetic benefits [3, 6, 25, 42, 56, 110, 133]. Yet, malfunction can

occur [65, 78, 110] and successive implant failures are classified as biological, mechanical, iatrogenic or functional [42]. Biologically conditioned issues are further subdivided into early (time span between placement and prosthetic restoration) or late (subsequent to prosthetic restoration) implant failures [42, 133], clinically result in either a fibrous encapsulation or a peri-implant bone loss [8, 37, 42] and rely on an aggravated immune reaction [6-8, 16, 123]. By reason of the considerable quantity of placed dental implants, progressive marginal bone loss constitutes a rising problem, therefore requiring consistent solution approaches [123].

1.1 Biomaterials as dental implants for tooth replacement

A biomaterial, as defined by David F. Williams, is '[…] a substance that has been engineered to take a form which […] is used to direct, by control of interactions with components of living systems, the course of any therapeutic or diagnostic procedure […]' [137]. In the stricter sense, leaving out novel technologies, such as tissue engineering or drug and gene delivering systems, a biomaterial comprises a material that interacts with a biological system thereby assessing, enhancing or even substituting a physiologic function a diseased or damaged tissue or organ can no longer perform [14, 137, 138, 145]. In order to allow for long-term functional coexistence of the inserted biomaterial and its encircling tissue, the former material has to be biocompatible [135, 136]. Regarding long-term implantable biomaterials in turn, biocompatibility is specified as 'the ability of [the biomaterial] to perform its intended function, with the desired degree of incorporation in the host, without eliciting any undesirable local or systemic effects […]' [136]. Although biomaterials have been advanced, their long-term *in vivo* functionality and survival are still predominantly dependent on the host's immune reaction to the biomaterial [71, 79].

1.1.1 Dental implants

A dental implant is a biomaterial correspondent to an artificial tooth root that is surgically inserted into the maxillary and prosthetically fitted to compensate for

tooth loss [38, 41, 56, 135]. Either a single tooth or multiple teeth up to the complete dentition can be replaced by oral implants, as they support restorations such as crowns, bridges and partial or full dentures [38, 56, 133]. Regarding the set-up ***(Figure (Fig.) 1)***, a dental implant with a prosthetic fitting consists of the implant fixture, that is incorporated into the bone, an abutment passing through the oral mucosa and connecting the fixture and the prosthetic restoration as well as the prosthetic restoration [21, 38, 56, 133]. The fixture itself is of tapered or parallel-walled screw-type shape, whereas cylindrically shaped implants with a smooth surface offering a facile insertion are declined due to an insufficient primary stability [38, 133]. Furthermore, one-piece implants with an inseparable connection between fixture and abutment are discriminated from two-piece implants, that consist of unconnected sections which are screwed together and can be placed in a two-stage technique enabling a submerged and unloaded healing of the fixture [133, 135]. The prosthetic superstructure on the contrary as an individual section is either screwed or cemented to the abutment [38, 133].

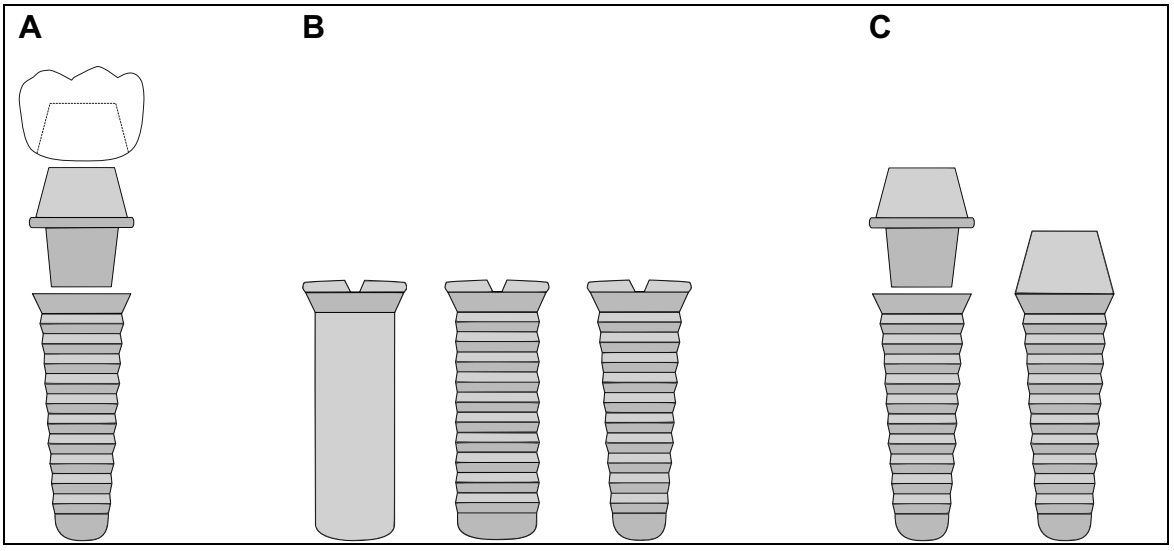

Figure 1: Schematic set-up of a dental implant *modified according to [133].* ***A*** *A dental implant commonly consists of the implant fixture, an abutment and a prosthetic fitting.* ***B*** *The implant fixture is of either a cylindrical or a parallel-walled or tapered screw-type shape.* ***C*** *A one-piece implant is characterized by an inseparable connection of fixture and abutment, whereas in a two-piece implant fixture and abutment are screwed together.*

An inserted oral implant is both conjunct to the maxillary and encircled by oral soft tissue [5, 133]. The interface between the implant fixture and the bone can either be established by connective tissue or can be directly osseous ***(Fig. 2)*** [5, 8, 37, 133, 135]: A connection set up of connective tissue, nowadays rarely occurrent if adequate dental implants are meticulously inserted, results from a fibrous encapsulation and is considered to be an early implant failure due to its constricted anchorage and its doubtful clinical long-term results [3, 5, 8, 42, 70, 133, 135]. In contrast, an intimate interface of the implant and its surrounding bone, referred to as osseointegration ***(Chapter (Chap.) 1.1.3),*** allows for a strong incorporation, an optimal function as well as reliable longevity and is therefore strived for [3, 5, 7, 42, 70, 133, 135].

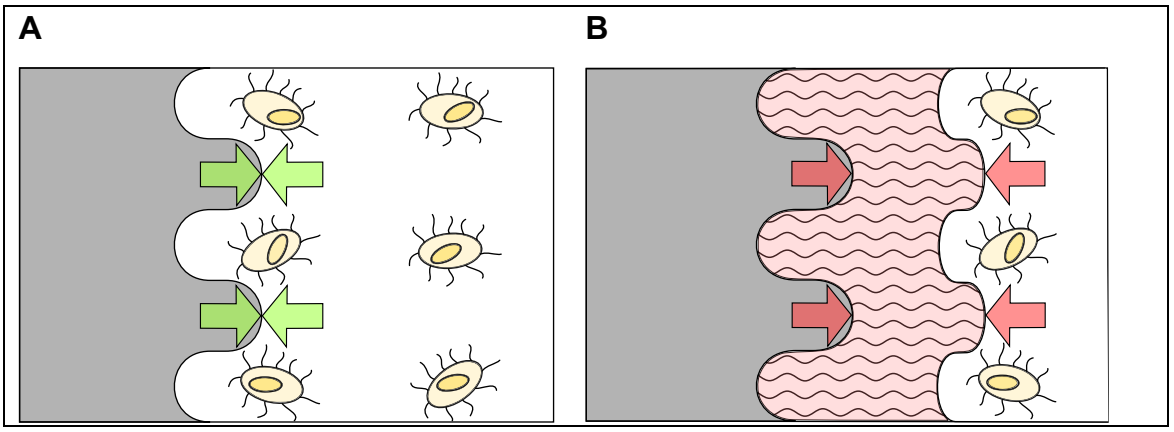

Figure 2: Different types of interfaces between the implant fixture and its surrounding bone *modified according to [5, 135].* ***A*** *The connection to the fixture is directly osseous corresponding to a successful osseointegration.* ***B*** *A sheath of connective tissue is interposed between the fixture and the bone corresponding to fibrous encapsulation.*

The implant's connection to its surrounding oral soft tissue is located at the coronal portion of the fixture or at the abutment [133]. Alike the physiologic contact between a natural tooth and the oral soft tissue, this interface is constituted of connective tissue and a hemi-desmosomal attachment of the mucosa [5, 133]. If in a good order, the soft tissue provides for a sealing of the maxillary, impeding the penetration of microbes and therefore facilitating the success of an implant [3, 5, 133].

1.1.2 Biomaterials used as dental implants

Concerning the selection of biomaterials employed for the fabrication of oral implants both the bulk material relevantly determining the mechanical characteristics as well as the surface properties affecting the establishment and retention of osseointegration in the first instance have to be considered [14, 39, 65, 70, 110]. Due to the beneficial chemical and physical characteristics, dental implants are predominantly composed of either commercially pure titanium or its titanium-6 alumium-4 vanadium alloy (Ti6Al4V), furthermore the usage of zirconium dioxide is on the increase [14, 38, 39, 41, 70, 110, 111, 135]. Thereby, titanium and its alloy are hallmarked by favorable mechanical characteristics, pronounced resistance to corrosion as well as the establishment of osseointegration [5, 39, 135]. Immediate oxidation processes at the titanium surface resulting in a thin and enduring oxide layer consisting of titanium oxides, such as titanium oxide (TiO), titanium dioxide (TiO_2) or titanium(III) oxide (Ti_2O_3), is underlying [5, 142]. Regarding the surface properties, titanium implants originally were machined without any further modification resulting in a smooth surface with parallel grooves at micron scale [9, 25, 39, 41, 110, 142]. As physical and chemical surface characteristics, however, may expedite healing and enhance osseointegration (***Chap. 1.3.2***), several modifications have been introduced [6, 9, 14, 39, 41, 70, 104, 110, 142]. Both subtractive surface conditioning, like blasting or acid-etching, and additive surface conditioning, such as spraying and electrochemical anodization, are implemented and may furthermore be combined [14, 39, 65, 70, 104, 110]. Converted to the clinical application, as to subtractive treatment, dental implants bearing sandblasted and acid-etched titanium surfaces, amongst others so-called sandblasted with large grits and acid-etched (SLA) titanium, allow for enhanced osseointegration along with high implant survival [14, 25, 110, 142]. Likewise, additively treated implant surfaces by means of anodic oxidation, exhibiting an augmented titanium dioxide layer, for instance of the so-called titanium anatase allotropic form, promote osseointegration while showing high implant survival rates [110, 111].

1.1.3 Osseointegration of dental implants

Osseointegration, a type anchorage of an implant within its surrounding bone, was first discovered in 1962 and subsequently termed in 1977 each by Per-Ingvar Brånemark [4, 5, 7, 8]. Originally, the latter phenomenon was defined as an immediate contact between foreign material and living bone without any interposition of soft tissue as light microscopically apparent [3, 5, 7]. Along with an increasing insight in healing processes and immunology the understanding of osseointegration refined to being an immunological response termed foreign body reaction (FBR, ***Chap. 1.3.1***) that enables a biological shield of the implant by means of interfacial bone [4, 7, 8, 37]. The establishment and retention of an osseointegration requires the compliance with specific prerequisites concerning the implant design, the implant material and its finish as well as the status of the maxillary, surgical techniques and the implant loading conditions (***Fig. 3***) [5, 8, 21, 38, 133].

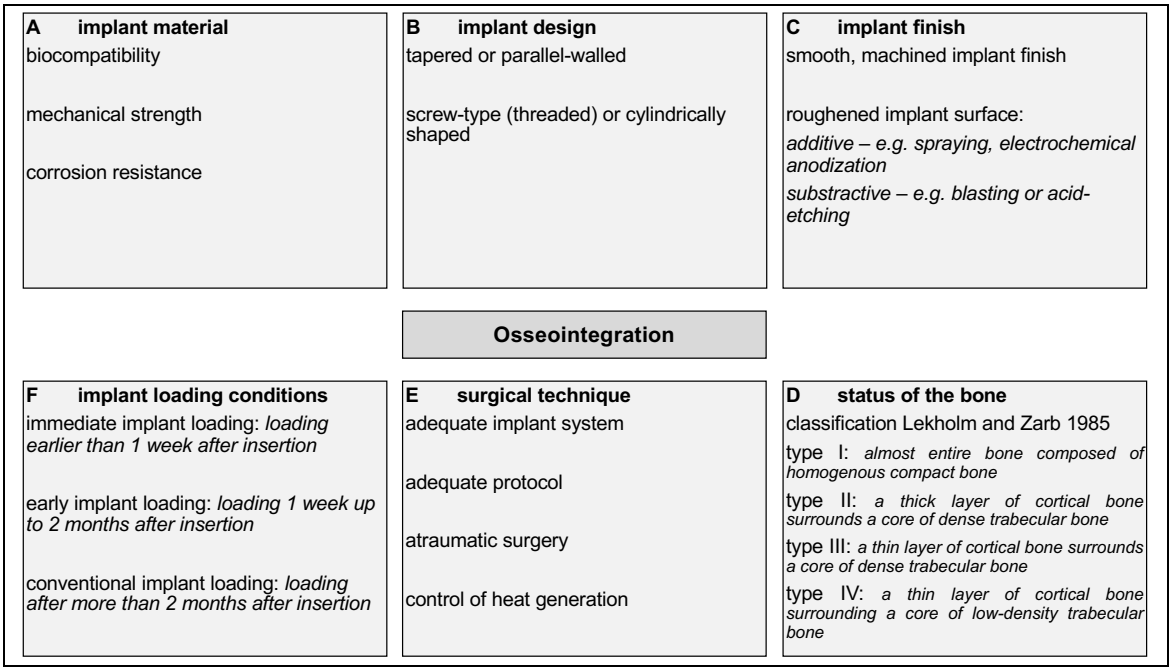

Figure 3: Prerequisites for establishment and retention of osseointegration*. Osseointegration is influenced on part of the implant by its bulk material, the implant design as well as the finish, on part of the patient by the status of the bone and on part of the therapy by the surgical technique as well as the prosthetic implant loading [5, 8, 21, 38, 133].* ***A*** *Regarding the implant material, the usage of a tissue-tolerant and corrosion-resistant biomaterial is inevitable concerning biocompatibility, furthermore mechanical strength should be concerted to the assumable load [5, 133].* ***B*** *A threaded implant design enhances the primary stability by means of reduced implant movement and thus fosters osseointegration [5, 133].* ***C*** *Eventually, the implant finish again affects the biocompatibility as well as possibly the surface area of the inserted implant [5, 133].* ***D***

As to the status of bone, failure rate increases with implants inserted into both bone of reduced quality and the maxilla [3, 133]. ***E*** *On the part of the surgical technique, a meticulous and atraumatic procedure strictly obviating heat generation using an adequate implant system and a protocol adapted to the individual patient is to be respected [3, 21, 133].* ***F*** *For implant loading conditions, early loading is reasonable for optimum clinical conditions, whereas conventional implant loading should be followed in case of impeded clinical situations [133].*

1.1.4 Peri-implant bone loss

A minor peri-implant bone loss is regularly observed in particular during the first year after a dental implant was placed and is attributed to an adaptation in the context of healing and occlusal loading [3, 6, 8, 93, 95]. Yet, concomitant with a high number of oral implants being inserted, progressive crestal bone loss constitutes a rising problem confining an implant's function as far as its failure [8, 95, 123]. Originally, marginal bone loss was ascribed a pathomechanism on the lines of periodontitis, therefore classifying the former condition as a biofilm-mediated infectious disease [4, 7, 8], and appropriately named 'peri-implantitis' [8, 95]. However, nowadays peri-implant bone loss is considered to result from an aggravated FBR with macrophages (MΦ) predominantly being involved for the most part (***Chap. 1.3.1***) [6-8, 16, 123], notably emerging if the abovementioned prerequisites (***Chap. 1.1.3***) are not met [5, 6, 8, 95] or in case of medically compromised or smoking patients [6, 8]. Thus, marginal bone loss constitutes an immunologically provoked clinical complication related to the therapy instead of a disease, although downstream an exacerbation due to microbial infection is possible [4, 8, 123]. Crestal bone loss does not necessarily result in an implant failure but can instead be brought to a stop, if with a reduced osseous connection, once its source, for instance remnants of cement particles or occlusal overload, is eliminated [6, 8].

1.2 Macrophages

The human immune system allows for the defense against invading and internal threats [36, 73, 90]. It comprises soluble molecules as well as cells and is subclassified into an innate and an acquired section [36, 73, 90]. The innate immune system on the one hand serves as an initial and unspecific defense and reacts

with consistent immune responses independent of the underlying threat and the quantity of previous encounters [36, 73, 90]. Molecules, like cytokines and acute phase proteins, enzymes, such as the complement system and lactoferrin, as well as cells, encompassing MΦ and neutrophils as phagocytic cells, basophils and eosinophils as secreting cells and natural killer cells, set up the innate immunity [36, 73, 90]. The acquired immune system on the other hand follows to the innate immune response and is highly specific to the threat, yet refining its specificity with every encounter [36, 73, 90]. Analogously, it is composed of molecules, such as antibodies, and cells, like B-cells for the humoral immunity and T-cells for the cellular immunity [36, 73, 90]. Both components, the innate and the acquired immune system are connected through messenger molecules and cells, in which MΦ play a key role through phagocytosis and antigen presentation as well as secretion of messenger molecules [36, 53, 62, 73, 90, 94, 144].

MΦ were first characterized by Elie Metchnikoff in 1882 [27, 40, 53, 114, 120]. Within the human organism, these cells constitute a heterogenous population with different subsets being in charge of, amongst others, immune defense, wound healing as well as tissue homeostasis [20, 40, 52-54, 62, 80, 108, 109, 119].

1.2.1 Origin of macrophages

Human MΦ ontologically originate from 2 different sources ***(Fig. 4)***: The first subset is derived from erythromyeloid precursors located in the yolk sac and the fetal liver and is allotted throughout most tissues during embryogenesis [40, 53, 57]. These cells remain resident in a long time, constituting a self-regulating and regenerating subset controlling the local trophic by means of phagocytosis [40, 53, 57]. The second subset on the other hand postnatally evolves from hematopoietic stem cells through several stadia of differentiation involving monoblasts, promonocytes and monocytes [40, 53, 54, 57, 80]. The monocytes themselves circulate within the blood until they migrate to their destination and differentiate into MΦ, so-called monocyte-derived MΦ (MdM), under the influence of local growth factors, cytokines as well as pathogens [53, 80, 108]. This subset complements the

former, embryonically derived one, particularly in tissues featuring a high turnover of MΦ, such as physiologically the gastrointestinal tract or pathologically inflamed or damaged tissues [53, 57, 108].

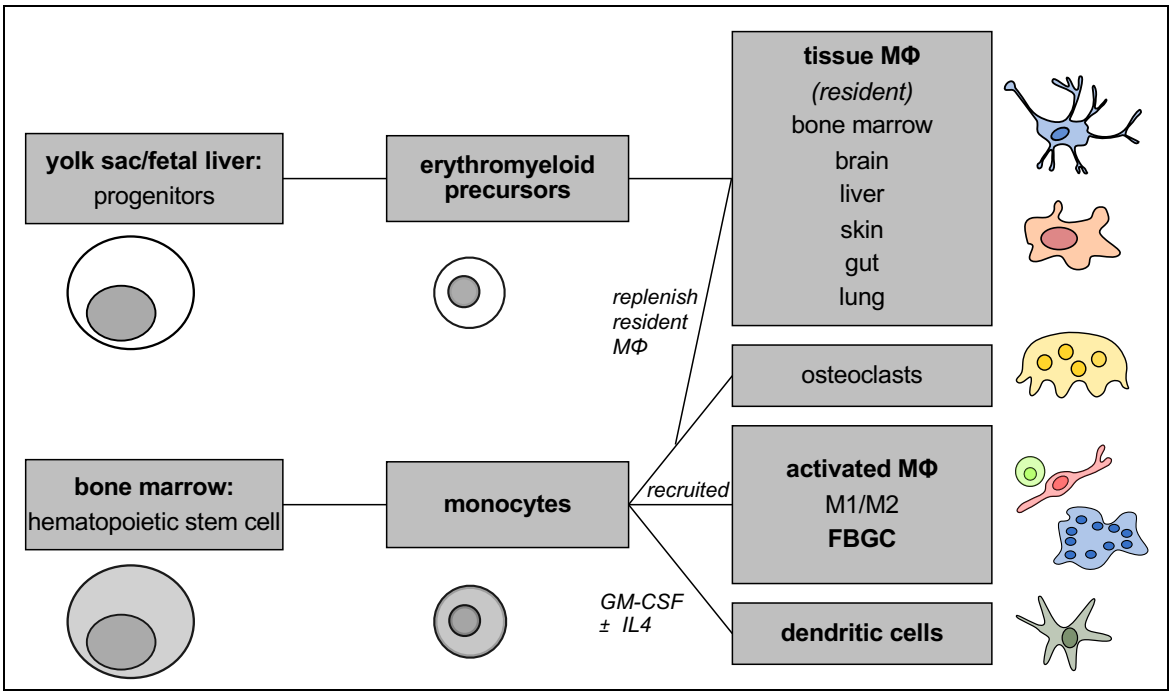

Figure 4: Origin of MΦ *modified according to [53, 80]. Throughout development, MΦ originate from erythromyeloid precursor cells within the yolk sac and the fetal liver resulting in long-lived tissue-resident MΦ. Postnatally, MΦ evolve from the hematopoietic stem cells so as to complement the embryonically derived MΦ. FBGC = foreign body giant cell; GM-CSF = granulocyte macrophage colony stimulating factor; IL = interleukin; MΦ = macrophage.*

1.2.2 Polarization of macrophages

MΦ adapt their function as well as their phenotype dependent upon the local micro-environment within the tissue they reside, a phenomenon referred to as polarization ***(Fig. 5)*** [53, 55, 62, 81, 94, 108, 109, 119, 130]. Resident MΦ as well as migrating MdM can be polarized by a multitude of stimuli, for instance growth factors, cytokines, glucocorticoids as well as pathogens or their associated molecules [20, 81, 108]. MΦ polarization is generally subclassified into 2 main groups distinguishing M1-polarization, also termed classical activation, from M2-polarization, or alternative activation, respectively [18, 20, 45, 53, 61, 62, 80, 94, 108, 130]. On the basis of type 1 T helper-cells (T_h1 cells) and their related spectrum

of cytokine secretion, M1-polarized MΦ are named M1-MΦ, as they originate particularly based on interferon (IFN) γ and tumor necrosis factor (TNF) α [53, 59, 72, 76, 108, 109]. Analogously, the influence of interleukin (IL) 4 and IL13, both cytokines specific to type 2 T helper-cells (T_h2 cells), effects the emergence of M2-MΦ [53, 59, 76, 108, 109]. There is, however, no unmitigated dichotomy of M1- and M2-polarization [53, 72, 76, 94, 108]. Rather, polarization should be regarded as a spectrum and especially the M2-polarization exhibits marked heterogeneity, taken into consideration by further subdivision into M2a-, M2b-, M2c- and M2d-polarization [72, 74, 76, 81, 94, 103, 108, 130]. Besides, a polarized state is not fixed, but MΦ are highly plastic instead, adjusting to their present micro-environment [72, 80, 94, 108, 109, 119].

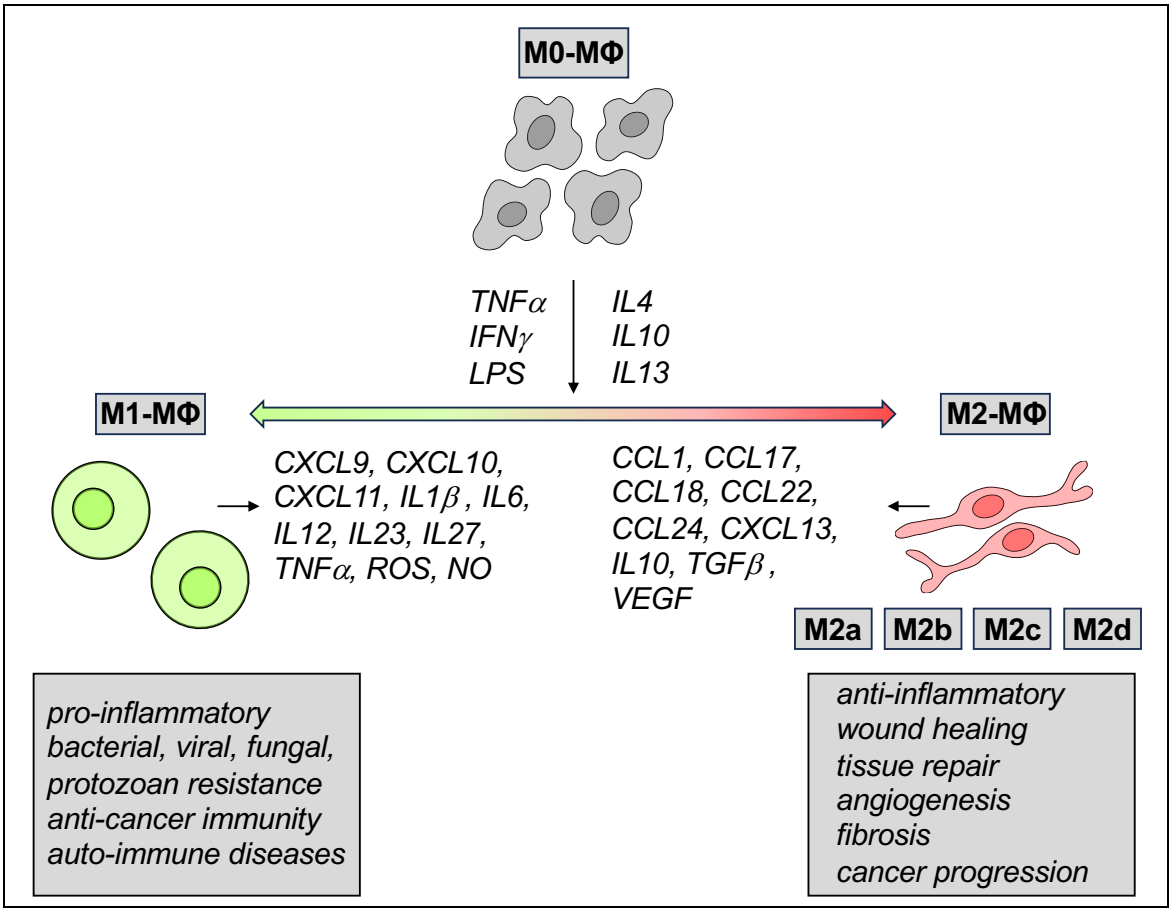

Figure 5: Polarization of MΦ *modified according to [81, 108, 141]. Depending on tissue-specific micro-environment, immunologic milieu and phenotypic influences, MΦ can polarize into an M0-, M1- and M2-phenotype. Due to the distinct plasticity of the latter cells, polarization is versatile. CCL = chemokine C-C motif ligand; CXCL = chemokine C-X-C motif ligand; IFN = interferon; IL = interleukin; LPS = lipopolysaccharide; NO = nitric oxide; ROS = reactive oxygen species; TGF*

= transforming growth factor; TNF = tumor necrosis factor; VEGF = vascular endothelial growth factor.

Concerning function and phenotype, M1-MΦ exhibit pro-inflammatory characteristics and commonly and show a round phenotype expressing markers, such as major histocompatibility complex (MHC) II or cluster of differentiation (CD) 80, CD86 and chemokine C-C motif receptor (CCR) 7 [20, 62, 75, 91, 100, 109]. In contrast, M2-MΦ have anti-inflammatory features and bear an elongated phenotype with expression of markers like CD1A, CD163, CD206 and CD209 [20, 62, 75, 91, 100, 109].

1.2.3 Function of macrophages

Corresponding to their polarization, MΦ execute a multiplicity of heterogenous and fractionally contrastive functions [20, 53, 62, 108, 114]. Accordingly, pro-inflammatory M1-MΦ are present within inflamed, infected or damaged tissue to engulf intruding pathogens, foreign bodies as well as debris [20, 62, 94, 108, 114, 130]. Thus, spreading of a pathological process is restricted and the affected tissue is prepared for subsequent wound healing [94, 108]. Following to the phagocytosis, MΦ present sections of the engulfed particles to lymphocytes using MHCII and associated surface markers, such as CD80 and CD86 [72, 108]. Moreover, inflammatory messenger molecules, amongst others TNFα, IL1, IL6, IL12, IL23, as well as reactive oxygen species (ROS) and reactive nitrogen species (RNS) are secreted to draw further immune cells and to destruct remaining pathogens [45, 72, 108, 114]. Anti-inflammatory M2-MΦ on the other hand succeed the M1-MΦ and guard the tissue from prolonged and extensive inflammation [20, 94, 108, 114, 130]. Their secreted cytokines, for instance IL10 and transforming growth factor (TGF) β, limit the pro-inflammatory effect of the aforementioned messenger molecules as well as of the activated immune cells [108, 114]. By means of phagocytosis, M2-MΦ remove debris and furthermore, release of growth factors and enzymes effectuates angiogenesis and sprouting of cells, all of which fosters wound healing [20, 62, 108, 114]. Eventually, tissue-resident MΦ

are accountable for constant phagocytosis eliminating aged, excessive and deteriorated cells, thus enabling accurate tissue formation and homeostasis [80, 114].

Besides their physiological functions, MΦ are involved in the genesis and progression of diseases, such as autoimmune disorders, arteriosclerosis and malignant neoplasia [20, 45, 53, 64, 81, 91, 108, 109, 130]. Furthermore, exuberant pro- as well as anti-inflammatory MΦ responses can cause pathological consequences [53, 80]. Accordingly, prolonged pro-inflammatory influences might lead to local tissue damage up to generalized sepsis and, in case of an implant, result in destruction of the involved biomaterial [44, 91, 108, 145]. On the other hand, continuous anti-inflammatory stimuli impede wound healing and forward the emergence of fibrosis, as existent in fibrous encapsulation of implants [20, 80, 108, 130].

1.3 Immunomodulatory effects of biomaterials

Implanted biomaterials unpreventably affect the immune system causing an inflammatory response termed FBR [8, 11, 32, 37, 44, 123, 145]. With regard to dental implants, the FBR on the one hand can result in the strived osseointegration or on the other hand, if aggravated or prolonged, can cause severe damage to the implant and its surrounding tissue resulting in up to early or late implant failure [8, 123]. As different characteristics of the biomaterial used can have modulatory effects on the FBR, influencing the healing and the functional retention of an oral implant by means of immunomodulation is aimed at [44, 123, 145].

1.3.1 Foreign body reaction and foreign body reaction equilibrium

As defined by David F. Williams, an FBR comprises the ‘overall response of a host to the presence of a foreign body’ [123, 138]. The latter reaction is considered to be an unspecific and downwelling, chronic immune reaction aiming at withdrawal, degradation or shielding of the biomaterial [8, 32, 37, 97, 123, 145]. Thereby, shielding is up to the establishment of an equilibrium of the FBR, termed

foreign body reaction equilibrium (FBE) [37, 123]. With regard to bone, this FBE results in osseointegration (***Chap. 1.1.3***), whereas within soft tissue, a minor fibrous encapsulation without evidence of a marked inflammation ensues [8, 37]. However, if an FBE is not attained, the ongoing FBR causes damage to the implanted biomaterial as well as the loss of osseointegration or the formation of a fibrous encapsulation within bone and an aggravated fibrous encapsulation as to soft tissue [8, 37, 44, 145]. An established FBE can be disturbed, restarting the FBR, which either leads to another, yet possibly reduced, equilibrium or results in the damage of the biomaterial and its surrounding tissue [8, 123]. The extent as well as the endurance of an FBR hinge on, amongst others, the surgically caused trauma associated to the implantation, the characteristics of the receiving tissue and the biomaterial used [10-12, 44, 145]. In case of absorbable biomaterials, resulting products of decomposition and concomitant changes of the biomaterial's surface properties may additionally modulate the prevailing FBR or even provoke an independent response [1, 44].

An FBR originates from the surgically provoked trauma going along with the implantation and effectuating contact between the foreign body as well as the host's tissue and blood [8, 10-12, 44, 71, 145]. Upon exposure, interstitial and blood proteins, such as fibronectin, vitronectin, albumin, immunoglobulins (Ig), coagulation and complement factors immediately adsorb to the biomaterial surface [1, 12, 22, 32, 44, 51, 63, 118, 131, 142, 145]. These proteins opsonize the foreign body and furthermore effect the onset of the coagulation as well as the complement cascade [10, 11, 44, 145]. Subsequently, not only platelets adhere and are activated, but also immune cells migrate due to chemotaxis and bind to the proteins [10-12, 32, 44, 51, 145]. Diverse biomaterial surface characteristics influence the type and composition as well as conformational changes of the proteins, thereby modulating the FBR downstream [12, 22, 145]. The adsorbed proteins therefore may thoroughly control the course of the FBR [12, 32, 118, 145].

As to the migrating immune cells, neutrophilic granulocytes initially predominate within the FBR [11, 12, 32, 44, 145]. These cells engulf intruded pathogens as well as debris and secrete proteolytic enzymes and ROS as defense mechanism [10, 44, 145]. Furthermore, the neutrophilic granulocytes release cytokines, such

as IL8, to attract further granulocytes and chemokines, like monocyte chemotactic protein-1 (MCP-1) or MΦ inflammatory protein-1β (MIP-1β) to allure monocytes and MΦ [1, 44, 48, 69, 140]. Due to a short life span of the granulocytes, monocytes and MΦ subsequently briskly prevail at the biomaterial surface [10-12, 44, 145]. The latter cells feature an increased endurance and, either as mere MΦ or as foreign body giant cells (FBGC), reside on the implant for its entire *in vivo* lifetime [11, 22, 24, 145]. The circumjacent micro-environment initially fosters the migrated MΦ to polarize towards a pro-inflammatory M1-phenotype furthering inflammation [1, 32, 44, 145]. Via secretion of cytokines, like IL1, IL6, IL8 and TNFα, as well as the aforementioned chemokines, other monocytes and MΦ are chemo-attracted [22, 44, 145]. Consequently, the antimicrobial defense as well as the phagocytic capacity, as regards debris, accrete in preparation for wound healing [1, 32, 44, 145]. Over time, MΦ polarization shifts towards the M2-phenotype educing regulatory as well as wound-healing MΦ [1, 32, 44, 145]. By means of secreting the immunosuppressive cytokine IL10, the regulatory M2-subtype curtail the ongoing inflammation [32, 44]. The wound-healing MΦ on the other hand, elicit the activation of osteoblasts, as to bone, or fibroblasts, concerning soft tissue resulting in the synthesis of extracellular matrix to substitute for the marred tissue and to shield the foreign body [44, 145]. Furthermore, MΦ residing on the implanted biomaterial fuse forming FBGC mediated through the cytokines IL4 and IL13 [10, 24, 44, 145]. If at this point anti-inflammatory influences as well as wound healing markedly exceed the pro-inflammatory immune activation being equivalent to an FBE, osseointegration as to the bone or a minor fibrous encapsulation without further active inflammation with regard to the soft tissue result [8, 10, 12, 37, 44, 123, 145]. Conversely, in case of sustained immune activation correspondent to a lasting FBR, intensified MΦ fusion occurs [1, 44, 123, 145]. Following, these FBGC can release proteolytic enzymes and ROS to an increasing degree making for an exacting degradative capacity [12, 23, 31, 44]. Otherwise, fused MΦ may also secrete growth factors, such as TGFβ, vascular endothelial growth factor (VEGF) or platelet derived growth factor (PDGF) fostering extensive fibrosis of the implanted biomaterial [1, 12, 31, 44, 145]. ***Fig. 6*** summarizes the sequences of an FBR.

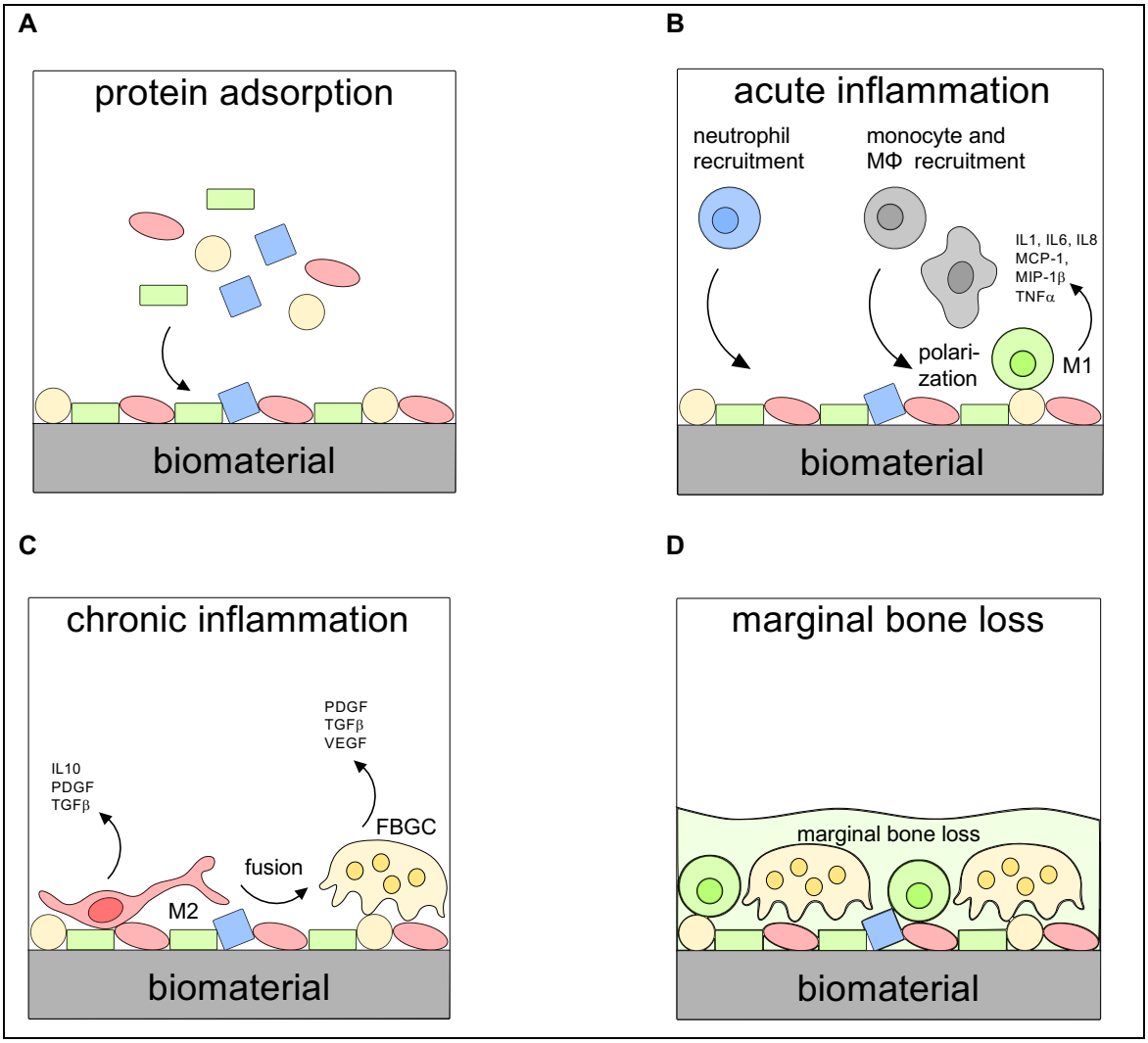

Figure 6: Foreign body reaction *modified according to [145].* ***A*** *Immediately after implant insertion interstitial and blood proteins adsorb to the biomaterial surface and effect the onset of the coagulation and complement cascade [12, 44, 145].* ***B*** *Subsequently, immune cells, particularly neutrophils, monocytes and MΦ, migrate due to chemotaxis and bind to the adsorbed proteins [10-12, 44, 145]. These cells engulf intruded pathogens as well as debris and secrete enzymes as well as ROS as defense mechanism [10, 44, 145]. Due to a short life span of neutrophils, monocytes and MΦ briskly prevail at the biomaterial surface and polarize to a pro-inflammatory M1-phenotype [10-12, 44, 145]. Via secretion of cytokines, like IL1, IL6, IL8 and TNFα other monocytes and MΦ are attracted and invaded pathogens as well as debris is phagocytosed to prepare for wound healing [44, 145].* ***C*** *Over time, MΦ polarization shifts towards the M2-phenotype bearing wound healing as well as regulatory MΦ [1, 32, 44, 145]. These MΦ secrete the anti-inflammatory cytokine IL10 [44]. Furthermore, MΦ residing on the implanted biomaterial fuse forming FBGC mediated through the cytokines IL4 and IL13 [10, 24, 44, 145]. If at this point anti-inflammatory influences as well as wound healing markedly exceed the pro-inflammatory immune activation being equivalent to an FBE, osseointegration as to the bone ensues [8, 10, 12, 123].* ***D*** *Conversely, in case of sustained immune activation correspondent to a lasting FBR, intensified MΦ fusion, resulting in peri-implant bone loss or fibrous encapsulation, follows [1, 12, 31, 44, 145]. FBGC = foreign body giant cell, IL = interleukin, MCP = monocyte chemotactic protein, MIP = MΦ inflammatory protein, PDGF = platelet derived growth factor, TGF = transforming growth factor, TNF = tumor necrosis factor, VEGF = vascular endothelial growth factor.*

For the purpose of avoiding the aforesaid, potentially damaging implications of the FBR, dental implants originally were intended to be biologically and chemically inert, thus preventing a pronounced cellular and immunological response [1, 44, 136]. Owing to a growing knowledge of immunology, however, it is recognized that an interaction between a foreign body and its surrounding cells is inevitable [8, 44, 145] and furthermore that, if the interaction is well-directed, healing as well as function of a dental implant can be enhanced [44, 97, 145]. Immunomodulatory effects of biomaterial characteristics on the FBR are therefore actively and extensively investigated [1, 24, 31, 32, 44, 145].

1.3.2 Immunomodulation by means of physicochemical surface characteristics

Physicochemical surface characteristics encompass physical properties, such as surface topography, roughness and porosity, on the one hand and chemical attributes, like wettability, electrical charge and surface chemistry, on the other hand [1, 39]. Concerning physical characteristics, a simulation of the physiological extracellular matrix comprising micro- and nanostructures is aimed at, as these structures *in vivo* have an effect on cell adhesion, proliferation, migration as well as gene expression [31, 44, 143, 145]. Immunomodulatory effects on MΦ, amongst others the facilitation of M2-polarization caused by groovings that induce MΦ elongation [71, 75], have been demonstrated within respective studies [1, 31, 71, 75, 145]. Chemical characteristics, on the contrary, affect the type as well as the quantity and conformational changes of proteins initially adsorbing to the biomaterial surface [22, 23, 44, 145]. As these proteins function as binding sites for the migrating immune cells, concomitant changes in cell binding provoke a modified cell signal transduction [22, 143, 145]. Accordingly, hydrophilic and anionic surfaces feature anti-inflammatory effects through inhibition of monocyte and MΦ binding and fusion to FBGC as well as shifting of cytokine secretion towards anti-inflammatory IL10 [22-24, 44, 145]. Hydrophobic and cationic biomaterials on the other hand foster protein binding as well as their conformational changes and thus forward immune cell adherence and the release of pro-inflammatory mediators resulting in an enhanced immune reaction [22-24, 32, 38, 145].

1.3.3 Immunomodulation by means of bioactive molecules

Furthermore, bioactive molecules for the purpose of effectuating immunomodulatory effects involve the exhibition of binding sites as well as the release of immunosuppressive molecules and growth factors [44, 145]. At this juncture, protein binding sites are implemented as oligopeptides, either solely or along with non-biofouling coatings, coupled to the biomaterial's surface oftentimes consisting of integrin molecules [44, 66, 97]. In this way, the binding of immune cells and therefore the course of the FBR may be regulated [44, 66, 97]. Especially in conjunction with non-biofouling biomaterial coatings, an enhancement of immunomodulation can be attained, as protein adsorption is additionally affected [44, 97, 106, 127, 145]. The release of immunosuppressive molecules and growth factors, otherwise, encompasses, amongst others, glucocorticoids and nitric oxide as well as molecules like epidermal growth factor (EGF), fibroblast growth factor (FGF), granulocyte MΦ colony stimulating factor (GM-CSF), TGFβ, VEGF, PDGF and bone morphologic proteins (BMP) [44, 58, 79, 87, 92, 145]. Glucocorticoids as well as nitric oxide impede the secretion of pro-inflammatory mediators and the migration of immune cells and thus diminish inflammation [44, 58, 79]. Particularly with regard to glucocorticoids however, an enduring release is required as to circumvent a reversion of the immunomodulation [44, 87]. The aforementioned growth factors in contrast, influence migration, adhesion, differentiation and proliferation of cells involved in wound healing, such as keratinocytes, fibroblasts and endothelial cells which on their part have an effect on immune cells [44].

1.3.4 Immunomodulation by means of extracellular matrix

Eventually, coating of biomaterial surfaces with an extracellular matrix strives for the imitation of physiological conditions and thereby modulation of immune responses [44, 145]. At this juncture, artificial extracellular matrix on the one hand features binding sites for migrating cells and on the other hand either includes several exogenous bioactive molecules or provides binding sites for endogenous molecules [44]. In this way, suchlike coatings are to direct, amongst others,

migration, differentiation as well as proliferation of immune and wound healing cells [44].

1.4 State of the art

MΦ are critically involved in the FBR and thus are considered to be a major starting point to engross the knowledge on the FBR and to research immunomodulation [44, 71, 145].

1.4.1 Origin of MΦ for *in vitro* research

Human primary MΦ are differentiated, thus limitedly proliferating, and tissue-resident cells that cannot be obtained in sufficient quantity for *in vitro* studies without disproportional impairment of their donor [13, 34, 52, 53, 67, 96, 105, 144]. Furthermore, the heterogeneity of the primary cells may limit the validity and reproducibility of research [29]. To investigate the involvement of MΦ in the FBR and immunomodulation nonetheless, the usage of either murine MΦ, appropriate human cell lines or MdM constitutes an alternative solution [81, 119, 145].

Murine MΦ for *in vitro* research are either obtained as bone marrow-derived MΦ (BMdM) from the red bone marrow or are isolated as differentiated and tissue-resident cells [101]. In the former case, undifferentiated stem cells are gathered from red bone marrow and are subsequently differentiated using growth factors, such as GM-CSF or MΦ colony stimulating factor (M-CSF) [101]. Tissue-resident MΦ on the other hand, are primarily extracted from peritoneum that might previously be pro-inflammatorily stimulated to augment MΦ quantity [101, 144]. However, differences between human and murine cells have to be taken into consideration and findings cannot unrestrictedly be transferred to the *in vivo* situation [61, 62, 119].

Cell lines comprise cells featuring unrestricted proliferation, if cultured [26]. Concerning MΦ, within the *in vitro* research several human cell lines of varying degree of differentiation exist ***(Table (Tab.) 1)*** [13, 29, 30, 34, 96]. Frequently, THP1 cells are utilized owing to their similarity to primary cells concerning morphology and

functionality as well as their ability to being polarized [13, 28-30, 96, 105, 119, 145]. These cells exhibit a consistent geno- as well as phenotype, proliferate readily up to a high passage and are modest as to their cultivation [13, 29, 30, 105, 145]. However, due to the malignant origin of THP1 cells, gene expression may be unphysiological and deviant expression of surface molecules compared to primary MΦ is described [29, 30, 119]. Findings therefore may be biased [29, 30, 34, 96, 105, 119].

Table 1: Cell lines as to monocytes or MΦ

Cell line	Origin	Differentiation to monocytes or MΦ
ML2	Monoblastic leukemia [29]	Phorbol-12-myristate-13-acetate (PMA) [29]
Mono Mac 6	Monoblastic leukemia [29]	Lipopolysaccharide (LPS) [29, 146] Prostaglandin E_2 (PGE_2) [29, 146] PMA [29, 146]
THP1	Acute monocytic leukemia [13, 29, 30, 125]	M-CSF [30] PMA [13, 30, 34, 124] 1,25-dihydroxyvitamin D3 (vD3) [13, 30, 34]
U937	Promonocytic, human myeloid leukemia [30]	Retinoic acid vD3 [29] PMA [29, 30, 47]

To circumvent the aforementioned limitations of murine MΦ and of human cell lines, human primary monocytes are frequently deployed for *in vitro* research [119, 144]. These cells are accessible in sufficient count and without unjustifiable impairment of their donor, as they can be isolated from peripheral blood and consecutively differentiated as well as polarized *in vitro* [67, 68, 84].

1.4.2 Preparation of human polarized MdM *in vitro*

A multiplicity of protocols as to the isolation, differentiation and polarization of human MdM is outlined in the literature [18, 55, 59, 61, 62, 67, 68, 84, 98-100, 119, 130].

Monocytes along with lymphocytes constitute the peripheral blood mononuclear cells (PBMC), that are separated in the first instance and can be obtained either

from whole blood or from buffy coat, consisting of leukocytes and platelets [68, 84, 99]. Isolation is attained by means of density gradient centrifugation [18, 33, 55, 59, 61, 67, 68, 84, 98-100, 119, 130, 144]. For this purpose, whole blood or buffy coat is layered onto a substrate of specific molecular weight and adjacently centrifuged [18, 33, 46, 61, 67, 68, 84, 98-100, 130]. On the basis of varied density, distinct layers compassing plasm, platelets and PBMC as well as red blood cells and granulocytes are deposited (***Fig. 7***) [33, 46, 68, 99, 100]. Subsequent to the removal of the overhead plasm, PBMC are accessible and can be isolated [46, 68, 99, 100].

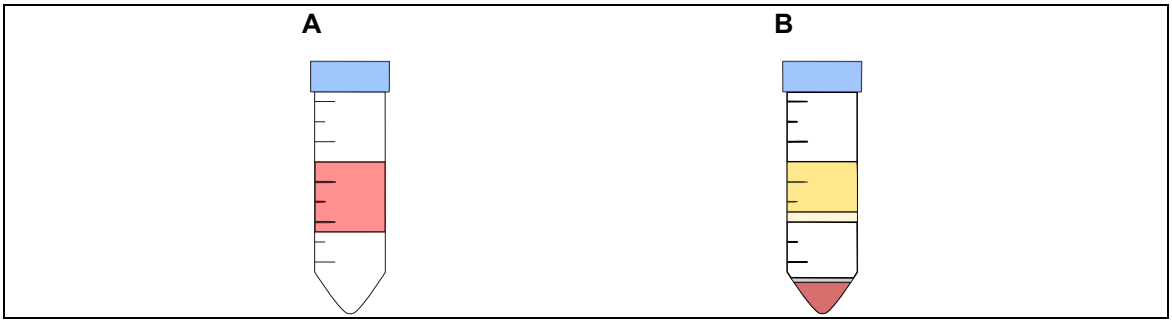

Figure 7: Density gradient centrifugation *modified according to [46, 68, 100].* ***A*** *Whole blood layered onto a substrate of specific molecular weight: whole blood (light red) and substrate (white).* ***B*** *Separation of whole blood components following density gradient centrifugation: plasm and platelets (orange), PBMC (yellow), substrate (white), granulocytes (grey) and erythrocytes (dark red).*

Regarding the separation of monocytes and lymphocytes hereinafter, either density gradient centrifugation [17, 33, 35, 50, 98], immunoselection [18, 33, 55, 59, 67, 84, 100, 119, 130] or monocyte adhesion [55, 61, 84, 100, 144] are employed. Concerning density gradient centrifugation, specific substrates are used that take account of the slight difference in density of monocytes and lymphocytes [17, 33, 35, 50, 98] and variation in the substrate's osmolarity is ascribed to enhance separation [98]. Regarding immunoselection, either a selective isolation of CD14+ monocytes, termed CD14+ immunoselection, or a directed removal of lymphocytes subject to their specific surface markers, named negative immunoselection, is conducted [33, 59, 84, 100, 130]. Monocyte adhesion, at last, relies on the capability of monocytes to adhere to plastic or glass surfaces, whereas lymphocytes remain loose and may thus be discarded [61, 84, 100].

Subsequently, monocytes are differentiated towards MdM by means of incubation with growth factors such as GM-CSF or M-CSF for 3 to 7 days [18, 59, 61, 62, 84, 100, 119, 130].

In order to polarize the MdM, another stimulation using cytokines, lipopolysaccharide (LPS), immune complexes as well as glucocorticoids for 24 hours up to 3 days may be undertaken [18, 55, 61, 62, 84, 100, 119, 130]. To this, the M1-phenotype is obtained via incubation with IFNγ and LPS [18, 55, 59, 61, 84, 100, 119, 130]. The M2-polarization on the other hand is, amongst others, induced by IL4 and IL13 as to the M2a-phenotype, by immunoglobulins, IL1β and LPS as to the M2b-phenotype and by IL10 and glucocorticoids as to the M2c-phenotype [18, 55, 59, 61, 84, 100, 103, 119, 130]. ***Tab. 2*** summarizes the protocols concerning monocyte isolation and differentiation as well as polarization of MdM.

1.4.3 Characterization of human polarized MdM *in vitro*

Various features of human polarized MdM may be investigated *in vitro*, so as to characterize these cells [61, 62, 119, 130]. To begin with, MΦ morphology is commonly assigned to the state of polarization with M1-polarized cells being rather round whereas the M2-phenotype is considered to be fusiform and elongated [62, 119]. Morphologic characteristics can be assessed light microscopically and by means of confocal laser scanning microscopy (CLSM) following staining of the cytoskeleton [62, 130]. Furthermore, MΦ can be classified regarding their secreted cytokines [61, 119]. M1-polarized MΦ typically secrete proinflammatory cytokines like TNFα, IL1β or IL6, whereas the M2-phenotype involves the release of, amongst others, IL10, TGFβ, chemokine C-C motif ligand (CCL) 13 and CCL17 [55, 61, 62, 108, 119, 130]. Enzyme-linked immunosorbent assay (ELISA) is implemented to measure messenger molecules secreted to the cell culture supernatant [55, 61, 130]. MΦ specifically express surface and intracellular markers rendering it possible to discern their polarization [18, 61, 62, 119, 130]. At this

Table 2: Protocols for preparation of human polarized MdM in vitro

Author	Isolation of PBMC	Isolation of monocytes	Differentiation of MdM	M1-polarization	M2-polarization
Beyer et al. [18]	Density gradient centrifugation (Pancoll) using buffy coat	$CD14^+$ immunoselection	GM-CSF 500 U/ml (3 days)	GM-MdM: IFNγ 200 U/ml (3 days)	GM-MdM: IL4 1000 U/ml (3 days)
Fujiwara et al. [45]	-	$CD14^+$ immunoselection	GM-CSF 10 ng/ml (7 days) *or* M-CSF 50 ng/ml (7 days)	GM-MdM or M-MdM: IFNγ 50 ng/ml + LPS 10 ng/ml (24 hours) *or* IFNγ 50 ng/ml (24 hours)	GM-MdM or M-MdM: IL4 10 ng/ml (24 hours) (M2a) *or* IL1β 10 ng/ml (24 hours) (M2b) *or* IL10 10 ng/ml (24 hours) (M2c)
Graff et al. [55]	Density gradient centrifugation (Ficoll Paque PLUS) using the leukocyte fraction	Monocyte adhesion (4 days) *or* $CD14^+$ immunoselection	Monocyte adhesion (4 days) in Roswell Park Memorial Institute (RPMI) 1640 + 10 % FBS	MdM: LPS 10 ng/ml + IFNγ 20 ng/ml (up to 72 hours)	MdM: IL4 20 ng/ml (up to 72 hours) (M2a) *or* IgG + LPS 100 ng/ml (up to 72 hours) (M2b) *or* TGFβ1 0,5 ng/ml (up to 72 hours) (M2c)
Hoppstädter et al. [59]	Density gradient centrifugation (Pancoll) using buffy coat	$CD14^+$ immunoselection	GM-CSF 10 ng/ml (5 days) *or* M-CSF 10 ng/ml (5 days)	GM-MdM: LPS 1 µg/ml + IFNγ 20 ng/ml (40 hours)	M-MdM: IL10 200 ng/ml (40 Stunden)
Iqbal et al. [61]	Density gradient centrifugation (Ficoll Paque) using whole blood	Monocyte adhesion (3 hours)	M-CSF 10 ng/ml (6 days)	M-MdM: IFNγ 20 ng/ml (2 days)	M-MdM: IL4 20 ng/ml (2 days) (M2a) *or* LPS 1 µg/ml+ IL1β 10 ng/ml (2 days) (M2b) *or*

					IL10 10 ng/ml (2 days) (M2c)
Jaguin et al. [62]	Density gradient centrifugation (Ficoll) using buffy coat [126]	Monocyte adhesion (2 hours) [126]	GM-CSF 400 IU/ml (6 days) *or* M-CSF 50 ng/ml (6 days)	GM-MdM or M-MdM: LPS 100 ng/ml + IFNγ 20 ng/ml (24 hours)	M-MdM: M-CSF 10 ng/ml + IL4 20 ng/ml (24 hours)
Kelly [67]	Density gradient centrifugation (Ficoll) using buffy coat	$CD14^+$ immunoselection	GM-CSF 50 ng/ml (6 days) *or* M-CSF 50 ng/ml (6 days)	GM-MdM: IFNγ 50 ng/ml (24 hours)	M-MdM: IL4 20 ng/ml (24 hours) *or* IL10 20 ng/ml (24 hours)
Nielsen et al. [84]	Density gradient centrifugation (Histopaque-1077) using buffy coat	$CD14^+$ immunoselection	GM-CSF 1 ng/ml + M-CSF 10 ng/ml (5 days)	GM-M-MdM: LPS 100 ng/ml + IFNγ 20 ng/ml (24 hours)	GM-M-MdM: IL4 10 ng/ml + IL13 10 ng/ml (24 hours) *or* IL10 10 ng/ml (24 hours)
Tarique et al. [119]	Density gradient centrifugation (Lymphoprep) using buffy coat	$CD14^+$ immunoselection	GM-CSF 50 ng/ml (6 days) *or* M-CSF 50 ng/ml (6 days)	GM-MdM or M-MdM: LPS 20 ng/ml (2 days) *or* IFNγ 20 ng (ml (2 days) *or* LPS 20 ng/ml + IFNγ (20 ng/ml (2 days)	GM-MdM or M-MdM: IL4 20 ng/ml (2 days) *or* IL13 20 ng/ml (2 days) *or* IL4 20 ng/ml + IL13 20 ng/ml (2 days)
Vogel et al. [130]	Density gradient centrifugation (Lymphoprep) using buffy coat	$CD14^+$ immunoselection	GM-CSF 10 ng/ml (5 days) or M-CSF 25 ng/ml (5 days) *or* Normal human serum (NHS) (5 days)	GM-MdM *or* M-MdM *or* NHS-MdM: IFNγ $1x10^3$ U/ml (2 days) + after 24 hours LPS 10 ng/ml (24 hours)	GM-MdM *or* M-MdM *or* NHS-MdM: IL4 10 ng /ml (2 days) (M2a) *or* IL10 10 ng/ml (2 days) (M2b) *or* Dexamethasone 10 µM (2 days) (M2c)

juncture, CD14 as well as CD68 are considered to be general markers of the monocytic cell line whereas molecules such as CD64, CD80 and CD86 are classified as marker of M1-polarization and molecules like CD1, CD163, CD206 and CD209 mark the M2-phenotype [18, 61, 62, 108, 115, 119, 121, 134]. Flow cytometry as well as fluorescence microscopy are used to characterize the expression of markers [18, 61, 62, 115, 130]. Lastly, gene expression of MΦ can be assessed isolating RNA and using quantitative real-time polymerase chain reaction (qRT-PCR) [45, 62, 119]. ***Tab. 3*** summarizes characteristics of polarized MΦ.

Table 3: Characterization of MΦ

Phenotype	Morphology	Cytokine and chemokine secretion	Marker expression	Gene expression	Function
M1-MΦ	fried-egg-like morphology [126]	CCL5 [108, 119] chemokine C-X-C motif ligand (CXCL) 9 [108] CXCL10 [62, 108, 119] CXCL11 [108] CXCL16 [108] IFNγ [119] IL1β [55, 62, 91, 108] IL6 [55, 91, 108] IL8 [119] IL12p40 [62, 130] IL12 [55, 91, 108] IL23 [108] IL27 [108] IL28 [91] TNFα [55, 59, 62, 91, 108, 119, 130]	CD40 [130] CD64 [18, 130] CD68 [108] CD80 [59, 61, 62, 91, 108, 119] CD86 [18, 61, 91, 108] IL1 receptor (R) 1 [91, 108] Inducible nitric oxide synthase (iNOS) [108] MHCII [91, 108] Nitric oxide synthase (NOS) 2 [91] toll-like receptor (TLR) 2 [91, 108] TLR4 [91, 108]	apolipoprotein L (APOL) 3 [119] CCL5 [62] CCR7 [62] CXCL 9 [18, 45, 55] CXCL10 [18, 62] CXCL11 [18, 45, 62, 119] Fcγ receptor (FcγR) 1α [18] FcγR1β [18] indolamine 2,3-dioxygenase (IDO) 1 [62] IL1β [18] IL6 [18] IL12 [62, 91] IL23α [18] IL28 [91] interferon regulatory factor (IRF) 5 [119] TNFα [18, 119]	pro-inflammatory immune response, tumor resistance [108]
M2-MΦ	spindle-shape [62, 119] elongated, stellate shape [126]	CCL17 [62, 119] CCL18 [119] CCL22 [62] CD163 [130] CD206 [130] IL10 [61]	CD1a [119] CD1b [119] CD11b [119] CD23 [18, 119] CD200R [62] CD209 [119]	CCL17 [18] CCL18 [18, 119] CCL22 [18, 62] CD23 [18] CD36 [62] fibronectin (FN) 1 [119] IL27 receptor antagonist (RA) [18] IRF4 [119] peroxisome proliferator activated receptor (PPAR) γ [62] Scanvenger receptor class B (SRB) 1 [62]	

					TGFβ [62]	
	M2a-MΦ		CCL17 [108] CCL18 [108] CCL22 [108] CCL24 [108] IL5 [61] IL10 [61, 108] IL22 [61] TGFβ [91, 108]	CD86 [61] CD163 [91] CD200R [61] CD206 [91, 108] IL1RA [108] IL1RII [91, 108] transglutaminase (TGM) 2 [91]	CCL13 [55] CCL17 [55]	anti-inflammatory immune response, tissue remodeling [108]
	M2b-MΦ		CCL1 [108] IL1β [55, 108] IL6 [55, 61, 108] IL10 [55, 61, 108] TNFα [55, 61, 108]	CD14 [61] CD80 [61] CD86 [91, 108]	IL1 [91] IL6 [91] IL10 [91] TNFα [91]	immunoregulation [108]
	M2c-MΦ		CCL13 [108] CCL18 [108] IL5 [61] IL10 [59, 108] IL22 [61] TGFβ [108]	CD14 [59] CD163 [59, 61, 91] CD206 [108] TLR1 [91, 108] TLR8 [91, 108]	IL10 [91] TNFβ [91]	phagocytosis of apoptotic cells [108]
	M2d-MΦ		IL10 [108] VEGF [108]	VEGF [91, 108]	IL10 [91] IL12 [91] TNFα [91] TNFβ [91]	angiogenesis, tumor progression [108]

1.5 Objective

Due to their beneficial functional, aesthetic and psychologic aspects along with promising long-term results, dental implants are frequently used in the treatment of tooth loss or edentulism [3, 38, 56]. However, peri-implant bone loss can occur [110] and marks an increasing problem [93, 123] that can lead up to implant failure, as reliable solution approaches are currently lacking [123]. Marginal bone loss is related to either a failed establishment of or the loss of an established FBE [93, 123, 133]. On a molecular level, MΦ critically control major phases of the FBR and the FBE, being present on an implant during its entire *in vivo* lifetime [11, 22, 24, 106, 123]. Efforts to unfailingly overcome peri-implant bone loss should therefore aim at disclosing cellular and molecular mechanisms of the FBR and the FBE bringing MΦ into focus [123].

On this account, the conducted study strived for the establishment of a protocol to isolate and differentiate human peripheral blood monocytes towards polarized MdM to subsequently deepen knowledge on the FBR and investigate potential immunomodulatory effects of biomaterials on the latter cells *in vitro*. ***Fig. 8*** depicts the research outline.

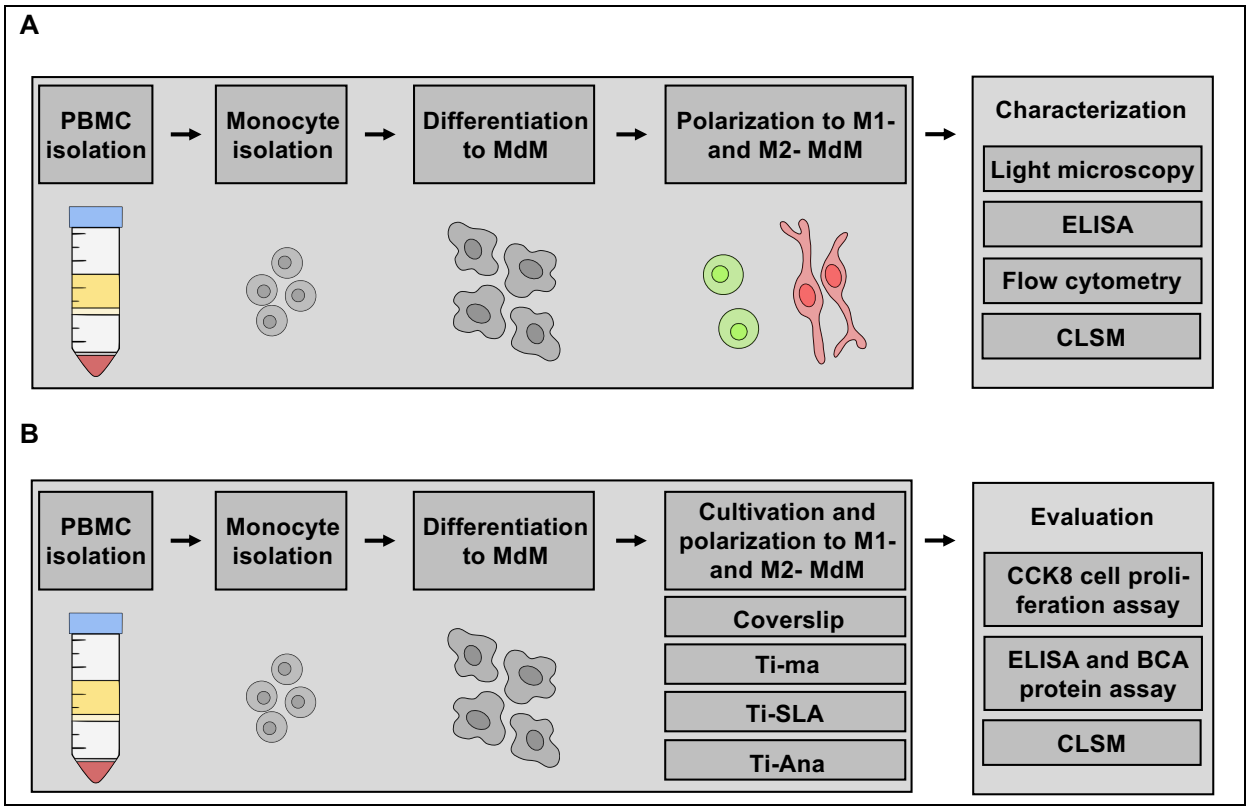

***Figure 8: Research outline**. **A** Establishment of a protocol comprised the set-up of an isolation method for PBMC and monocytes hereinafter, the set-up of a method for differentiation to MdM and for their polarization. M0-, M1- and M2-MdM were then characterized by means of light microscopy, ELISA, flow cytometry and CLSM. **B** Implementation of the established protocol comprised the seeding of the MdM on different surfaces (coverslip, machined titanium discs (Ti-ma), SLA titanium discs (Ti-SLA) or titanium anatase discs (Ti-Ana)) and the subsequent polarization to M0-, M1- and M2-MdM to test on potential immunomodulatory effects of the latter biomaterials. Evaluation was conducted using cell counting kit (CCK) 8 cell proliferation assay, ELISA, bicinchoninic acid assay (BCA protein assay) and CLSM.*

Within the first section of this study, monocytes were initially separated from human blood by density gradient centrifugation and monocyte adhesion on plastic surfaces. Differentiation towards MdM was then accomplished using the growth factor M-CSF and polarization to either M0-, M1- or M2-MdM was obtained through incubation with complete medium, the cytokines IFNγ and LPS or the cytokines IL4 and IL13, respectively. The polarized MdM were finally characterized morphologically as well as by means of ELISA, flow cytometry and CLSM.

The second part of this study aimed at the implementation of the established protocol and hence comprised the investigation of biomaterial-related immunomodulatory effects on MdM. To this, differentiated MdM were cultivated on titanium surfaces comprising either Ti-SLA discs or Ti-Ana discs as modified titanium surfaces, whereas Ti-ma discs as well as tissue culture plastic coverslips were utilized as control surfaces. Incubation with either complete medium, the cytokines IFNγ and LPS or the cytokines

IL4 and IL13 was deployed to induce M0-, M1- or M2-MdM phenotype, respectively. Potential immunomodulatory effects on polarized MdM were then controlled by means of CCK8 cell proliferation assay, ELISA, BCA protein assay and CLSM.

2 Materials and Methods

The study conducted is approved by the ethics committee of the Eberhard Karls University of Tübingen (ethical approval: 286/2021 BO).

2.1 Cells

Primary human monocytes were used to prepare differentiated and polarized MdM ***(Chap. 2.6.1, Chap. 2.6.2, Chap. 2.6.3, Chap. 2.6.4)***. The monocytes were obtained from ethylendiaminetetraacetic acid (EDTA) -anticoagulated whole blood drawn by peripheral venipuncture from healthy and voluntary subjects independent of their sex and age. Their written consent is documented. Blood was taken prior to each experiment and was immediately used for monocyte isolation.

2.2 Chemicals and reagents

Chemicals and reagents used within this study are listed below in ***Tab. 4***.

Table 4: List of chemicals and reagents

Chemical	Manufacturer	Catalog number
Accutase in DPBS, 0.5 mM EDTA	EMD Millipore Corp. (Burlington, USA)	SCR005
Ammonium chloride Molecular biology grade NH_4Cl M_r 53,50	Serva Electrophoresis GmbH (Heidelberg, Germany)	39752.01
Antibody anti-human CCR7, purified Mouse Monoclonal IgG, Clone 150503	R & D Systems® (Minneapolis, MN, USA)	MAB197
Antibody anti-human CD68 Clone: eBioY1/82A, Alexa Fluor 647	Life Technologies Corp. (Carlsbad, CA, USA)	50-0689-42
Antibody anti-human/mouse Arginase 1 monoclonal antibody Clone: A1exF5, PerCP-eFluor 710 Invitrogen	Thermo Fisher Scientific (Waltham, MA, USA)	46-3697-80
Antibody Anti-human CD1A Clone: SK9, PE invitrogen	Thermo Fisher Scientific (Waltham, MA, USA)	12-001741
Antibody anti-human CD86 Clone: IT2.2, PE invitrogen	Thermo Fisher Scientific (Waltham, MA, USA)	12-0869-42

Antibody anti-human CD197 (CCR7) Clone: 3D12, PE Invitrogen	Thermo Fisher Scientific (Waltham, MA, USA)	12-1979-41
Antibody DC-SIGN (D7F5C) XP Rabbit mAB	Cell Signaling Technology (CST) (Denvers, NA, USA)	13193
Antibody goat anti-mouse IgG (H+L) highly cross absorbed secondary antibody Alexa Fluor Plus 488 invitrogen	Thermo Fisher Scientific Inc. (Waltham, MA, USA)	A32723TR
Antibody Goat anti-rabbit IgG (H+L) Alexa Fluor 488	Abcam (Cambridge, Great Britain)	A150077
Antibody goat anti-rabbit IgG (H+L) cross absorbed secondary antibody Cyanine3 invitrogen	Thermo Fisher Scientific Inc. (Waltham, MA, USA)	A10520
Antibody mouse anti-human CD14 Clone: M5E2, Alexa Fluor 647	BioLegend (San Diego, CA, USA)	301818
Antibody mouse anti-human CD80 Clone 2D10, Briliant Violet 421	BioLegend (San Diego, CA, USA)	305222
Antibody mouse anti-human CD163 Clone:GHI/61, FITC BD Pharmingen	BD Biosciences (San Jose, CA, USA)	563697
Antibody mouse anti-human CD206 Clone:19.2, PE BD Pharmingen	BD Biosciences (San Jose, CA, USA)	555954
Antibody mouse anti-human CD209 Clone: DCN46, FITC BD Pharmingen	BD Biosciences (San Jose, CA, USA)	561764
Anti-fade fluorescence mounting medium - aqueous, fluoroshield	abcam (Cambridge, UK)	ab104135
Ampuwa irrigation solution 1000 mL Plastipur	Fresenius Kabi (Bad Homburg, Germany)	B230673
BD Cytofix Fixation Buffer	Becton, Dicinson and Company (Franklin Lakes, NJ, USA)	554655
BD Pharmingen Purified NA/LE Human BD Fc Block	Becton, Dicinson and Company (Franklin Lakes, NJ, USA)	564765
Bovine serum albumin (BSA)	VWR International bvba (Leuven, Belgium)	422361V
Cell Counting Kit-8	Dojindo Laboratories (Mashiki, Japan)	CK04
Dimethyl sulfoxide	Sigma-Aldrich Co. (St. Louis, MO, USA)	D2438-5X10ML
DPBS (1X) Dulbecco's Phosphate Buffered Saline [-] $MgCl_2$ [-] $CaCl_2$	Gibco (Paisley, United Kingdom)	14109-094
DRAQ5 staining solution	Milteny Biotec (Bergisch Gladbach, Germany)	130-117-344
EDTA-Solution pH 8.0 (0.5 M) for molecular biology	AppliChem GmbH (Darmstadt, Germany)	A3145

Ethanol	VWR Chemicals (Rosny-sous-Bois, France)	20.821.330
Ethylenediaminetetraacetic acid disodium salt dihydrate Suitable for electrophoresis, for molecular biology, 99.0-101.0 % (titration)	Sigma-Aldrich Co. (St. Louis, MO, USA)	E5134-50G
FBS SUPERIOR stabil Steril filtriert	Bio&Sell (Nürnberg, Germany)	FBS.S 0615
Human CCL13 (MCP-4) ELISA kit invitrogen	Thermo Fisher Scientific (Carlsbad, CA, USA)	EHCCL13
Human CCL17 (TRAC) ELISA kit invitrogen	Thermo Fisher Scientific (Carlsbad, CA, USA)	EHCCL17
Human IFN-gamma recombinant protein	invitrogen (Rockford, IL, USA)	RIFNG100
Human IL4	Miltenyi Biotec (Bergisch Gladbach, Germany)	130-095-373
Human IL13	Miltenyi Biotec (Bergisch Gladbach, Germany)	130-112-409
Human M-CSF	Peprotech (Cranbury, NJ, USA)	300-25
Human TNF-α ELISA Kit invitrogen	Thermo Fisher Scientific (Carlsbad, CA, USA)	KHC3011
Immersion oil	Ibidi (Gräfelfing, Germany)	50101
Lipopolysaccharides from Escherichia coli O111:B4	Sigma Aldrich Co. (St. Louis, MO, USA)	L4391-1MG
Lymphocyte Separation Medium 1077	PromoCell (Heidelberg, Deutschland)	C-44010
Monocyte Attachment Medium	PromoCell (Heidelberg, Deutschland)	C-28051
Pen Strep Penicillin Streptomycin [+]10 000 Units/ml Penicillin [+]10 000 µg/ml Streptomycin	Gibco (Grand Island, NY, USA)	15140-122
Phalloidin-fluorescein isothiocyanate (FITC)	Sigma-Aldrich (St. Louis, MO, USA)	P5282
Pierce BCA protein assay kit thermo scientific	Thermo Fisher Scientific (Carlsbad, CA, USA)	23227
Potassium bicarbonate ACS reagent, 99,7 %, powder, crystals or granules	Sigma-Aldrich Co. (St. Louis, MO, USA)	237205-100G
Paraformaldehyde reagent grade, crystalline	Sigma Aldrich Co. (St. Louis, MO, USA)	P6148-500G
RNase free DPEC-treated water	Thermo Fisher Scientific (Carlsbad, CA, USA)	AM9916
RPMI 1640, 1X with L-glutamine	Mediatech Inc. (Manassas, VA, USA)	10-040-CV
Triton 100X	Merck KGaA (Darmstadt, Germany)	112298
Trypan blue solution 0.4%	Carl Roth GmbH + Co. KG (Karlsruhe, Germany)	1680.1
Tween 20	Carl Roth (Karlsruhe, Germany)	9127.2

2.2.1 Solutions and buffers

As to the experimental procedure, solutions and buffers were prepared for the isolation of monocytes, their differentiation towards polarized MdM as well as the subsequent

assessment using ELISA, flow cytometry, CLSM and BCA protein assay. ***Tab. 5*** summarizes these solutions and buffers.

Table 5: List of solutions and buffers

Solution/buffer	Contents	Application notes
BCA protein assay		
Working reagent for BCA protein assay	BCA reagent A + BCA reagent B 50:1	Preparation prior to usage Utilization: room temperature
CLSM		
Fixation buffer for CLSM	PBS + 3% paraformaldehyde (PFA)	Storage: room temperature Utilization: room temperature
Permeabilization buffer for CLSM	PBS + 0.2% Triton 100X	Storage: room temperature Utilization: room temperature
Staining buffer for CLSM	PBS + 1% BSA + 0.1% Tween 20	Storage: +4° C Utilization: room temperature
Storage buffer for CLSM	PBS + 1% penicillin and streptomycin	Storage: +4° C Utilization: room temperature
Wash buffer for CLSM	PBS + 0.1% Tween 20	Storage: +4° C Utilization: room temperature
ELISA		
Assay diluent B 1X for CCL13 ELISA	5-fold dilution of assay diluent B 5X with deionized or distilled water	Preparation prior to usage Utilization: room temperature
Assay diluent B 1X for CCL17 ELISA	5-fold dilution of assay diluent B 5X with deionized or distilled water	Preparation prior to usage Utilization: room temperature
Assay diluent C for CCL17 ELISA	-	Storage: +4° C Utilization: room temperature
Biotin concentrate for CCL13 ELISA	Biotin (vial) + 100 µl assay diluent B 1X	Storage: +4° C Utilization: room temperature
Biotin conjugate for CCL13 ELISA	80-fold dilution of biotin concentrate with assay diluent B 1X	Preparation prior to usage Utilization: room temperature
Biotin concentrate for CCL17 ELISA	Biotin (vial) + 100 µl assay diluent B 1X	Storage: +4° C Utilization: room temperature
Biotin conjugate for CCL17 ELISA	80-fold dilution of biotin concentrate with assay diluent B 1X	Preparation prior to usage Utilization: room temperature
Biotin conjugate for TNFα ELISA	-	Storage: +4° C Utilization: room temperature
Incubation buffer for TNFα ELISA	-	Storage: +4° C Utilization: room temperature
Stabilized chromogen for CCL13 ELISA	-	Storage: +4° C Utilization: room temperature
Stabilized chromogen for CCL17 ELISA	-	Storage: +4° C Utilization: room temperature
Stabilized chromogen for TNFα ELISA	-	Storage: +4° C Utilization: room temperature
Standard diluent buffer for TNFα ELISA 1X	-	Storage: +4° C Utilization: room temperature
Stop solution for CCL13 ELISA	-	Storage: +4° C Utilization: room temperature
Stop solution for CCL17 ELISA	-	Storage: +4° C Utilization: room temperature
Stop solution for TNFα ELISA	-	Storage: +4° C

		Utilization: room temperature
Streptavidin-horse raddish peroxidase (HRP) solution 1X for CCL13 ELISA	200-fold dilution of streptavidin HRP (200X) with assay diluent B 1X	Preparation within 15 minutes of usage Utilization: room temperature
Streptavidin-HRP solution 1X for CCL17 ELISA	400-fold dilution of streptavidin HRP (400X) with assay diluent B 1X	Preparation within 15 minutes of usage Utilization: room temperature
Streptavidin-HRP solution 1X for TNFα ELISA	10 µl streptavidin-HRP (100X) solution + 1 ml streptavidin-HRP diluent	Preparation within 15 minutes of usage Utilization: room temperature
Wash buffer 1X for CCL13 ELISA	20 ml wash buffer concentrate (20X) + 380 ml of deionized or distilled water	Storage: +4° C Utilization: room temperature
Wash buffer 1X for CCL17 ELISA	20 ml wash buffer concentrate (20X) + 380 ml of deionized or distilled water	Storage: +4° C Utilization: room temperature
Wash buffer 1X for TNFα ELISA	16 ml wash buffer concentrate (25X) + 384 ml of deionized or distilled water	Storage: +4° C Utilization: room temperature
Fluorescence-activated cell sorting (FACS)		
FACS buffer	PBS + 0.5 % BSA	Storage: +4° C Utilization: ice-cold/+4° C
FACS Fc-blocking buffer	FACS buffer + 2,5 % Fc block	Preparation prior to usage Utilization: +4° C
Monocyte isolation, MdM differentiation and polarization		
Complete medium	RPMI + 10 % FBS + 1 % penicillin and streptomycin in PBS	Storage: +4° C Utilization: +37° C
Dilution buffer for PBMC isolation	500 ml DPBS + 2 ml 0.5 M EDTA	Storage: +4° C Utilization: +37° C
Erythrocyte lysis buffer	1000 ml H_2O + 8.29 g NH_4Cl + 1 g $KHCO_3$ + 0.37 g $C_{10}H_{14}N_2O_8 \bullet 2\ Na \bullet 2\ H_2O$	Sterile-filtered Storage: +4° C Utilization: +37° C
FBS	-	Heat inactivation: +56° C, 30 minutes Storage: +4° C Long-term storage: -20° C
Lymphocyte Separation Medium	-	Storage: room temperature, under protection from light Utilization: room temperature, under protection from light
Monocyte Adhesion Medium	-	Storage: +4° C Utilization: +37° C
Wash buffer for PBMC isolation	500 ml DPBS + 50 ml FBS + 2 ml 0.5 M EDTA	Storage: +4° C Utilization: +37° C

Furthermore, the growth factor M-CSF, the cytokines IFNγ, IL4 and IL13, LPS as well as phalloidin were prepared according to the manufacturers' specific instructions prior to their utilization.

2.2.2 IFNγ

IFNγ was obtained as lyophilizate, was stored at -20° C and was reconstituted to a concentration of 1 mg/ml using ribonuclease (RNase) -free water. Further dilution to a concentration of 50 µg/ml was prepared with phosphate buffered saline (PBS) + 0.1 % bovine serum albumin (BSA). Diluted IFNγ was then aliquoted into protein low-binding tubes and kept at -20° C until its utilization. Repeated freeze-thaw cycles were avoided.

2.2.3 IL4

IL4 was obtained as lyophilizate, was stored at -20° C and was reconstituted to a concentration of 0.1 mg/ml using RNase-free water. Further dilution to a concentration of 10 µg/ml was prepared with PBS + 0.1 % BSA. Diluted IL4 was then aliquoted into protein low-binding tubes and kept at -20° C until its utilization. Repeated freeze-thaw cycles were avoided.

2.2.4 IL13

IL13 was obtained as lyophilizate, was stored at -20° C and was reconstituted to a concentration of 0.1 mg/ml using RNase-free water. Further dilution to a concentration of 10 µg/ml was prepared with PBS + 0.1 % BSA. Diluted IL13 was then aliquoted into protein low-binding tubes and kept at -20° C until its utilization. Repeated freeze-thaw cycles were avoided.

2.2.5 LPS

LPS was obtained as lyophilizate, was stored at -20° C and was reconstituted to a concentration of 1 mg/ml using 0.9 % sodium chloride (NaCl) solution. Reconstituted LPS was then aliquoted and kept at -20° C. Prior to its utilization further dilution to a concentration of 10 µg/ml was done using complete medium. Repeated freeze-thaw cycles were avoided.

2.2.6 M-CSF

M-CSF was obtained as lyophilizate, was stored at -20° C and was reconstituted to a concentration of 0.1 mg/ml using RNase-free water. Further dilution to a concentration

of 10 µg/ml was prepared with PBS + 0.1 % BSA. Diluted M-CSF was then aliquoted into protein low-binding tubes and kept at -20° C until its utilization. Repeated freeze-thaw cycles were avoided.

2.2.7 Phalloidin

Phalloidin was obtained as lyophilizate, was stored at -20° C and was reconstituted to a concentration of 0.5 mg/ml using dimethyl sulfoxide (DMSO). Reconstituted phalloidin was then aliquoted and kept at -20° C. Prior to its utilization further dilution to a concentration of 5 µg/ml was done using PBS + 0.1 % BSA. Repeated freeze-thaw cycles were avoided.

2.3 Consumables

Consumables used within this study are listed below in ***Tab. 6***.

Table 6: List of consumables

Consumable	Manufacturer	Catalog number
Cell culture dish 35x10 mm Cellstar	Greiner Bio-One GmbH (Frickenhausen, Germany	627160
Cell Scraper Costar	Corning Incorporated (Corning, NY, USA)	3010
Descosept sensitive	Dr. Schumacher GmbH (Malsfeld, Deutschland)	00-653-050
Eppendorf tubes protein LoBind tube 1.5 ml	Eppendorf SE (Hamburg, Germany)	022431081
Eppendorf tubes safe-lock tubes 1.5 ml	Eppendorf SE (Hamburg, Germany)	0030 120.086
Eppendorf tubes safe-lock tubes 2.0 ml	Eppendorf AG (Hamburg, Germany)	0030 120.094
FACS tubes Falcon 5 ml polysterene round-bottom tube	Corning Science México S. A. de C. V. (Reynosa, Tamaulipas, México)	352054
Filter paper	Macherey-Nagel (Düren, Germany)	431 009
Filtration system Millipore Membrane, 33 mm ⌀	Merck Millipore Ltd. (Cork, Ireland)	SLG033SS
Filtration system Steritop 45 mm Neck Size Millipore Express PLUS	Merck KGaA (Darmstadt, Germany)	S2GPT02RE
Gloves, Peha-soft nitrile FINO	Paul Hartmann AG (Heidenheim, Germany)	110699
Hemocytometer, C-Chip, disposable	NanoEntek Inc. (Hwaseong-si, Gyeonggi-do, Korea)	DHC-N01
Leukoplast soft Skin friendly adhesive dressing	BSN medical GmbH (Hamburg, Germany)	79297-03

Microscope cover glass, 10 mm ⌀	Paul Marienfeld GmbH & Co. KG (Lauda-Königshofen, Germany)	111500
Microscope cover glass 12 mm ⌀ Assistent	Karl Hecht GmbH & Co KG (Sondheim vor der Rhön, Germany)	1001
Microscope cover glass, 20 x 20 mm	Menzel Gläser (Braunschweig, Deutschland)	1
Microscope slide Objektträger	Carl Roth GmbH (Karlsruhe, Germany)	4HX4.1
Nail polish Colour shield top coat Essence	Cosnova GmbH (Sulzbach, Germany	N/A
octenisept antiseptic Wässriges Wund- und Schleim-Haut-antiseptikum	Schülke & Mayr GmbH (Nordersted, Germany)	173711
Parafilm	Bemis Company, Inc. (Oshkosh, WI, USA)	PM999
Pipette tips Finntip Flex 300 Volume range 30-300 µl	Thermo Fisher Scientific OY (Vantaa, Finland)	94060520
Pipette tips ratiolab tips 100-1200 µl blue	Ratiolab GmbH (Dreireich, Germany)	2100610
Pipette tips ratiolab tips 1-200 µl yellow	Ratiolab GmbH (Dreireich, Germany)	2100600
Pipette tips ratiolab tips 0.5-20 µl crystal	Ratiolab GmbH (Dreireich, Germany)	2500170
Pipet tip Sapphire 1000 µl	Greiner Bio-One GmbH (Kremsmünster, Austria)	777350
Pipette tip Sapphire 200 µl	Greiner Bio-One GmbH (Kremsmünster, Austria)	775350
Pipette tip Spitzen 10 µl	Biozym Scientific GmbH (Hessisch Oldendorf, Germany)	720011
Pipette tip Ultratip 200 µl	Greiner Bio-One GmbH (Frickenhausen, Germany	739290
Plate, 24-well Cellstar for suspension culture	Greiner Bio-One GmbH (Frickenhausen, Germany)	662102
Plate, 24-well Costar not-treated	Corning Incorporated (Kennebunk, ME, USA)	3738
Plate, 24-well Costar tissue culture-treated	Corning Incorporated (Kennebunk, ME, USA)	3524
Plate, 96-well	Greiner Bio-One GmbH (Frickenhausen, Germany)	655101
Pur-Zellin Zellstofftumpfer von der Rolle Cellulose swabs on a roll	Paul Hartmann AG (Heidenheim, Germany)	143 253
S-Monovette 9 ml K3E K3E: 1,6 ml EDTA/ml	Sarsted AG & Co. KG (Nümbrecht, Germany)	02.1066.001
Safety-Multifly® 21G tube 200 mm	Sarsted AG & Co. KG (Nümbrecht, Germany)	85.1638.235
Serological pipet, 10 ml graduated in 1/10 ml Cellstar	Greiner Bio-One GmbH (Frickenhausen, Germany	F220934U
Serological pipet, 10 ml graduated in 1/10 ml, Corning Advantage	Corning Incorporated (Corning, NY, USA)	356551
Serological pipet, 25 ml graduated in 1/4 ml, Falcon Advantage	Corning Incorporated (Durham, NC, USA)	356525

Serological pipet, 25 ml graduated in 2/10 ml, Costar Stripette	Corning Incorporated (Corning, NY, USA)	4489
Serological pipet, 5 ml graduated in 1/10 ml, Corning Advantage	Corning Incorporated (Corning, NY, USA	4487
The green Tourniquet	Prämeta (Köln, Germany)	902
Tissue Culture Coverslips 13 mm (plastic)	Sarsted, Inc. (Newton, NC, USA)	83.1840.002
Tissue culture flask T75	Sarsted AG & Co. KG (Nümbrecht, Germany)	83.3911.002
Titanium-Anatase discs 12 mm	Medentis medical GmbH (Bad Neuenahr-Ahrweiler, Germany)	N/A
Titanium-machined discs 12 mm	Medentis medical GmbH (Bad Neuenahr-Ahrweiler, Germany)	N/A
Titanium-SLA discs 10 mm	Medentis medical GmbH (Bad Neuenahr-Ahrweiler, Germany)	N/A
Tube, 15 ml, Cellstar conical bottom, graduated, sterile	Greiner Bio-One GmbH (Frickenhausen, Germany)	188261-N
Tube, 50 ml, Cellstar, conical bottom, graduated, sterile	Greiner Bio-One GmbH (Frickenhausen, Germany)	227261
Tube, 50 ml, Cellstar, conical bottom with support skin	Greiner Bio-One GmbH (Frickenhausen, Germany	210270

2.4 Appliances

Appliances used within this study are listed below in ***Tab. 7***.

Table 7: List of appliances

Appliance	**Manufacturer**	**Catalog number/ Item number**
Absorbance reader Infinite F50	TECAN Austria GmbH (Grödig, Austria)	TCAT91000001
Canon EOS 550D	Canon (Tokyo, Japan)	4463B017AA
Centrifuge Multifuge 1S-R	Kendro Laboratory Products GmbH (Langenselbold, Germany)	40662891
Centrifuge Biofuge 15	Heraeus instruments (Hanau, Germany)	236384
CLSM Leica TCS SP5	Leica Microsystems CMS GmbH (Mannheim, Germany)	
FACS BD FACSCalibur Flow cytometer	BD Biosciences (San Jose, CA, USA)	E97500055
Freezer +4° C/-20° C	Liebherr (Ochsenhausen, Germany)	GSN3226
Heracell 150 i CO2 incubator	Thermo Fisher Scientific (Waltham, MA, USA)	51032720
Laboratory balance Sartorius analytic	Sartorius GmbH (Göttingen, Germany)	39010016
Light microscope CK2	Olympus Deutschland GmbH (Hamburg, Germany)	601663
Pipette Eppendorf Research plus 0.5-10 µl	Eppendorf SE (Hamburg, Deutschland)	3123000020
Pipette Eppendorf Research plus 10-100µl	Eppendorf SE (Hamburg, Deutschland)	**3**123000047
Pipette Eppendorf Research plus 100-1000 µl	Eppendorf SE (Hamburg, Deutschland)	3123000063

Pipette Eppendorf Research plus 10-100 µl, 8-Kanal	Eppendorf SE (Hamburg, Deutschland)	3125000036
Pipette controller Pipetus	Hirschmann Laborgeräte GmbH & Co. KG (Eberstadt, Germany)	8707199
Shaker DOS-20S	neoLab Migge GmbH (Heidelberg, Germany)	7DE048
Sterile bench, LaminarAir HB 2472	Heraeus instruments (Hanau, Germany)	51012197
Varioklav Dampfsterilisator	HP Labortechnik GmbH (Oberschleißheim, Germany)	41320797
Waterbath Medingen W6, 220 V 50/60 Hz, 1.0 KW	Medingen GmbH (Ottendorf-Okrilla, Germany)	40044

2.5 Software

Software used within this study is listed below in ***Tab. 8***.

Table 8: List of software

Software	Manufacturer	Version
BD CellQuestPro Software	BD Biosciences (San Jose, CA, USA)	Version 5.1
Endnote	Clarivate (Philadelphia, PA, USA)	Version 21.4
EOS Utility software	Canon Inc. (Tokyo, Japan)	Version 3.10.20.0
FlowJo	FlowJo, LLC (Ashland, OR, USA)	Version 10.10.0
GraphPad Prism	GraphPad Software (Boston, MA, USA)	Version 9.4.1
ImageJ	National Institutes of Health (Bethesda, MD, USA)	Version 1.53k
Inkscape	The Inkscape Project (N/A)	Version 1.4
Leica LAS AF Lite	Leica Microsystems CMS GmbH (Mannheim, Germany)	Version 3.3.10134.0
Microsoft Office 365	Microsoft Corporation (Redmond, WA, USA)	Version 16.90

2.6 Experimental setup

The protocol given hereinafter refers to the PBMC isolated from 72 ml of whole blood, corresponding to 8 EDTA-monovettes seizing 9 ml of volume. About 0.5 to 2.5 x 10^6 PBMC are comprised within 1 ml whole blood [46, 99], whereupon monocytes constitute 10 to 20 % of these cells [68]. Depending on the number of MdM needed for a particular repeat of the study, either 72 ml of whole blood were used in total or the volume was doubled or tripled, respectively.

2.6.1 Isolation of PBMC

Density gradient centrifugation was conducted for the isolation of PBMC from whole blood. To this end, 72 ml of whole blood were equally apportioned among 4 50 ml tubes transferring 18 ml of blood into each 50 ml tube. We then added 18 ml dilution buffer for PBMC isolation (+37° C) ***(Chap. 2.2.1)*** to all of the 50 ml tubes, diluting the whole blood 1:2, and mixed the suspensions by inverting the tubes. Another 8 50 ml tubes were then filled with 18 ml Lymphocyte Separation Medium ***(Chap. 2.2.1)*** at room temperature each and the blood suspensions were evenly distributed, carefully layering 18 ml diluted blood onto each 18 ml Lymphocyte Separation Medium using a Peleus ball and a serological pipette. Centrifugation was then conducted for 30 minutes at +21° C at 400 x g without acceleration and brake, respectively, to allow for the separation of blood cells and plasm. Following, plasm was carefully removed and discarded to expose the fraction of PBMC. We then collected the latter cells combining the PBMC from 2 50 ml tubes into a new 50 ml tube. These 4 new 50 ml tubes were then filled up with wash buffer for PBMC isolation (+37° C) ***(Chap. 2.2.1)*** to a total volume of 40 ml each and centrifuged for 10 minutes at +21° C at 300 x g with acceleration and brake for washing. The supernatant was discarded. To achieve depletion of contaminating erythrocytes, the PBMC were then resuspended in 40 ml of erythrocyte lysis buffer ***(Chap. 2.2.1)*** for each 50 ml tube and the cells were incubated for 5 minutes at room temperature. Adjacently, the cells were centrifuged for 10 minutes at +21° C at 400 x g with acceleration and brake and the supernatant was discarded. For each 50 ml tube, we resuspended the PBMC in 10 ml wash buffer for PBMC isolation and subsequently transferred all PBMC into one of the 50 ml tubes. This particular 50 ml tube was then filled up with wash buffer for PBMC isolation to 50 ml of total volume and the number of PBMC was counted using a hemocytometer. Terminally, the PBMC were centrifuged for 10 minutes at +21° C at 400 x g with acceleration and brake and the supernatant was discarded.

2.6.2 Isolation of monocytes

Following, monocytes were separated from lymphocytes by means of adhesion on plastic surfaces. For this purpose, we resuspended the isolated PBMC in 45 ml of prewarmed Monocyte Attachment Medium (+37° C) ***(Chap. 2.2.1)*** and subsequently distributed the cells equally to 3 T75-flasks. Depending on the number of isolated PBMC,

each T75-flask contained an approximate number of 30 x 10^6 to 40 x 10^6 cells suspended in 15 ml Monocyte Attachment Medium, respectively. We then incubated the PBMC for 90 minutes at +37° C and 5 % CO_2 to allow for the monocytes to adhere. After the incubation period, the supernatant was discarded and the adherent monocytes were carefully washed once with 15 ml pre-warmed complete medium (+37° C) ***(Chap. 2.2.1)*** per T75-flask, gently tilting and tapping the T75-flasks, in order to remove the non-adherent and loosely adherent fraction of PBMC.

2.6.3 Differentiation of monocytes to MdM

The adherent monocytes were then differentiated to MdM via incubation in 15 ml of fresh complete medium supplemented with the growth factor M-CSF ***(Chap. 2.2.6)*** at a concentration of 10 ng/ml for 6 days altogether. Incubation was done at +37° C and 5 % CO_2 with exchange of the medium every other day. As a lot of initially adhering cells detached during the first days of incubation, 15 ml of complete medium supplemented with 10 ng/ml M-CSF was used on day 1 and day 3 of differentiation and volume was reduced to 12 ml complete medium supplemented with 10 ng/ml M-CSF on day 5 of differentiation.

2.6.4 Polarization of MdM

Polarization of the MdM was conducted following to their differentiation to induce either M1- or M2-phenotype. For each phenotype, cells within 1 T75-flasks were used. The M0-phenotype was obtained through incubation in 12 ml of complete medium without any polarizing agents. M1-MdM were induced through incubation in 12 ml of complete medium supplemented with 50 ng/ml IFNγ **(*Chap. 2.2.2*)** and 10 ng/ml LPS ***(Chap. 2.2.5)***. For the M2-polarization, the MdM were incubated in 12 ml complete medium containing 20 ng/ml IL4 ***(Chap. 2.2.3)*** and 20 ng/ml IL13 ***(Chap. 2.2.4)***. Incubation was done for 2 days at +37° C and 5 % CO_2.

In order to characterize the resultant MdM, following to their polarization, the cells were assessed using light microscopy, ELISA, flow cytometry as well as CLSM as delineated below.

2.6.5 Characterization of polarized MdM using light microscopy

To begin with, polarized MdM were regularly assessed light microscopically regarding their morphology. For this purpose, during their differentiation as well as their polarization, MdM were observed and images were taken at a 10X and 20X magnification.

2.6.6 Characterization of polarized MdM using ELISA

Polarized MdM were then characterized regarding their secretion of cytokines using ELISA. To this, the concentration of TNFα was determined as a parameter for M1-polarization whereas the concentration of CCL-13 and CCL-17 was investigated as parameter for M2-polarization.

On day 2 of polarization, we collected the supernatant of M0-, M1- or M2-polarized cells, respectively, each in a 15 ml tube and centrifuged at 300 x g for 5 minutes at +21° C to seclude suspended cells and debris. Supernatant was then aliquoted into 1.5 ml protein low-binding tubes and either ELISA was directly performed or the samples were kept at -20° C until their future measurement. Repeated freezing and thawing of the samples was avoided. ELISA kits were chosen contingent on their sensitivity and their detection limit. For each of the latter cytokines, ELISA was conducted according to the manufacturer's specific instructions and all reagents were allowed to reach room temperature prior to their utilization. Standards, blanks as well as samples were investigated as doublets. We firstly identified the proper dilution of the diverse samples to be tested *(data not shown)*.

For the TNFα ELISA, the Invitrogen Human TNFα ELISA Kit was utilized and the M1-MdM samples were diluted 1:10 using complete medium. To begin with, standards were prepared according to the manufacturer's specific instructions and sole standard diluent buffer for TNFα ELISA ***(Chap. 2.2.1)*** was used as a blank ***(Tab. 9)***. Following, 50 µl of incubation buffer for TNFα ELISA ***(Chap. 2.2.1)*** for standards as well as blanks and 50 µl of standard diluent buffer for TNFα ELISA for samples, respectively, were laid to each well. We then added 100 µl of standard, blank or sample to the appropriate well and carefully tapped the plate for the purpose of mixing. The plate was incubated for 2 hours at room temperature to allow the antigens to bind and subsequently the wells were washed 4 times with wash buffer for TNFα ELISA ***(Chap. 2.2.1)*** and carefully dried. To each well 100 µl of biotin conjugate for TNFα ELISA ***(Chap. 2.2.1)*** was adjoined and

the plate was incubated for 1 hour at room temperature. Following to another 4 times of washing with wash buffer for TNFα and accurate drying, we added 100 µl of streptavidin-HRP solution for TNFα ELISA ***(Chap. 2.2.1)*** into each well and incubated the plate for 30 minutes at room temperature. The wells were washed for 4 times with wash buffer for TNFα ELISA again and after drying 100 µl of stabilized chromogen for TNFα ELISA ***(Chap. 2.2.1)*** was then added to each well. Incubation was done for 30 minutes at room temperature under protection form light. After this incubation period, we added 100 µl of stop solution for TNFα ELISA ***(Chap. 2.2.1)*** to each well, carefully tapped the plate as to mixing and read the absorbance as stated below.

Table 9: TNFα standard dilution scheme for TNFα ELISA

	Volume of diluent [µl]	Volume and source of TNFα [µl]	Final TNFα concentration [pg/ml]
A	300	300 of reconstituted standard	1000
B	300	300 of A	500
C	300	300 of B	250
D	300	300 of C	125
E	300	300 of D	62.5
F	300	300 of E	31.2
G	300	300 of G	15.6
H	300	-	0 = blank

Concerning the CCL13 ELISA, the Invitrogen Human CCL13 (MCP-4) ELISA Kit was used and a 1:12 fold dilution using assay diluent B for CCL13 ELISA ***(Chap. 2.2.1)*** was required for the M2-MdM samples. Again, standards were diluted according to the manufacturer's specific instructions at first and sole assay diluent B for CCL13 ELISA was used as a blank ***(Tab. 10)***. Next, 100 µl of standard, blank or sample were adjoined to the appropriate well and the plate was incubated for 2,5 hours at room temperature with gentle shaking to allow the antigens to bind. Subsequently, the solution within the wells was discarded and the wells were washed 4 times with wash buffer for CCL13 ELISA ***(Chap. 2.2.1)***. After accurate drying, 100 µl of biotin conjugate for CCL13 ELISA ***(Chap. 2.2.1)*** was added and the plate was incubated for 1 hour at room temperature with gentle shaking. Again, the wells were washed for 4 times with wash buffer for

CCL13 ELISA with careful drying after all. We then adjoined 100 µl of streptavidin-HRP solution 1X for CCL13 ELISA ***(Chap. 2.2.1)*** to each well and incubation was done for 45 minutes at room temperature with gentle shaking. The solution was discarded and the wells were washed 4 times with wash buffer for CCL13 ELISA and thoroughly dried. Adjacently, 100 µl of stabilized chromogen for CCL13 ELISA ***(Chap. 2.2.1)*** was then added to each well and the plate was incubated for 30 minutes at room temperature under protection from light with gentle shaking. Eventually, 50 µl of stop solution for CCL13 ELISA ***(Chap. 2.2.1)*** was adjoined and the plate was carefully tapped as to mixing. Absorbance was read as delineated below.

Table 10: CCL13 standard dilution scheme for CCL13 ELISA

	Volume of diluent [µl]	**Volume and source of CCL13 [µl]**	**Final CCL13 concentration [pg/ml]**
A	998	2 of reconstituted standard	200
B	300	300 of A	100
C	300	300 of B	50
D	300	300 of C	25
E	300	300 of D	12.5
F	300	300 of E	6.25
G	300	300 of G	3.13
H	300	-	0 = blank

As to the CCL17 ELISA, the Invitrogen Human CCL17 (TARC) ELISA Kit was utilized and no dilution was required. Initially, we prepared the standards according to the manufacturer's specific instructions and sole assay diluent C for CCL17 ELISA ***(Chap. 2.2.1)*** was used as a blank ***(Tab. 11)***. Then, 100 µl of standard, blank or sample was pipetted to the appropriate well and the plate was incubated for 2,5 hours at room temperature with gentle shaking to allow the antigens to bind. Following, we discarded the solution within the wells and washed the wells 4 times with wash buffer for CCL17 ELISA ***(Chap. 2.2.1)***. Subsequent to accurate drying, 100 µl of biotin conjugate for CCL17 ELISA ***(Chap. 2.2.1)*** was adjoined and the plate was incubated for 1 hour at room temperature with gentle shaking. The wells were washed for 4 times with wash buffer for CCL17 ELISA and carefully dried. We then added 100 µl of streptavidin-HRP solution for

CCL17 ELISA ***(Chap. 2.2.1)*** to each well. After incubation for 45 minutes at room temperature with gentle shaking, the supernatant was discarded and the wells were washed 4 times with wash buffer for CCL17 ELISA as well as thoroughly dried. Following, 100 µl of stabilized chromogen for CCL17 ELISA ***(Chap. 2.2.1)*** was added to each well and the plate was incubated for another 30 minutes at room temperature under protection from light with gentle shaking. Finally, we added 50 µl of stop solution for CCL17 ELISA ***(Chap. 2.2.1)*** to each well and the plate was carefully tapped as to mixing. Absorbance was read as delineated below.

Table 11: CCL17 standard dilution scheme for CCL17 ELISA

	Volume of diluent [µl]	**Volume and source of CCL17 [µl]**	**Final CCL17 concentration [pg/ml]**
A	570	30 of reconstituted standard	2500
B	300	200 of A	1000
C	300	200 of B	400
D	300	200 of C	160
E	300	200 of D	64
F	300	200 of E	25.6
G	300	200 of G	10.2
H	300	-	0 = blank

Immediately after appending the stop solution to each well of the plate, the absorbance was read at 450 nm. Adjacently, the standard curve was generated and the concentration of secreted TNFα, CCL13 or CCL17, respectively, was calculated subject to the correspondent curve according to the manufacturers' specific instructions. In case of prior sample dilution, calculated concentration values were then multiplied by their appropriate dilution factor. Lastly, normalization of the concentration of secreted TNFα, CCL13 or CCL17, each, to the number of cells within the corresponding T-75 flask was done and concentrations are presented relating to $1x10^6$ cells.

2.6.7 Characterization of MdM using flow cytometry

We furthermore assessed the polarized MdM as to their expression of surface and intracellular markers by means of flow cytometry. In this regard, the expression of CD14 and CD68 as MΦ-pan-markers was investigated, whereas CD80, CD86 and CCR7 were employed as markers for M1-polarization and the expression of CD1A, CD163, CD206, CD209 and Arg1 was tested as marker for M2-polarization.

On day 2 of polarization, the adherent cells were harvested in the first step. Therefore, after the culture medium from of each T75-flask had been collected for analysis of cytokine secretion (***Chap. 2.6.6***), the adherent MdM were washed once with 15 ml PBS per T75-flask. Following, we added 10 ml of pre-warmed Accutase (+37° C) to each T75-flask and incubated the cells for 30 minutes at +37° C and 5 % CO_2. To facilitate detachment, flasks were additionally tapped every 10 minutes. After the incubation period, floating cells were gathered and transferred into a separate 50 ml tube for each T75-flask. We then harvested still adherent MdM by adding 10 ml of PBS to each flask, mechanically scraping and then collecting the cells into their corresponding 50 ml tube. The detached MdM were centrifuged at 300 x g for 10 minutes at +21° C and the supernatant was discarded. We resuspended the cell pellets in 5 ml of complete medium for each 50 ml tube. Cell number as well as viability was assessed using the trypan blue exclusion method and a hemocytometer. For each sample 100 000 to 150 000 cells were then aliquoted into round bottom fluorescence activated cell sorting (FACS) tubes, for the unstained controls 200 000 to 300 000 cells were used. We added 2 ml of pre-chilled FACS buffer (+4° C) ***(Chap. 2.2.1)*** to the samples, centrifuged the tubes for 5 minutes at 300 x g at +21° C and discarded the supernatant. Following, the MdM of each sample were either stained at their surface or intracellularly. Single staining was done using the fluorochrome labelled antibodies shown in ***Tab. 12***.

Table 12: Antibodies used for flow cytometry

Marker	Location	Fluorochrome	Excitation wave length [nm]	Emission wave length [nm]	Clone	Amount [µl]/1-3 x 10^4 cells
CD14	cell surface	Alexa Fluor 468	650	671	M5E2	5
CD68	intracellular	Alexa Fluor 468	650	671	eBioY1/ 82A	5
CD80	cell surface	Brilliant Violet 421	405	421	2D10	5
CD86	cell surface	PE	488-561	578	IT2.2	5

CCR7 (CD197)	cell surface	PE	488-561	578	3D12	5
CD1A	cell surface	PE	488-561	578	SK9	5
CD163	cell surface	FITC	498	517	GHI/61	5
CD206	cell surface	PE	488-561	576	19.2	5
CD209	cell surface	FITC	498	517	DCN46	5
Arg1	intracellular	Per-CP	482	710	A1exF5	1.25

For cell surface staining, the cells of each FACS tube were resuspended in 102.5 µl of pre-chilled Fc-blocking buffer for FACS (+4° C) ***(Chap. 2.2.1)*** containing 2.5 µl of Fc-block and incubated for 10 minutes on ice. Subsequently, cells were centrifuged for 5 minutes at 300 x g at +21° C, supernatant was discarded and cells were washed once using the aforesaid adjustment for centrifugation and 2 ml of pre-chilled FACS buffer (+4° C) each for all samples. The cells of each FACS tube were then resuspended in 100 µl of pre-chilled FACS buffer (+4° C). The appropriate amount of fluorescence-labelled antibody, as listed in ***Tab. 12***, was added to the corresponding tube and un-stained samples were used as controls. We then incubated the samples for 30 minutes on ice in the dark. Afterwards, cells were centrifuged for 5 minutes at 300 x g at +21° C, supernatant was discarded and cells were washed twice using the aforesaid adjust-ment for centrifugation and 2 ml of pre-chilled FACS buffer (+4° C) each for all samples. For fixation, the samples were then resuspended in 250 µl of ice-cold BD Cytofix and incubated for 15 minutes on ice in the dark. Afterwards, 2 ml of pre-chilled FACS buffer (+4° C) was added to each sample and centrifugation for 5 minutes at 300 x g at +21° C was done. Supernatant was discarded and the cells were washed once more with 2 ml of FACS buffer and the latter adjustment for centrifugation. We then resuspended the MdM in 500 µl of pre-chilled FACS buffer (+4° C) for measurement.

As to intracellular staining, cells were fixed and permeabilized in the first step. For this purpose, MdM were resuspended in 250 µl ice-cold BD Cytofix and were incubated for 15 minutes on ice in the dark. Following, we added 2 ml of pre-chilled FACS buffer (+4° C) to each sample and centrifugation for 5 minutes at 300 x g at +21° C was done. The supernatant was discarded and the cells were washed with another 2 ml of pre-chilled FACS buffer (+4° C) with the aforesaid adjustment for centrifugation. The cells were then resuspended in 50 µl of ice-cold FACS buffer, 450 µl of 90 % ice-cold meth-anol was added to every sample and incubation for 10 minutes on ice in the dark was done. Adjacently, we adjoined 2 ml of ice-cold FACS buffer and centrifuged the sam-ples for 5 minutes at 300 x g at +21° C. The cells of each FACS tube were resuspended

in 102.5 µl of pre-chilled FACS Fc-blocking buffer (+4° C) containing 2.5 µl of Fc-block and incubated for 10 minutes on ice. Subsequently, cells were centrifuged for 5 minutes at 300 x g at +21° C, supernatant was discarded and cells were washed once using the aforesaid adjustment for centrifugation and 2 ml of pre-chilled FACS buffer (+4° C) each for all samples. Supernatant was discarded and cells were resuspended in 100 µl of ice-cold FACS buffer each for staining. The appropriate amount of fluorescence-labelled antibody either against CD68 or against Arg1, as listed in ***Tab. 12***, was added to the corresponding tube. The cells were incubated for 30 minutes on ice in the dark and afterwards centrifuged for 5 minutes at 300 x g at +21° C to discard the supernatant. 2 times of washing each with 2 ml of FACS buffer per sample and an adjustment of centrifugation with 5 minutes at 300 x g at +21° C was done. After discarding the supernatant, every sample was resuspended in 500 µl of ice-cold FACS buffer for measurement.

The stained samples were either directly analyzed by means of FACS or kept at +4° C in the dark for up to 24 hours until their future measurement. Flow cytometric measurements were conducted using FACSCalibur. As a start, the appropriate cell populations were identified assessing forward scatter and side scatter for M0-, M1- and M2-MdM, respectively. Subsequently, for each specimen, minimum 10 000 events were recorded and antibody-mediated fluorescence was contrasted with unstained controls. The acquired data were processed using FlowJo software and are presented as marker expression [%] for all of the markers tested and as mean fluorescence intensity (MFI) concerning CD206.

2.6.8 Characterization of MdM using CLSM

The protocol concerning phalloidin and antibody staining as well as imaging using CLSM was established by Hannah Conrady. Staining and imaging was done in collaboration with Hannah Conrady.

Lastly, the polarized MdM were examined using CLSM in order to confirm the characterization implemented afore. For this purpose, cell morphology was evaluated via cytoskeleton staining using phalloidin and surface marker expression of CCR7 and CD209 was tested using specific primary and fluorescently labelled secondary

antibodies. CCR7 as well as CD209 were chosen based on our preliminary studies *(data not shown)* as well as contingent to their specificity as disclosed within the flow cytometric investigations ***(Chap. 3.3)***. Concomitant with the cytoskeleton or surface marker staining, deep red anthraquinone (DRAQ) 5 was employed for staining of the nuclei. As CLSM imaging could not be conducted using tissue culture flasks, MdM were collected following to their differentiation and were seeded onto tissue culture plastic coverslips as to their polarization.

To this, the coverslips were transferred each into a well of a non-treated 24-well plate. MdM were then harvested from a T75-flask on day 6 of differentiation. Supernatant was discarded and the adherent MdM were washed once with 15 ml PBS at room temperature. Following, 10 ml of pre-warmed Accutase (+37° C) was added to the T75-flask and the cells were incubated for 30 minutes at +37° C and 5 % CO_2. In order to facilitate the detachment of the MdM, we additionally tapped the T75-flask every 10 minutes. Subsequent to the incubation, floating cells were gathered and transferred into a 50 ml tube. MdM that were still adherent to the T75-flask were then harvested by adding 10 ml of PBS to the flask, mechanically scraping and eventually collecting the cells into the 50 ml tube. We centrifuged the detached MdM at 300 x g for 10 minutes at +21° C and discarded the supernatant. The cell pellet was resuspended in 50 ml of pre-warmed complete medium (+37° C) and cell number as well as viability was determined using the trypan blue exclusion method and a Neubauer chamber. Following to another centrifugation at 300 x g for 10 minutes at +21° C, a cell suspension with 160 000 MdM per 1 ml of pre-warmed complete medium (+37° C) was prepared. To each coverslip, we then added 1 ml of the latter cell suspension. The cell suspension was pipetted directly onto the coverslips to direct cellular interaction with the surface. In order to obtain M0-MdM, cells were left incubating in complete medium without any polarizing agents. M1-polarization was induced via addition of IFNγ at 50 ng/ml and LPS at 10 ng/ml. For the M2-phenotype, MdM were treated with 20 ng/ml IL4 and 20 ng/ml IL13. All MdM were incubated for 2 days at +37° C and 5 % CO_2.

For the evaluation by means of CLSM, cells were fixed immediately after their polarization and staining as well as imaging were followed up within 1 to 6 weeks thereafter.

On day 2 of polarization, we gently washed the adherent MdM twice with 800 µl PBS per coverslip. Subsequently, fixation buffer for CLSM ***(Chap. 2.2.1)*** was added to the cells, using 300 µl of 3 % PFA in PBS for the coverslips. The MdM were incubated for

20 minutes at room temperature. Fixation buffer for CLSM was then discarded and all coverslips were washed 3 times in 400 µl PBS. We either stained the adherent cells immediately after fixation or kept the coverslips each in 1 ml of storage buffer for CLSM containing PBS + 1 % P/S ***(Chap. 2.2.1)*** at +4° C with the 24-well plate being sealed with parafilm until their future staining. After storage, cells were washed twice with 800 µl PBS per coverslip.

For cytoskeleton staining with phalloidin, the MdM were permeabilized with 400 µl CLSM permeabilization buffer ***(Chap. 2.2.1)*** containing 0.2 % Triton 100X in PBS for 10 minutes. The supernatant was discarded and cells were gently washed in 400 µl PBS 3 times. To prevent unspecific binding, the MdM were then incubated with 500 µl staining buffer for CLSM ***(Chap. 2.2.1)*** each for 30 minutes at room temperature. We discarded the staining buffer for CLSM and gently washed the cells twice in 500 µl PBS. Phalloidin was diluted in PBS + 1 % BSA to a final concentration of 5 µg/ml and coverslips were incubated with 300 µl of the latter solution. The samples were incubated for 40 minutes at room temperature in the dark. Following, the supernatant was discarded and the coverslips were gently washed 3 times with 400 µl PBS with an incubation period of 3 minutes for each repeat of washing. Eventually, counterstaining of the nuclei was done with DRAQ5. For this purpose, DRAQ5 was diluted in PBS to a final concentration of 10 µM and the cells were washed once with 400 µl of PBS per coverslip. We then added 300 µl of diluted DRAQ5 to the coverslips. The MdM were incubated for 15 minutes at room temperature in the dark. The supernatant was then discarded and the coverslips were gently washed in 400 µl of PBS once. We completely removed the PBS and the coverslips were transferred to microscope slides each. Mounting medium was added using 7 drops for the coverslips. After 5 minutes of incubation at room temperature in the dark, the coverslips were covered with cover glasses and let drying for 1 hour. Subsequently, we sealed the edges of the cover glasses with clear nail polish and stored the stained coverslips at +4° C in the dark until their future imaging.

For staining of the cell surface markers CCR7 and CD209, the MdM were incubated with 500 µl of staining buffer for CLSM for 30 minutes at room temperature to prevent unspecific binding. We then discarded the staining buffer for CLSM and added primary antibodies against either CCR7 or CD209 diluted in staining buffer for CLSM performing either single- or co-staining. The primary antibody concentrations as well as the

volumes used are listed in ***Tab. 13***. A total volume of 300 µl was added to the coverslips. The adherent cells were incubated for 60 minutes at room temperature.

Table 13: Concentration and volume of primary antibodies used for CLSM

Primary antibody	**Stock concentration**	**Final concentration**	**Volume of antibody per ml [ml]**	**Volume of CLSM staining buffer per ml [ml]**	**Volume of antibody per ml [ml]**	**Volume of CLSM staining buffer per ml [ml]**
			Single staining		Co-staining	
Mouse-anti-human CCR7 IgG	0.5 mg/ml	10 µg/ml	20 µl	980 µl	20 µl	975.5 µl
Rabbit-anti-human CD209 IgG	-	1:400 dilution	2.5 µl	997.5 µl	2.5 µl	

Following, the supernatant was discarded and the discs were gently washed 3 times in 400 µl of wash buffer for CLSM. We added fluorochrome-labelled secondary antibodies diluted in staining buffer for CLSM either doing single- or co-staining. The antibody concentrations as well as the volumes used are listed in ***Tab. 14***. Incubation was done for 60 minutes at room temperature in the dark.

Table 14: Concentration and volume of secondary antibodies used for CLSM

Secondary antibody	**Stock concentration**	**Final concentration**	**Volume of antibody**	**Volume of CLSM staining buffer**	**Volume of antibody**	**Volume of CLSM staining buffer**
			Single staining		Co-staining	
Goat- anti-mouse IgG Alexa488	2 mg/ml	5 µg/ml	2.5 µl	997.5 µl	2.5 µl	995 µl
Goat anti-rabbit IgG Cy3	-	1:200 dilution	2.5 µl	997.5 µl	2.5 µl	
Goat anti-rabbit IgG Alexa488	-	1:200 dilution	2.5 µl	997.5 µl	-	-

Again, the supernatant was discarded and the discs were gently washed 3 times with 400 µl of wash buffer for CLSM with an incubation period of 3 minutes for each repeat of washing. Eventually, counterstaining of the nuclei was done with DRAQ5 as

described afore ***(Chap 2.6.8)***. The coverslips were then transferred to glass slides each and prepared as aforementioned ***(Chap 2.6.8)*** using mounting medium and cover glasses. Storage was done at +4° C in the dark until their future imaging.

The stained samples were imaged using Leica TCS SP5 at a magnification of 25X to provide for an overview, whereas either a 63X magnification or 2.5X zoom to the 25X magnification was obtained for detailed assessment of morphology and marker expression. Images were acquired with a photomultiplier using CLSM with an argon laser (488 nm), diode pumped solid state (DPSS) laser (561 nm) and helium-neon (HeNe) laser (633 nm). At this point, we did not determine fluorescence intensity, as quantity of CCR7 and CD209 was measured before using flow cytometry ***(Chap. 2.6.7, Chap. 3.3)*** resulting in more precise results than deploying semi-quantitative CLSM analysis.

Following to successfully isolating monocytes, differentiating these cells towards polarized MdM as well as effectively and reliably characterizing the resultant cells ***(Chap. 3.1, Chap. 3.2, Chap. 3.3, Chap. 3.4)*** as delineated afore ***(Chap. 2.61, Chap. 2.6.2, Chap. 2.6.3, Chap. 2.6.4, Chap. 2.6.5, Chap 2.6.6, Chap. 2.6.7, Chap. 2.6.8)***, the established protocol was to be implemented investigating potential immunomodulatory effects of diverse titanium biomaterial surfaces.

2.6.9 Cultivation and polarization of MdM on titanium surfaces

As to the implementation, differentiated MdM were cultivated and polarized on different titanium surfaces to test for immunomodulatory influences. Ti-SLA discs as well as Ti-Ana discs were used as titanium modifications and Ti-ma discs constituted the control surfaces. Moreover, we deployed tissue culture plastic coverslips as further control surfaces to the examined titanium discs as coverslips are optimally adjusted to cell culture and allow for most natural cell behavior and growth *in vitro*.

Straight beforehand the cultivation of the MdM on the titanium surfaces, the Ti-ma-, Ti-SLA- as well as Ti-Ana-discs were sterilized in 70 % ethanol for 30 minutes. Adjacently, the discs were left to dry for 30 to 60 minutes and then transferred each into a well of a non-treated 24-well plate. Furthermore, coverslips were also allotted each.

For the cultivation and polarization of MdM on titanium surfaces, the PBMC were isolated by means of density gradient centrifugation and monocytes were adhered and differentiated towards MdM as described before ***(Chap. 2.6.1***, ***Chap. 2.6.2***, ***Chap. 2.6.3)***. On day 6 of differentiation, we harvested MdM from the T75-flasks as abovementioned ***(Chap. 2.6.8)*** using Accutase and mechanical scraping. Cell number and viability was assessed deploying the trypan blue exclusion method as well as a Neubauer chamber and a cell suspension with 160 000 MdM per 1 ml of pre-warmed complete medium (+37° C) was prepared ***(Chap.2.6.8)***. To each well of the 24-well plates containing either discs or coverslips, we then added 1 ml of the latter cell suspension. The cell suspension was pipetted directly onto the discs and coverslips to direct cellular interaction with the surface. In order to obtain M0-polarization, cells were left incubating in complete medium without any polarizing agents. M1-MdM again was induced through addition of IFNγ at 50 ng/ml and LPS at 10 ng/ml. For the M2-phenotype, MdM were treated with 20 ng/ml IL4 as well as 20 ng/ml IL13. All MdM were incubated for 2 days at +37° C and 5 % CO_2.

2.6.10 Evaluation of immunomodulatory effects using CCK8 cell proliferation assay

To preclude direct adverse effects of the titanium surfaces regarding metabolism and survival of the cultivated MdM, metabolic activity as a surrogate of viability, cell number and proliferation was assessed using CCK8 cell proliferation assay. The assay was done according to the manufacturer's specific instructions.

To this end, on day 2 of polarization, supernatant was removed and collected for further analysis using ELISA and BCA protein assay as described in ***Chap. 2.6.11***. We then gently washed the adherent MdM once with 1000 µl PBS at room temperature per disc. In order to obviate falsification due to MdM adhering to the surface of the wells but not contacting their respective disc, all discs and coverslips were each transferred to a well of a new 24-well plate thereafter. Subsequently, 500 µl of pre-warmed complete medium (+37° C) and 50 µl of CCK8 reagent was mixed and added to each well. The plates were incubated for 1 hour at 37° C under protection from light.

For the purpose of analysis, 100 µl of supernatant from each well was transferred into a separate well of a 96-well plate using doublets for each sample. The absorbance was read at 450 nm. As to the subsequent analysis, CCK8-mediated optical density

was normalized to a surface area of 10 mm^2 for each disc. Following, transformation was done and the optical density of the M0-MdM cultivated on coverslips was defined as reference. Results are presented as relative proliferation [%].

2.6.11 Evaluation of immunomodulatory effects using ELISA and BCA protein assay

As to the evaluation of potential immunomodulatory effects of the different titanium surfaces, polarized MdM were investigated regarding their secretion of cytokines using ELISA. Since the previous characterization ***(Chap. 2.6.6, Chap. 3.2)*** accented secretion of TNFα as a marker for M1-polarization and the secretion of CCL-13 as a marker for M2-phenotype, the two latter cytokines were selected for further assessment.

On day 2 of polarization, supernatant of M0-, M1- or M2-polarized MdM, respectively, was collected into a 15 ml tube and was centrifuged at 300 x g for 5 minutes at +21° C for separation of suspended cells and debris. We then aliquoted the supernatant into 1.5 ml protein low-binding tubes and either immediately conducted ELISA and BCA protein assay or kept the samples at -20° C until their future measurement. Repeated freezing and thawing of the samples was avoided.

ELISA for measurement of both, TNFα as well as CCL-13, was done according to the manufacturer's specific instructions as described above ***(Chap. 2.6.6)***. Following, the concentration of the secreted cytokines was calculated by means of the standard curve according to the manufacturer's specific instructions. As the adhered MdM on the one hand could hardly be removed from the discs and on the other hand were needed for continuative studies, the concentration of secreted cytokines could not be normalized to the cell number as before ***(Chap. 2.6.6)***. Instead, we normalized the measured concentration to the concentration of total protein within the supernatant.

On this account, BCA protein assay was conducted as to the determination of the concentration of total protein using Thermo Fisher Scientific Pierce BCA protein assay kit. The assay was done according to the manufacturer's specific instructions. Standards, blanks as well as samples were tested as doublets. We firstly identified the proper dilution of the diverse samples to be tested *(data not shown)*.

All samples were diluted 1:5 using Ampuwa. To begin with, standards were prepared according to the manufacturer's specific instructions using Ampuwa and sole Ampuwa

was employed as a blank ***(Tab. 15)***. We then prepared the working reagent for BCA protein assay by mixing BCA reagent A and BCA reagent B at a ratio of 50:1 ***(Chap. 2.2.1)***. Next, 25 µl of standards, blanks or samples was pipetted into separate wells of a 96-well plate each and 200 µl of working reagent for BCA protein assay was added, respectively. The plate was mixed on a plate shaker for 30 seconds and incubated at +37° C under protection from light for 30 minutes. After equilibration to room temperature the absorbance was read at 550 nm. Adjacently, the standard curve was generated and the concentration of total protein was calculated subject to the curve according to the manufacturer's specific instructions. As to prior dilution, concentration values were then multiplied by their appropriate dilution factor. Lastly, normalization of the concentration of secreted TNFα or CCL13, each, to the concentration of total protein was done to express results as [pg/ml/mg of total protein].

Table 15: BSA standard dilution scheme for BCA protein assay

	Volume of diluent [µl]	Volume and source of BSA [µl]	Final BSA concentration [µg/ml]
A	0	300 of stock	2000
B	125	375 of stock	1500
C	325	325 of stock	1000
D	175	175 of vial B dilution	750
E	325	325 of vial C dilution	500
F	325	325 of vial E dilution	250
G	325	325 of vial F dilution	125
H	400	100 of vial G dilution	25
I	400	0	0 = blank

2.6.12 Evaluation of immunomodulatory effects using CLSM

The statistical analysis of CCR7 and CD209 fluorescence intensity was done by Leila Mohammadnejad. Statistical analysis was done, notwithstanding that data resulting from only 2 repeats concerning M1- and M2-MdM cultivated on coverslips, Ti-ma discs, Ti-SLA-discs and Ti-Ana discs was available.

As the MdM adherent to all titanium discs could hardly be detached and hence were not available in sufficient quantity *(data not shown)*, we forwent flow cytometrical analysis. Potential immunomodulatory effects on the cells were instead further investigated using CLSM. For this purpose, MdM were stained for CCR7 as a marker of M1-polarization as well as CD209 as a marker of M2-phenotype, since both markers were identified to be specific using flow cytometry as well as CLSM afore ***(Chap. 2.6.7, Chap. 2.6.8, Chap. 3.3, Chap. 3.4)***. As before, DRAQ5 was employed for staining of the nuclei and the cells' morphology was depicted using cytoskeleton staining with phalloidin, additionally. For the evaluation by means of CLSM, cells were fixed immediately after their polarization and staining as well as imaging were followed up within 1 to 6 weeks thereafter.

On day 2 of polarization, following to the CCK8 cell proliferation assay ***(Chap. 2.6.10)***, fixation was conducted as described afore ***(Chap. 2.6.8)*** using 300 µl of CLSM fixation buffer for the coverslips and 400 µl of CLSM fixation buffer for the titanium discs. We either stained the adherent cells immediately after fixation or kept the discs each in 1 ml of storage buffer containing PBS + 1 % P/S at +4° C until their future staining. After storage, cells were washed twice with 800 µl PBS per disc.

For cytoskeleton staining with phalloidin, the MdM were permeabilized as abovementioned ***(Chap. 2.6.8)***. The supernatant was discarded and cells were gently washed in 400 µl PBS 3 times. To prevent unspecific binding, the MdM were then incubated with CLSM staining buffer as delineated afore ***(Chap. 2.6.8)***. Phalloidin was then diluted as aforementioned and coverslips were incubated with 300 µl of the latter solution, while 400 µl of the phalloidin solution was used for the discs ***(Chap. 2.6.8)***. Subsequently, the supernatant was discarded and the discs and coverslips were washed 3 times with 400 µl PBS with an incubation period of 3 minutes for each repeat of washing. Counterstaining of the nuclei was then done with DRAQ5 as described afore ***(Chap. 2.6.8)*** using 300 µl of diluted DRAQ5 for the coverslips and 400 µl of diluted DRAQ5 for the titanium discs. The supernatant was then discarded and the discs were gently washed in 400 µl of PBS once. We completely removed the PBS and transferred the coverslips to glass slides each, whereas the titanium discs were separately put into a cell culture plate. Mounting medium was added using 7 drops for the coverslips and 1 drop for each titanium disc. After 5 minutes of incubation at room temperature in the dark, the cover slips and the titanium discs were covered with cover glasses and let drying for 1

hour. Subsequently, we sealed the edges of the cover glasses with clear nail polish and stored the stained coverslips and titanium discs at +4° C in the dark until their future imaging.

For staining of the cell surface markers CCR7 and CD209, the MdM were incubated with CLSM staining buffer for 30 minutes as noted before ***(Chap. 2.6.8)*** to prevent unspecific binding. We then discarded the CLSM staining buffer and added primary antibodies against CCR7 and CD209 diluted in staining buffer for CLSM as aforementioned ***(Chap. 2.6.8)*** performing either single- or co-staining. The antibody concentrations as well as the volumes used are listed in ***Tab. 13***. A total volume of 300 µl was added to the coverslips and 400 µl were used for the titanium discs. Following, the supernatant was discarded and the discs were gently washed 3 times in 400 µl of wash buffer for CLSM. We added fluorochrome-labelled secondary antibodies diluted in staining buffer for CLSM either doing single- or co-staining as described afore ***(Chap. 2.6.8)***. The antibody concentrations as well as the volumes used are listed in ***Tab. 14***. Again, the supernatant was discarded and the discs were gently washed 3 times with 400 µl of wash buffer for CLSM with an incubation period of 3 minutes for each repeat of washing. Eventually, counterstaining of the nuclei was done with DRAQ5 as abovementioned ***(Chap. 2.6.8)***. using 300 µl of diluted DRAQ5 for the coverslips and 400 µl of diluted DRAQ5 for the titanium discs. The coverslips were then transferred to glass slides each, whereas the titanium discs were separately put into a cell culture plate and both were prepared as aforementioned ***(Chap 2.6.11)*** using mounting medium and cover glasses. Storage was done at +4° C in the dark until their future imaging.

The stained samples were imaged using Leica TCS SP5 at a magnification of 25X to provide for an overview, whereas either a 63X magnification or 2.5X zoom to the 25X magnification was obtained for detailed assessment of the morphology and the marker expression. Images were acquired with a photomultiplier using CLSM with an argon laser (488 nm), DPSS laser (561 nm) and HeNe laser (633 nm). Fluorescence intensity of CCR7 and CD209 was determined using ImageJ software. Hereunto, images were converted to 8-bit binary images, a threshold was set and the mean grey value of each image was determined. For each polarization state of the MdM as well as surface 3 images were analyzed at a time. Following, fluorescence intensity of either CCR7 or CD209 was normalized to DRAQ5 fluorescence intensity and means of the 3 images were calculated. Results are expressed as fluorescence intensity.

2.7 Statistics

All data are presented as mean ± standard error of the mean (SEM). Statistical analysis was performed using GraphPad Prism software. Data were first checked for outliers and normality was tested. As indicated in the figure legends, as to normally distributed data one-way analysis of variance (ANOVA) followed by Tukey's multiple test was exerted. In contrast, Friedman test and Dunn's multiple comparison test or Kruskal-Wallis test and Dunn's multiple comparison test were used for non-parametric paired or non-parametric unpaired data sets, respectively. n denotes the number of experimental repeats with different MdM specimens to ensure reproducibility. As different MdM specimens could react heterogeneously to experimental stimuli, we tested the same MdM specimens for control and experimental set up within one repeat. Statistical significance was defined as a p-value $p < 0.05$.

3 Results

The established protocol disclosed afore ***(Chap. 2.6.1, Chap. 2.6.2, Chap. 2.6.3, Chap. 2.6.4)*** allowed for a reliable as well as reproducible isolation of monocytes, their differentiation towards MdM as well as eventually the MdM polarization to the M1- and M2-phenotype. Regarding the PBMC isolation, 72 ml of whole blood resulted in a total of 106.4 x 10^6 ± 12.21 x 10^6 PBMC (n = 5). These cells in turn yielded 5.93 x 10^6 ± 0.62 x 10^6 MdM (n = 5) following to monocyte adhesion and MdM differentiation.

3.1 Morphologic characterization of MdM using light microscopy

Concerning the characterization of the resultant MdM, as a start, cells were regularly assessed using light microscopy and images were taken at 10X and 20X magnification. To this, monocytes were differentiated towards MdM using complete medium with 10 ng/ml M-CSF for 6 days. As illustrated in ***Fig. 9***, during their differentiation towards MdM, monocytes transitioned from a rather round conformation to a flattened, irregular and extended shape partly exhibiting elongation. Moreover, differentiation was marked by an increase in cell volume.

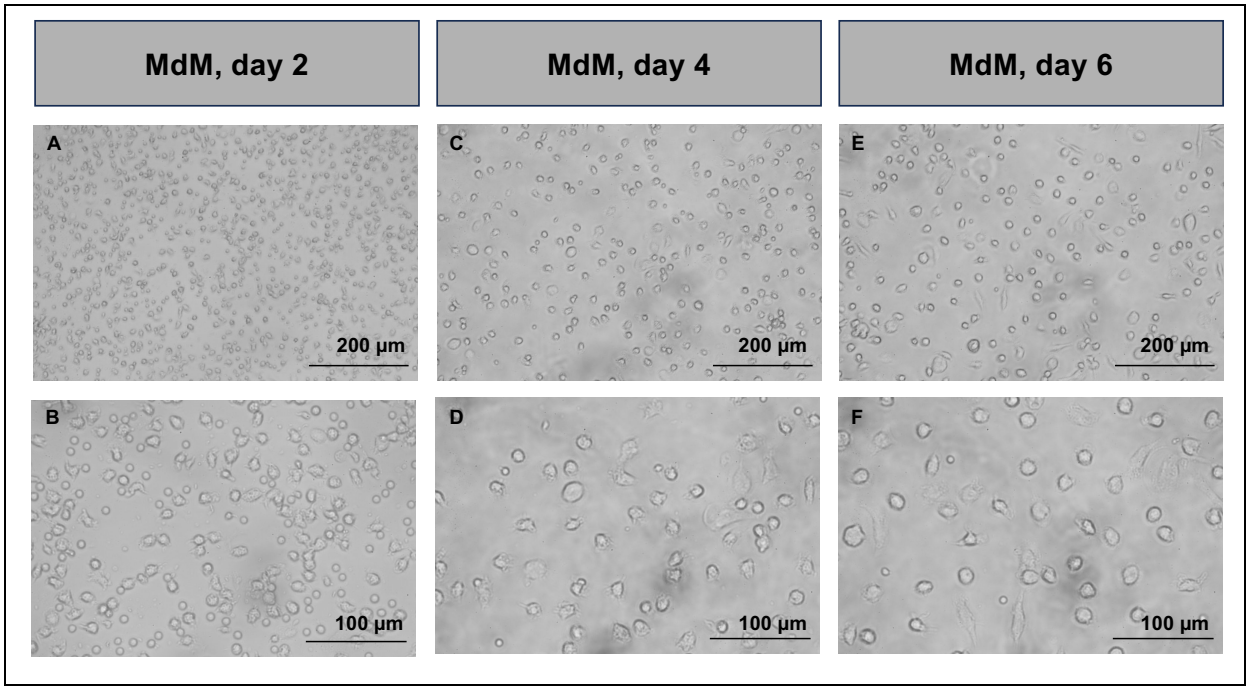

Figure 9: Morphology of monocytes during their differentiation towards MdM*. Representative monocyte and MdM phenotype using light microscopy during incubation with complete medium with 10*

ng/ml M-CSF to induce differentiation towards MdM. ***A*** *Monocytes/MdM on day 2 of differentiation, 10X magnification,* ***B*** *Monocytes/MdM on day 2 of differentiation, 20X magnification,* ***C*** *Monocytes/MdM on day 4 of differentiation, 10X magnification,* ***D*** *Monocytes/MdM on day 4 of differentiation, 20X magnification,* ***E*** *MdM on day 6 of differentiation, 10X magnification,* ***F*** *MdM on day 6 of differentiation, 20X magnification.*

Following to differentiation, treatment with complete medium without any polarizing agents, complete medium with 50 ng/ml IFNγ and complete medium with 10 ng/ml LPS or 20 ng/ml IL4 and 20 ng/ml IL13 for 2 days was undertaken to allow for polarization to the M0-, M1- or M2-phenotype, respectively. As shown in ***Fig. 10***, M0-MdM maintained an irregular and extended constitution with some cells being elongated. M1-MdM exhibited a round phenotype with only few cells being extended effectuating a rather consistent morphology. In contrast, M2-MdM showed distinct elongation as well as stellate-like branching as to most cells.

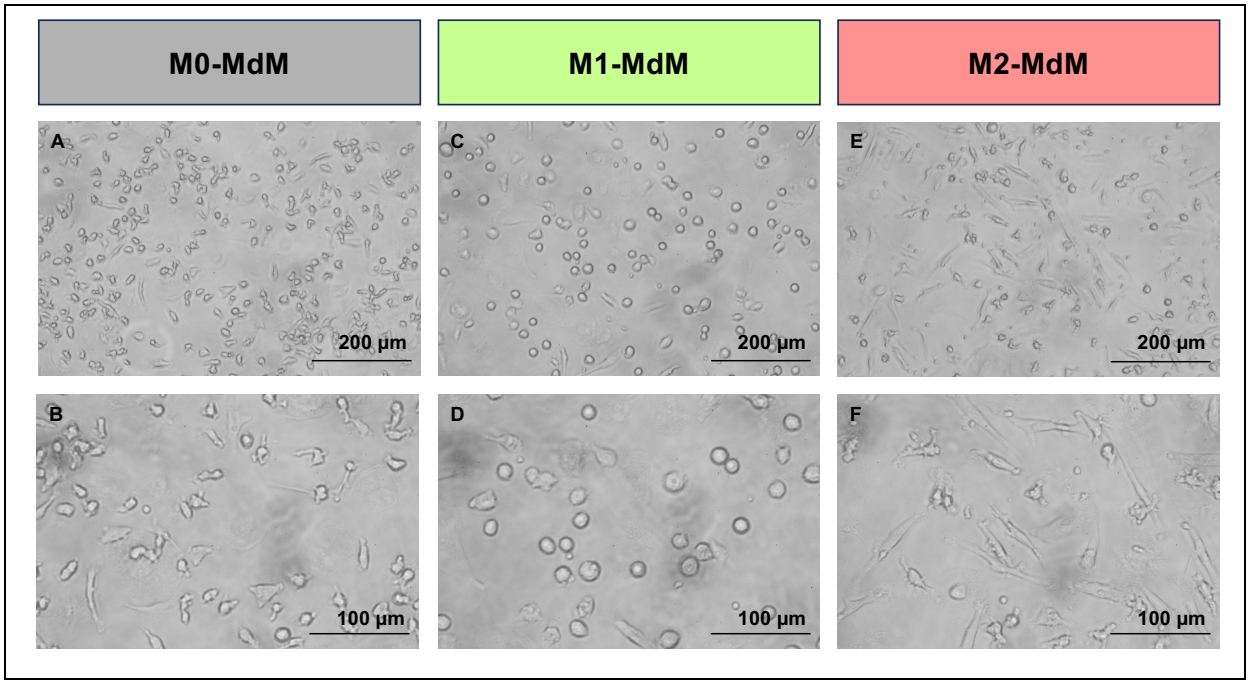

Figure 10: Morphology of M0-, M1- and M2-MdM*. Representative MdM phenotype using light microscopy following incubation with complete medium without addition of polarizing agents, complete medium with 50 ng/ml IFNγ and 10 ng/ml LPS or 20 ng/ml IL4 and 20 ng/ml IL13 for 2 days to induce M0-, M1- or M2-polarization, respectively.* ***A*** *M0-MdM, 10X magnification,* ***B*** *M0-MdM, 20X magnification,* ***C*** *M1-MdM, 10X magnification,* ***D*** *M1-MdM, 20X magnification,* ***E*** *M2-MdM, 10X magnification,* ***F*** *M2-MdM, 20X magnification.*

3.2 Characterization of MdM using ELISA

Moreover, M0-, M1- and M2-MdM were analyzed concerning their cytokine secretion by means of ELISA. On this, TNFα concentration in the cell culture supernatant was determined concerning M1-polarization, whereas secretion of CCL13 and CCL17 as markers of the M2-phenotype was evaluated.

3.2.1 Secretion of TNFα

Secretion of the cytokine TNFα is commonly ascribed to M1-MdM and therefore regarded as a marker of M1-polarization. As to the characterization of the polarized MdM, TNFα concentration in the cell culture supernatant was therefore studied using ELISA. Prior to the measurement, the MdM were polarized for 2 days using complete medium without any polarizing agents, complete medium with addition of 50 ng/ml IFNγ and 10 ng/ml LPS as well as complete medium with addition of 20 ng/ml IL4 and 20 ng/ml IL13 for the M0-, M1- and M2-phenotype, respectively. As depicted in ***Fig. 11***, the TNFα concentration in the cell culture supernatant was specifically and significantly increased for the M1-phenotype compared to the M0- and M2-MdM. The arithmetic means ± SEM of the TNFα concentration for n = 5 repeats were 1.02 ± 0.28 pg/ml/1x10^6 cells, 901.50 ± 205.60 pg/ml/1x10^6 cells and 4.63 ± 1.33 pg/ml/1x10^6 cells for the M0-, M1- and M2-MdM, respectively.

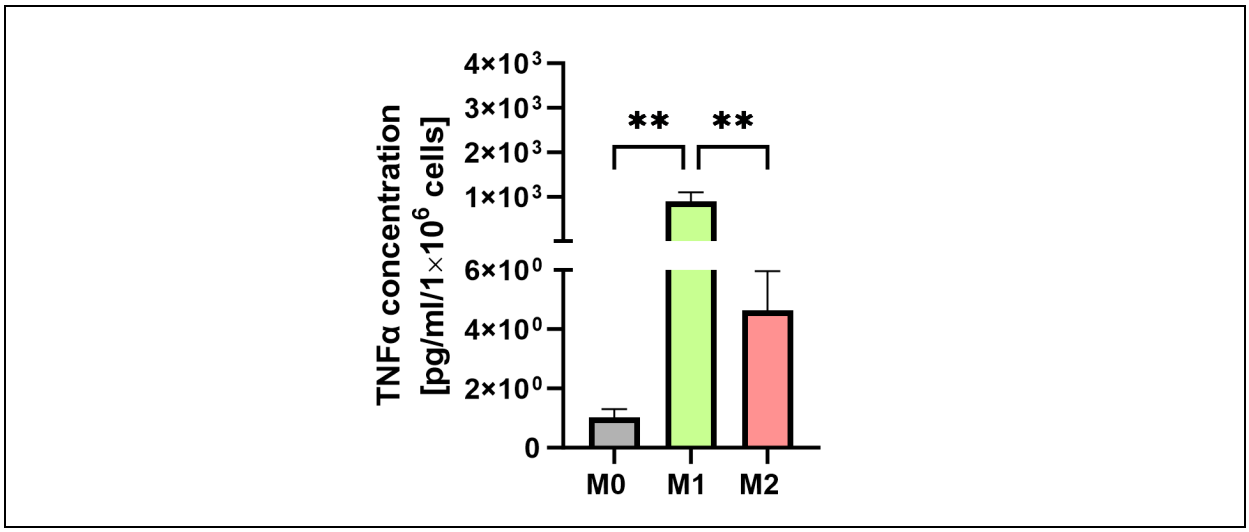

Figure 11: MdM secretion of TNFα subsequent to polarization to M0-, M1-, and M2-phenotype. *Arithmetic means ± SEM (n = 5) of TNFα concentration [pg/ml/1x10^6 cells] in the cell culture supernatant*

*after polarization to M0- (grey), M1- (green) and M2- (red) MdM for 2 days using ELISA. **p ≤ 0.01 indicates significant difference (one-way ANOVA).*

3.2.2 Secretion of CCL13

Furthermore, secretion of the cytokine CCL13 is regarded to be specific for M2-MdM. Hence, the concentration of CCL13 was analyzed using ELISA in view of a marker of M2-polarization as to characterize the MdM. Prior to the measurement, the MdM were polarized for 2 days using complete medium without any polarizing agents, complete medium with addition of 50 ng/ml IFNγ and 10 ng/ml LPS as well as complete medium with addition of 20 ng/ml IL4 and 20 ng/ml IL13 for the M0-, M1- and M2-phenotype, respectively. CCL13 was distinctly elevated regarding M2-polarization and moreover, the increase was significant as compared to M0-MdM. As represented in ***Fig. 12***., the arithmetic means ± SEM of the CCL13 concentration for n = 5 repeats are 16.77 ± 5.35 pg/ml/1x10^6 cells, 17.78 ± 5.65 pg/ml/1x10^6 cells and 1624.00 ± 524.30 pg/ml/1x10^6 cells for the M0-, M1- and M2-MdM, respectively.

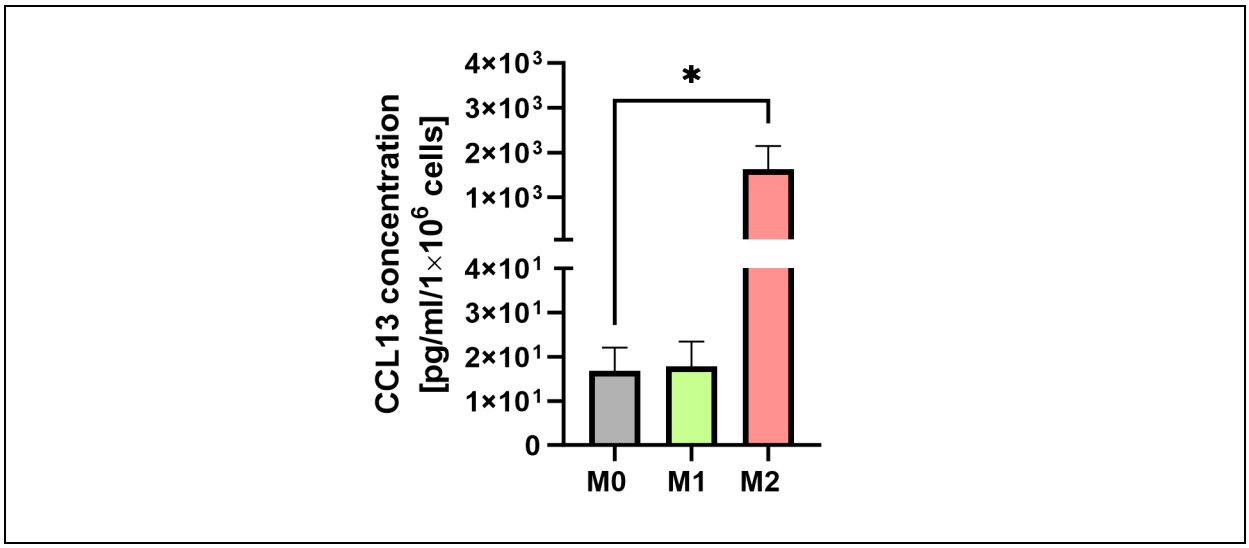

***Figure 12: MdM secretion of CCL13 subsequent to polarization to M0-, M1-, and M2-phenotype**. Arithmetic means ± SEM (n = 5) of CCL13 concentration [pg/ml/1x10^6 cells] in the cell culture supernatant after polarization to M0- (grey), M1- (green) and M2- (red) MdM for 2 days using ELISA. *p ≤ 0.05 indicates significant difference (Friedman test).*

3.2.3 Secretion of CCL17

Lastly, the cytokine CCL17 is also considered to be specifically secreted by M2-MdM and therefore classified to be a marker of M2-polarization. Accordingly, we studied the

CCL17 concentration in the cell culture supernatant. Subsequent to the polarization of the MdM for 2 days using complete medium without any polarizing agents, complete medium with addition of 50 ng/ml IFNγ and 10 ng/ml LPS and complete medium with addition of 20 ng/ml IL4 and 20 ng/ml IL13 for the M0-, M1- and M2-phenotype, respectively, ELISA was done. ***Fig. 12*** shows an elevated concentration of CCL17 specific for M2-MdM being significantly different from the secretion of M0-MdM. The arithmetic means ± SEM of the CCL17 concentration for n = 3 repeats were 49.59 ± 41.96 pg/ml/1x10^6 cells, 216.70 ± 104.60 pg/ml/1x10^6 cells and 3505.00 ± 471.5 pg/ml/1x10^6 cells for the M0-, M1- and M2-MdM, respectively.

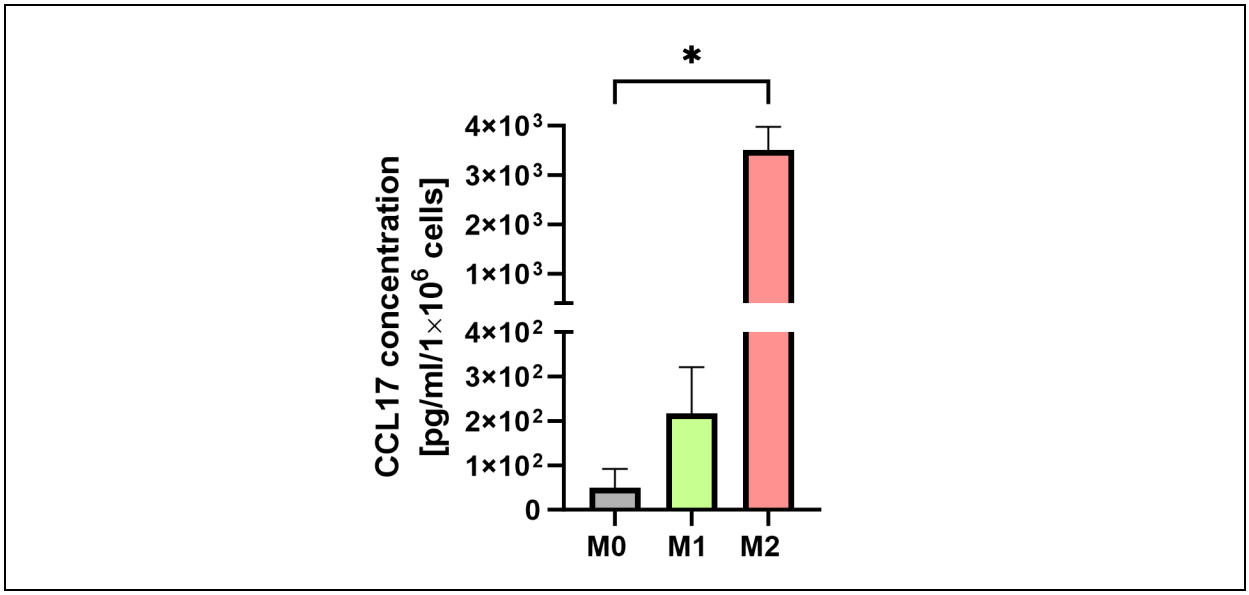

Figure 13: MdM secretion of CCL17 subsequent to polarization to M0-, M1-, and M2-phenotype*. Arithmetic means ± SEM (n = 3) of CCL17 concentration [pg/ml/1x10^6 cells] in the cell culture supernatant after polarization to M0- (grey), M1- (green) and M2- (red) MdM for 2 days using ELISA. *p ≤ 0.05 indicates significant difference (Friedman test).*

3.3 Characterization of MdM using flow cytometry

Furthermore, the M0- as well as the polarized M1- and M2-MdM were characterized regarding to their expressed surface or intracellular markers, respectively, using FACS. To this, we studied CD14 as well as CD68 correspondent to pan-markers, CD80, CD86 and CCR7 as markers for the M1-phenotype and CD1A, CD163, CD206, CD209 as well as Arg1 as markers for the M2-polarization.

3.3.1 Expression of CD14

The surface marker CD14 is commonly considered to be a pan-marker for monocytes and MΦ. As to the characterization of the polarized MdM, the CD14 expression was therefore studied flow cytometrically. Prior to the measurement, the MdM were polarized for 2 days using complete medium without any polarizing agents, complete medium with addition of 50 ng/ml IFNγ and 10 ng/ml LPS as well as complete medium with addition of 20 ng/ml IL4 and 20 ng/ml IL13 for the M0-, M1- and M2-phenotype, respectively. As shown in ***Fig. 14***, CD14 expression was high for all MdM, irrespective of their polarization. Moreover, the level of expression was significantly increased for M0- and M1-MdM, each compared to the M2-phenotype. The representative histogram depicts a distinct increase of the Alexa 647 fluorescence of all MdM-phenotypes, being most pronounced for the M0- and M1-polarization. The arithmetic means ± SEM of the percentage of CD14 expression for n = 3 repeats are 98.57 ± 0.29 %, 99.13 ± 0.12 % and 79.63 ± 3.52 % for the M0-, M1- and M2-MdM, respectively.

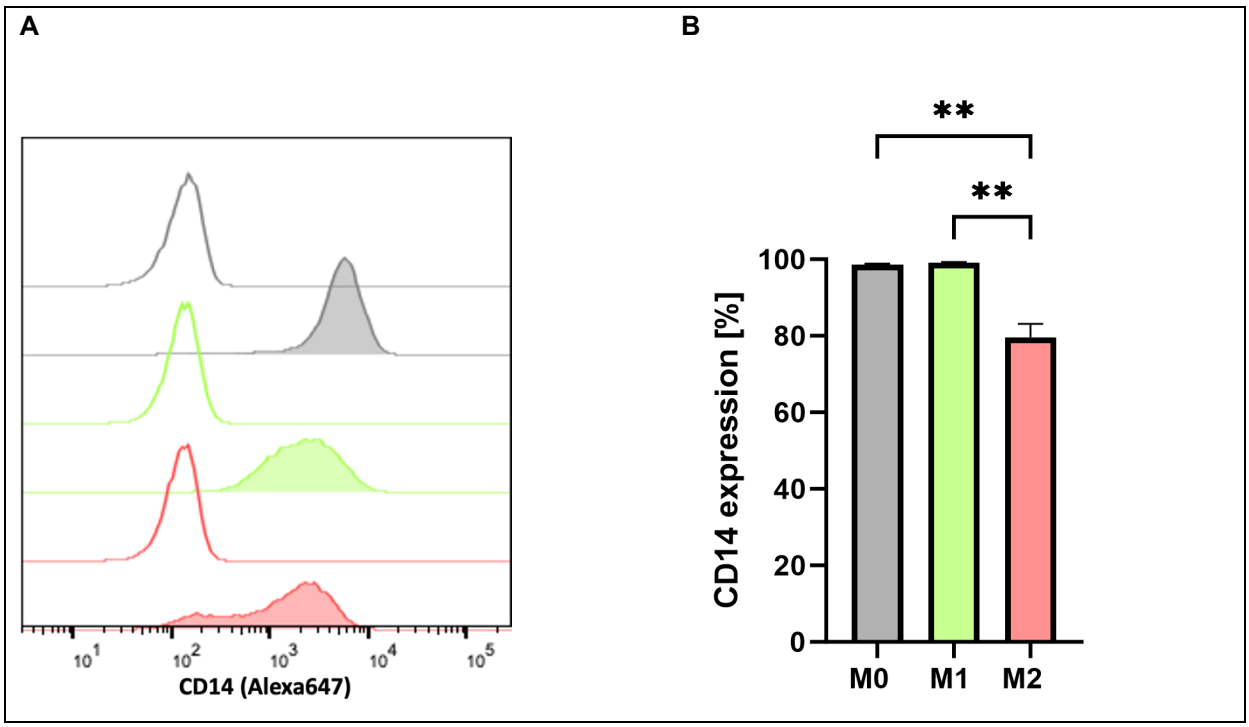

Figure 14: MdM expression of CD14 subsequent to polarization to M0-, M1- and M2-phenotype. ***A*** *Representative histogram of Alexa 647 fluorescence of MdM using flow cytometric assessment following their polarization to M0- (grey area), M1- (green area), and M2- (red area) phenotype for 2 days. Referentially, autofluorescence of unstained MdM is depicted for M0- (grey line), M1- (green line) and M2- (red line) phenotype.* ***B*** *Arithmetic means ± SEM (n = 3) of MdM CD14 expression [%] following their polarization to M0- (grey), M1-(green), and M2- (red) phenotype for 2 days. **p ≤ 0.01 indicates significant difference (one-way ANOVA).*

3.3.2 Expression of CD68

As furthermore the intracellular marker CD68 is generally regarded to be a pan-marker for monocytes and MΦ, the CD68 expression of the polarized MdM was also analyzed. To this, the MdM were either treated for 2 days with complete medium without any polarization agents, complete medium with 50 ng/ml IFNγ and 10 ng/ml LPS or complete medium with 20 ng/ml IL4 and 20 ng/ml IL13 to allow for polarization towards the M0-, M1 or M2-phenotype, respectively. The cells were then analyzed concerning their CD68 expression by means of flow cytometry. ***Fig. 15*** depicts a minor expression of CD68 without any significant difference between the M0-, M1- and M2-polarization with M1-MdM showing an increased expression by trend. The representative histogram illustrates only a slight increase of Alexa 647 fluorescence for the MdM, irrespective of their polarization, compared to the unstained cells. The arithmetic means ± SEM of the percentage of CD68 expression for n = 3 repeats were 5.55 ± 5.42 %, 13.29 ± 12.95 % and 8.02 ± 5.44 % for the M0-, M1- and M2-MdM, respectively.

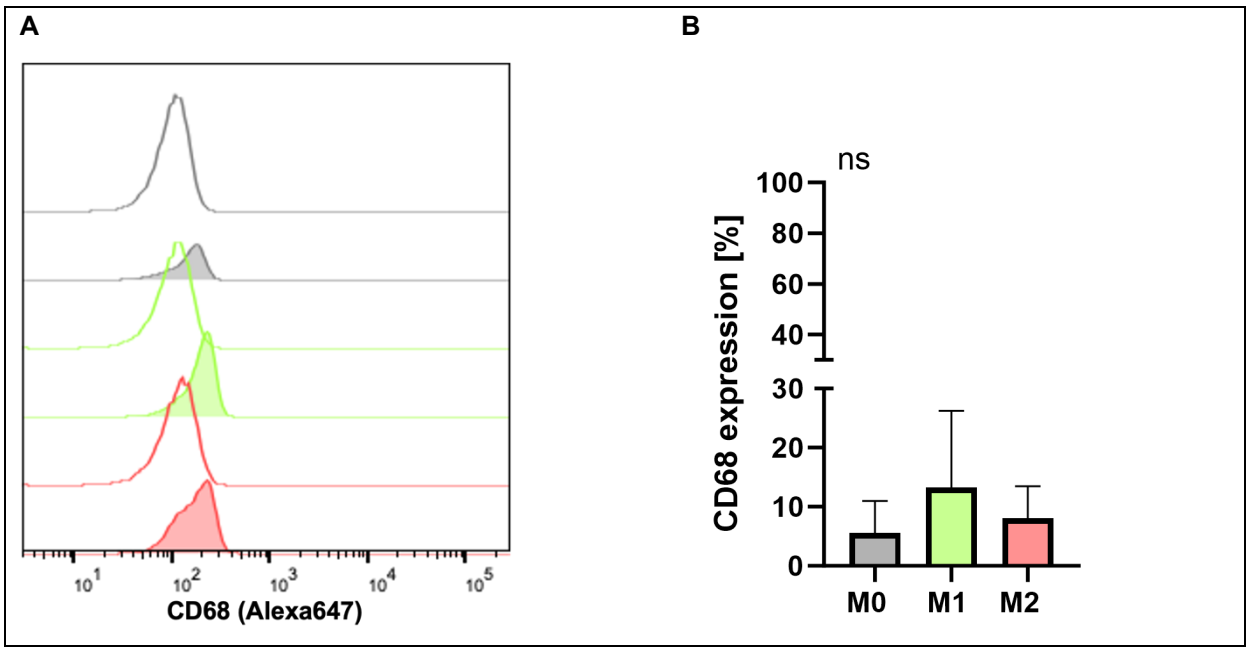

Figure 15: MdM expression of CD68 subsequent to polarization to M0-, M1- and M2-phenotype. ***A*** *Representative histogram of Alexa 647 fluorescence of MdM using flow cytometric assessment following their polarization to M0- (grey area), M1- (green area), and M2- (red area) phenotype for 2 days. Referentially, autofluorescence of unstained MdM is depicted for M0- (grey line), M1- (green line) and M2- (red line) phenotype.* ***B*** *Arithmetic means ± SEM (n = 3) of MdM CD68 expression [%] following their polarization to M0- (grey), M1-(green), and M2- (red) phenotype for 2 days. ns indicates non-significancy (Friedman test).*

3.3.3 Expression of CD80

The surface marker CD80 is commonly classified as a marker of M1-polarization. As to the characterization of the polarized MdM, we thus studied the expression of CD80 by means of flow cytometry. For this purpose, prior to the measurement, the MdM were polarized for 2 days using complete medium without any polarizing agents, complete medium with addition of 50 ng/ml IFNγ and 10 ng/ml LPS as well as complete medium with addition of 20 ng/ml IL4 and 20 ng/ml IL13 for the M0-, M1- and M2-phenotype, respectively. ***Fig. 16*** shows a significant increase of the CD80 expression of M1-MdM compared to M0- as well as M2-MdM. Still, the M0- and the M2-phenotype both expressed CD80, although M2-MdM were marked by a significantly higher expression compared to M0-MdM. The representative histogram depicts a distinct increase of the Brilliant Violet 421 fluorescence of M1-MdM relating to M0- and M2-MdM, as well as a slight increase of the Brilliant Violet 421 fluorescence of M2-MdM compared to M0-MdM. The arithmetic means ± SEM of the percentage of CD80 expression for n = 5 repeats were 36.24 ± 8.36 %, 99.22 ± 0.17 % and 67.28 ± 4.36 % for the M0-, M1- and M2-MdM, respectively.

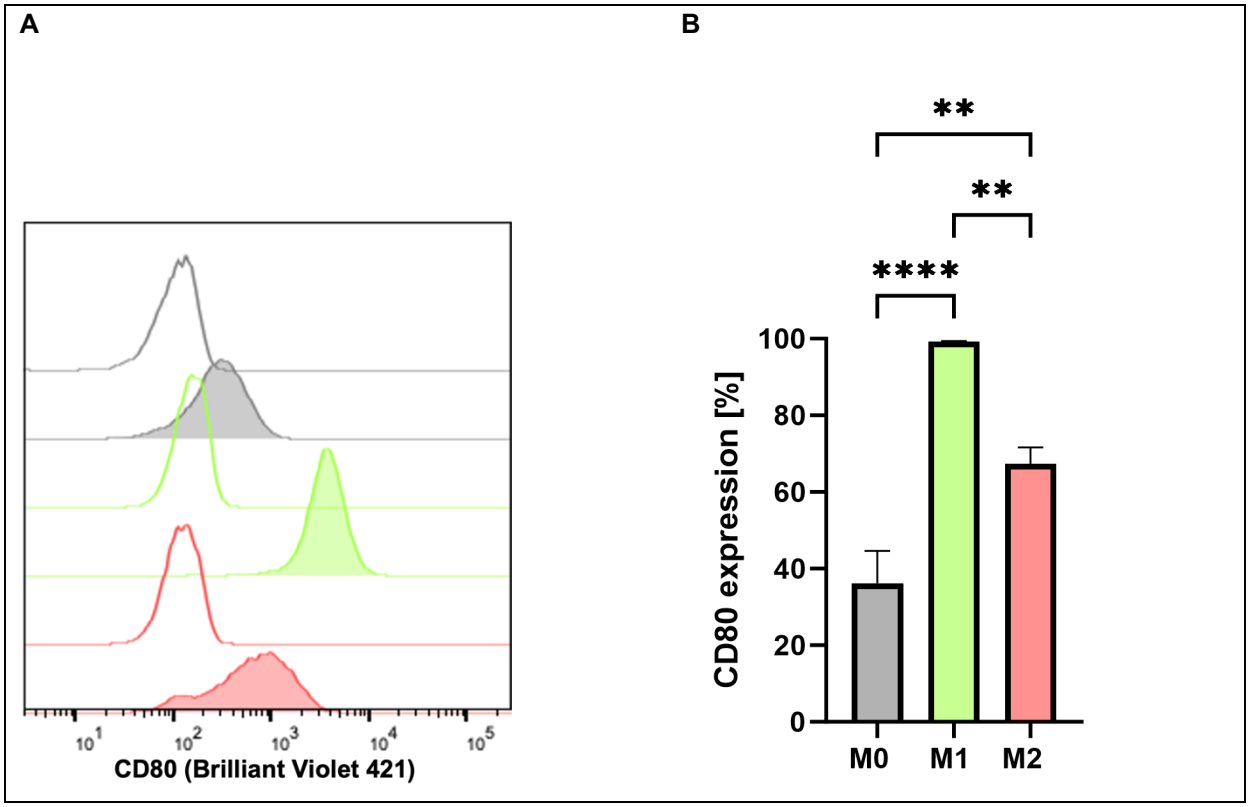

Figure 16: MdM expression of CD80 subsequent to polarization to M0-, M1- and M2-phenotype. ***A*** *Representative histogram of Brilliant Violet 421 fluorescence of MdM using flow cytometric*

assessment following their polarization to M0- (grey area), M1-(green area), and M2- (red area) phenotype for 2 days. Referentially, autofluorescence of unstained MdM is depicted for M0- (grey line), M1- (green line) and M2- (red line) phenotype. ***B*** *Arithmetic means ± SEM (n = 5) of MdM CD80 expression [%] following their polarization to M0- (grey), M1- (green), and M2- (red) phenotype for 2 days. **p ≤ 0.01 and ****p ≤ 0.0001 indicate significant difference (one-way ANOVA).*

3.3.4 Expression of CD86

The surface marker CD86 is generally regarded as another marker of the M1-phenotype. For the purpose of characterization of the polarized MdM, the expression of CD86 was hence analyzed. Subsequent to the polarization of the MdM for 2 days using complete medium without any polarizing agents, complete medium with addition of 50 ng/ml IFNγ and 10 ng/ml LPS and complete medium with addition of 20 ng/ml IL4 and 20 ng/ml IL13 for the M0-, M1- and M2-phenotype, respectively, flow cytometry was done. As presented in ***Fig. 17***, the surface marker CD86 was highly and nonspecifically expressed by all MdM, irrespective of their polarization. The representative histogram illustrates high PE fluorescence for the M0-, M1- as well as M2-phenotype. The arithmetic means ± SEM of the percentage of CD86 expression for n = 3 repeats were 99.30 ± 0.21, 99.60 ± 0.06 and 99.37 ± 0.07 for the M0-, M1- and M2-MdM, respectively.

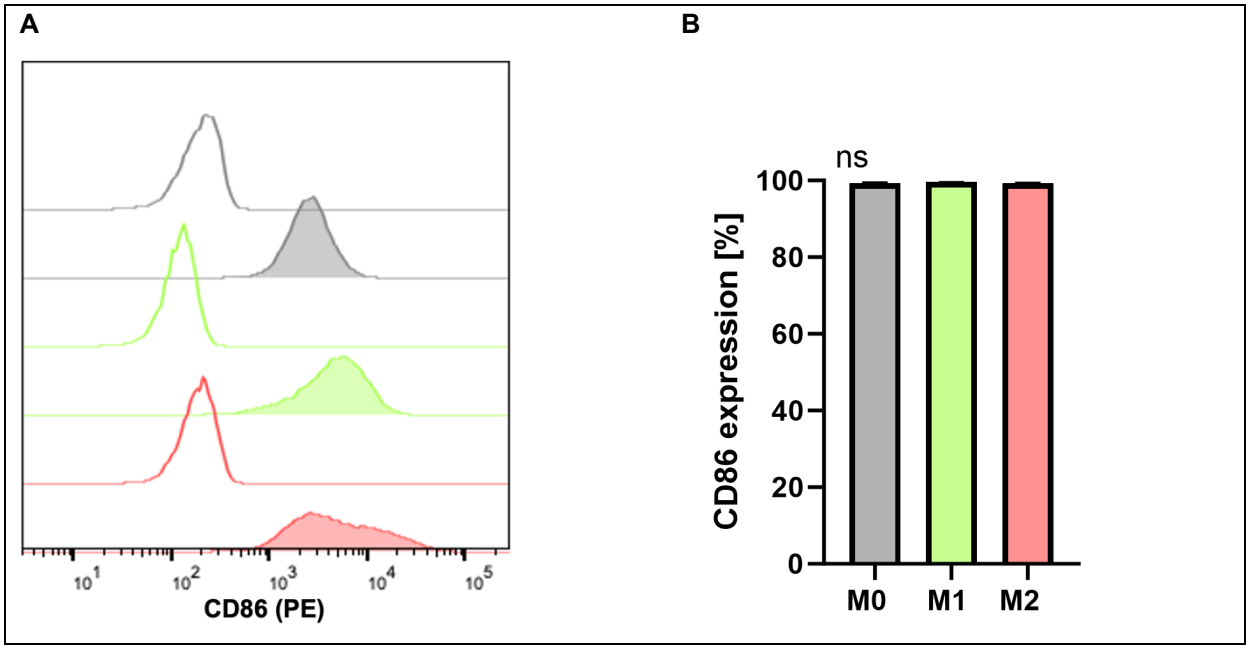

Figure 17: MdM expression of CD86 subsequent to polarization to M0-, M1- and M2-phenotype*. **A** Representative histogram of PE fluorescence of MdM using flow cytometric assessment following their polarization to M0- (grey area), M1- (green area), and M2- (red area) phenotype for 2 days. Referentially, autofluorescence of unstained MdM is depicted for M0- (grey line), M1- (green line) and M2- (red line) phenotype.* ***B*** *Arithmetic means ± SEM (n = 3) of MdM CD86 expression [%] following their*

polarization to M0- (grey), M1-(green), and M2- (red) phenotype for 2 days. ns indicates non-significancy (Friedmann test).

3.3.5 Expression of CCR7

As moreover the surface marker CCR7 is commonly considered to be a marker of M1-phenotype, the CCR7 expression of the polarized MdM was also studied. To this, the MdM were either treated for 2 days with complete medium without any polarization agents, complete medium with 50 ng/ml IFNγ and 10 ng/ml LPS or complete medium with 20 ng/ml IL4 and 20 ng/ml IL13 to allow for polarization to the M0-, M1 or M2-phenotype, respectively. The cells were then analyzed concerning their CCR7 expression by means of flow cytometry. ***Fig. 18*** depicts a significant as well as specific increase of the CCR7 expression of M1-MdM compared to M0- and M2-MdM. The representative histogram shows a distinct and specific increase of PE fluorescence of M1-MdM. The arithmetic means ± SEM of the percentage of CCR7 expression for n = 3 repeats were 5.21 ± 2.45 %, 61.57 ± 11.60 % and 1.61 ± 0.23 % for the M0-, M1- and M2-MdM, respectively.

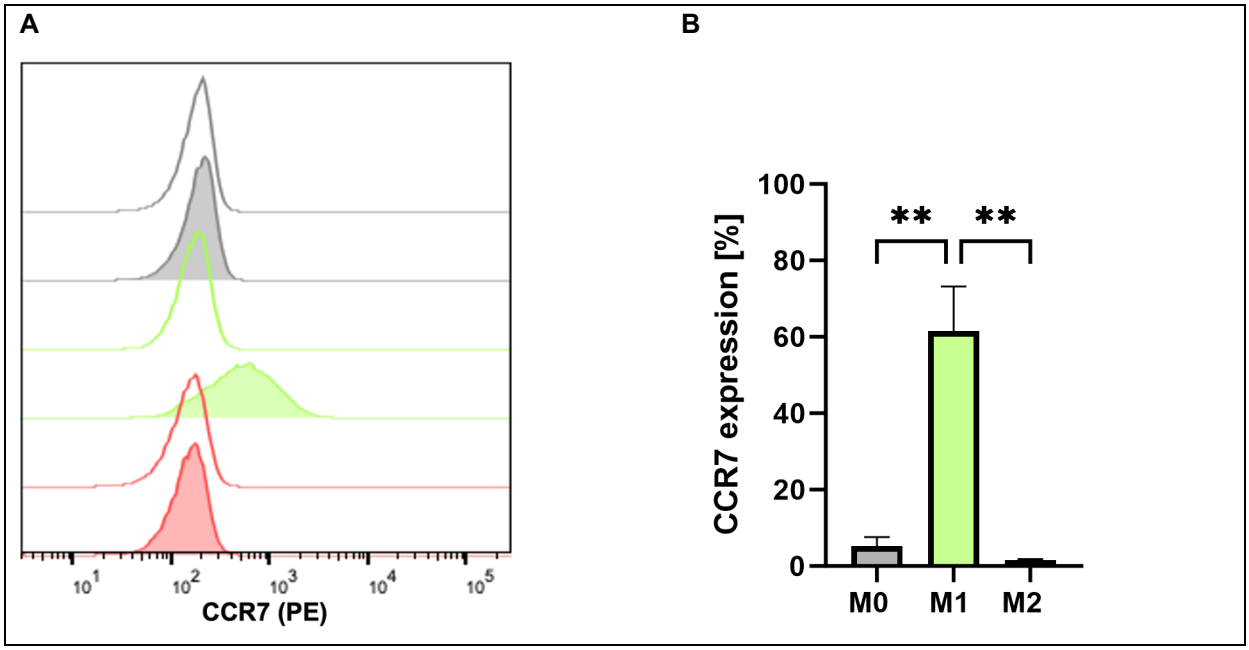

Figure 18: MdM expression of CCR7 subsequent to polarization to M0-, M1- and M2-phenotype. ***A*** *Representative histogram of PE fluorescence of MdM using flow cytometric assessment following their polarization to M0- (grey area), M1- (green area), and M2- (red area) phenotype for 2 days. Referentially, autofluorescence of unstained MdM is depicted for M0- (grey line), M1- (green line) and M2- (red line) phenotype.* ***B*** *Arithmetic means ± SEM (n = 3) of MdM CCR7 expression [%] following their polarization to M0- (grey), M1-(green), and M2- (red) phenotype for 2 days. **p ≤ 0.01 indicates significant difference (one-way ANOVA)*

3.3.6 Expression of CD1A

Regarding the M2-polarization, the surface marker CD1A is considered to be characteristic. We thus studied the CD1A expression for the purpose of characterization of the polarized MdM. Subsequent to the polarization of the MdM for 2 days using complete medium without any polarizing agents, complete medium with addition of 50 ng/ml IFNγ and 10 ng/ml LPS and complete medium with addition of 20 ng/ml IL4 and 20 ng/ml IL13 for the M0-, M1- and M2-phenotype, respectively, flow cytometry was done. As ***Fig. 19*** shows, M2-MdM moderately but specifically expressed the surface marker CD1A. Expression of M2-MdM was significantly heightened as compared to M0- or M1-polarization. The representative histogram shows a slight increase in the PE fluorescence for the M2-phenotype, whereas no increment results for the M0- as well as M1-phenotype. The arithmetic means ± SEM of the percentage of CD1A expression for n = 3 repeats were 4.01 ± 0.57, 2,23 ± 0.47 and 24.47 ± 5.84 for the M0-, M1- and M2-MdM, respectively.

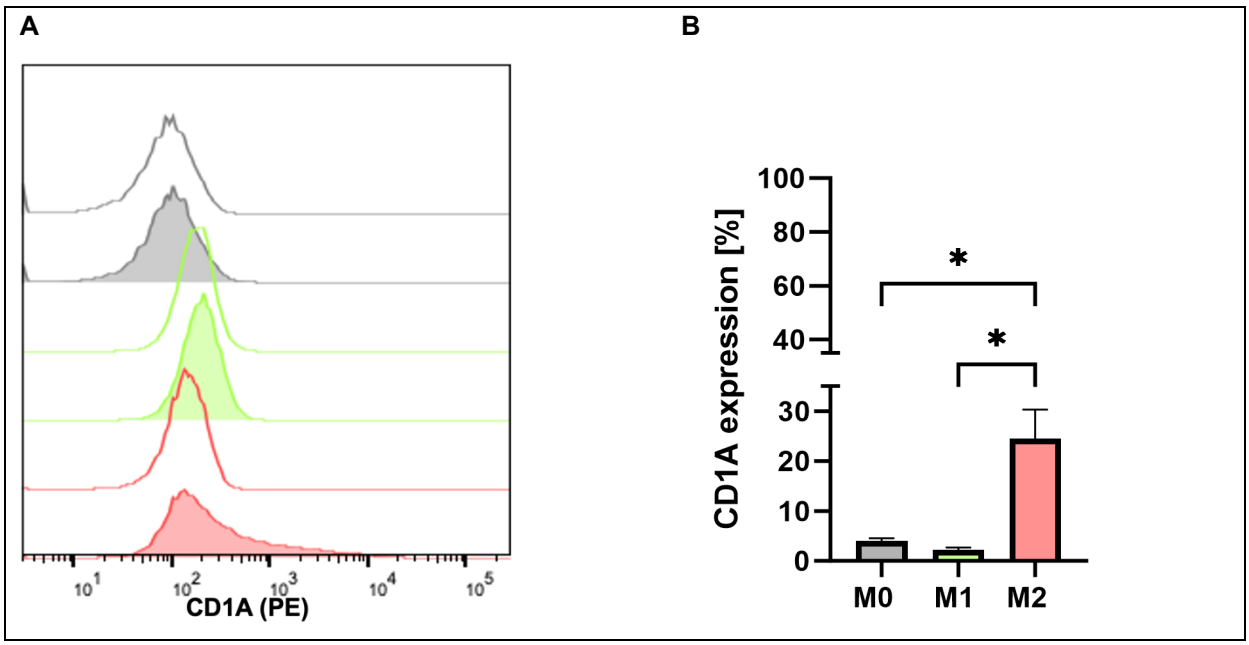

Figure 19: MdM expression of CD1A subsequent to polarization to M0-, M1- and M2-phenotype. ***A*** *Representative histogram of PE fluorescence of MdM using flow cytometric assessment following their polarization to M0- (grey area), M1- (green area), and M2- (red area) phenotype for 2 days. Referentially, autofluorescence of unstained MdM is depicted for M0- (grey line), M1- (green line) and M2- (red line) phenotype.* ***B*** *Arithmetic means ± SEM (n = 3) of MdM CD1A expression [%] following their polarization to M0- (grey), M1-(green), and M2- (red) phenotype for 2 days. *p ≤ 0.05 indicates significant difference (one-way ANOVA).*

3.3.7 Expression of CD163

Furthermore, the surface marker CD163 is commonly regarded as a marker of M2-phenotype. CD163 expression was hence analyzed to characterize the polarized MdM. To this, the latter cells were either treated for 2 days with complete medium without any polarization agents, complete medium with 50 ng/ml IFNγ and 10 ng/ml LPS or complete medium with 20 ng/ml IL4 and 20 ng/ml IL13 to allow for polarization to the M0-, M1 or M2-phenotype, respectively. The MdM were then flow cytometrically analyzed concerning their CD163 expression. ***Fig. 20*** shows a considerable increment of CD163 expression for M0- and M1- MdM, whereas the CD163 expression of the M2-phenotype was only moderately increased. As compared to the M2-phenotype, the CD163 expression of M0-MdM was significantly increased. The representative histogram depicts a marked increase of FITC fluorescence for M0- as well as M1-MdM, FITC fluorescence of M2-MdM in contrast is only slightly heightened. The arithmetic means ± SEM of the percentage of CD163 expression for n = 3 repeats were 66.73 ± 4.92 %, 44.33 ± 10.47 % and 31.60 ± 7.30 % for the M0-, M1- and M2-MdM, respectively.

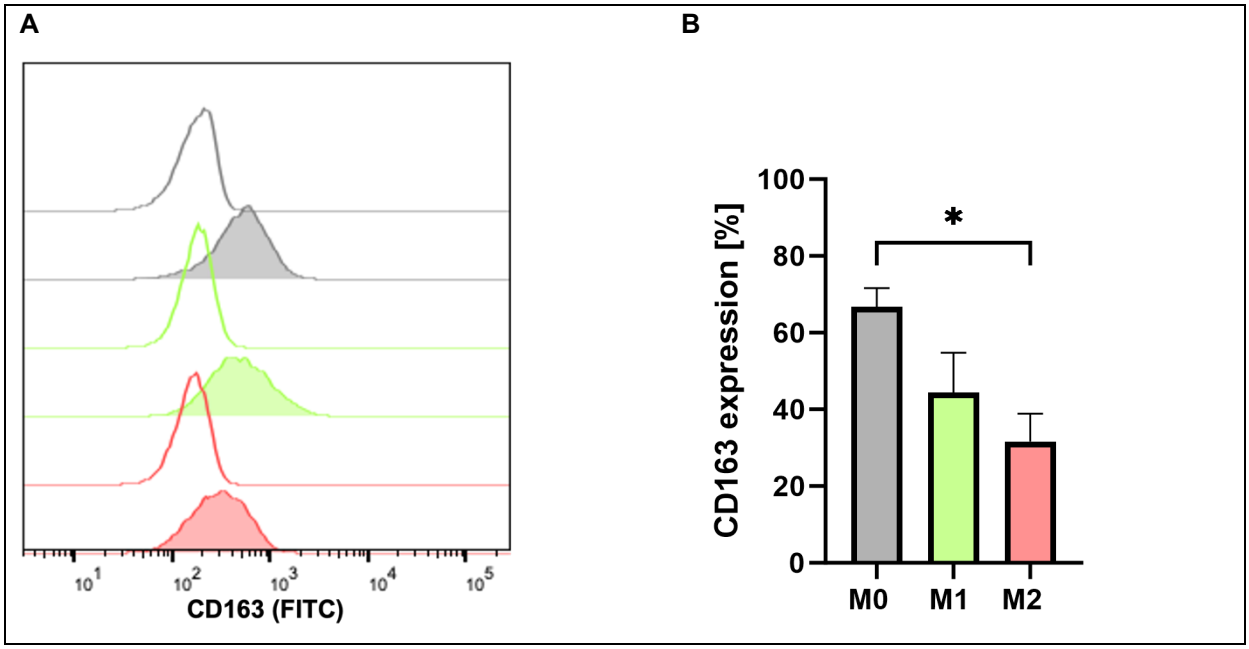

Figure 20: MdM expression of CD163 subsequent to polarization to M0-, M1- and M2-phenotype. ***A*** *Representative histogram of FITC fluorescence of MdM using flow cytometric assessment following their polarization to M0- (grey area), M1- (green area), and M2- (red area) phenotype for 2 days. Referentially, autofluorescence of unstained MdM is depicted for M0- (grey line), M1- (green line) and M2- (red line) phenotype.* ***B*** *Arithmetic means ± SEM (n = 3) of MdM CD163 expression [%] following their polarization to M0- (grey), M1-(green), and M2- (red) phenotype for 2 days. *p ≤ 0.05 indicates significant difference (one-way ANOVA).*

3.3.8 Expression of CD206

Likewise, the surface marker CD206 is commonly classified as a marker of M2-polarization. In order to characterize the polarized MdM, we thus studied the expression of CD206 by means of flow cytometry. To this, prior to measurement, the cells were polarized for 2 days using complete medium without any polarizing agents, complete medium with addition of 50 ng/ml IFNγ and 10 ng/ml LPS as well as complete medium with addition of 20 ng/ml IL4 and 20 ng/ml IL13 for the M0-, M1- and M2-phenotype, respectively. As illustrated in ***Fig. 21***, CD206 expression was high for M0-, M1- as well as M2-MdM, although the M2-phenotype CD206 expression wass most pronounced. M0- as well as M2-MdM CD206 expression was significantly elevated compared to the M1-phenotype. With reference to the CD206 MFI, M2-MdM showed significantly heightened fluorescence intensity deviating from the M0- and M1-phenotype. The representative histogram depicts a marked increase of the PE fluorescence of M0-, M1- as well as M2-MdM being most pronounced for the M2-phenotype and least distinct for the M1-phenotype. The arithmetic means ± SEM of the percentage of CD206 expression for n = 5 repeats were 90.98 ± 3.41 %, 75.72 ± 3.66 % and 97.14 ± 0.62 % for the M0-, M1- and M2-MdM, respectively. The arithmetic means ± SEM of the CD206 MFI for n = 5 repeats were 1021 ± 95.01, 768.8 ± 106.2 and 2825 ± 433.4 for the M0-, M1- and M2-MdM, respectively.

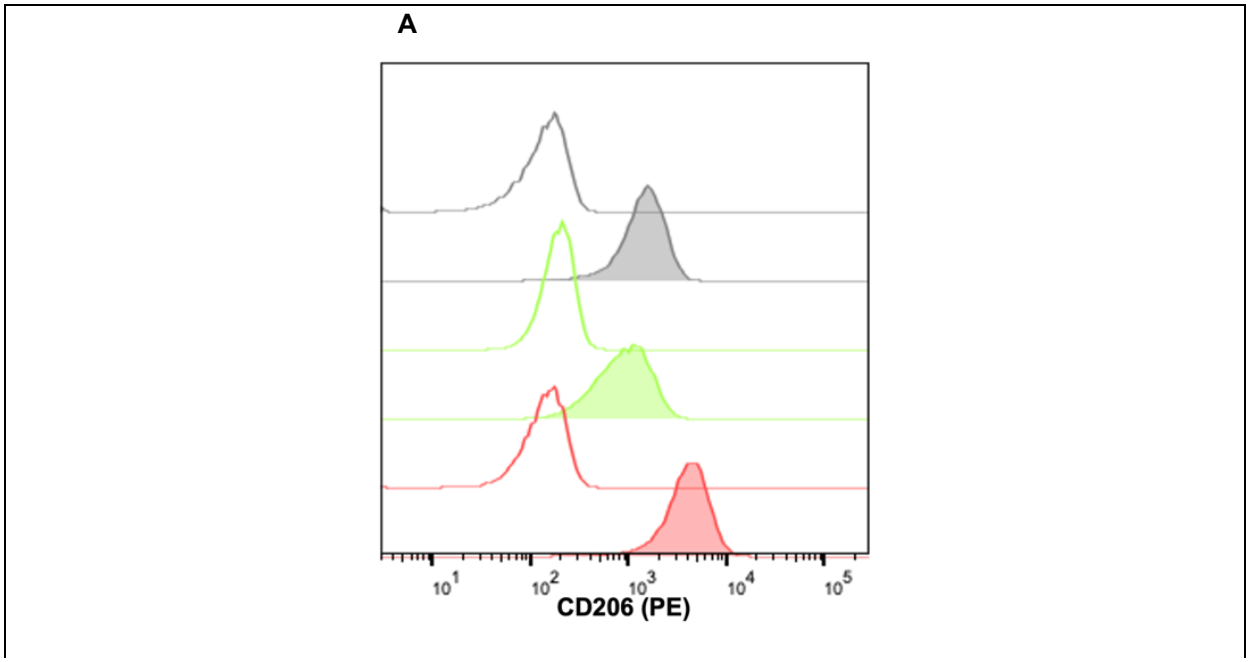

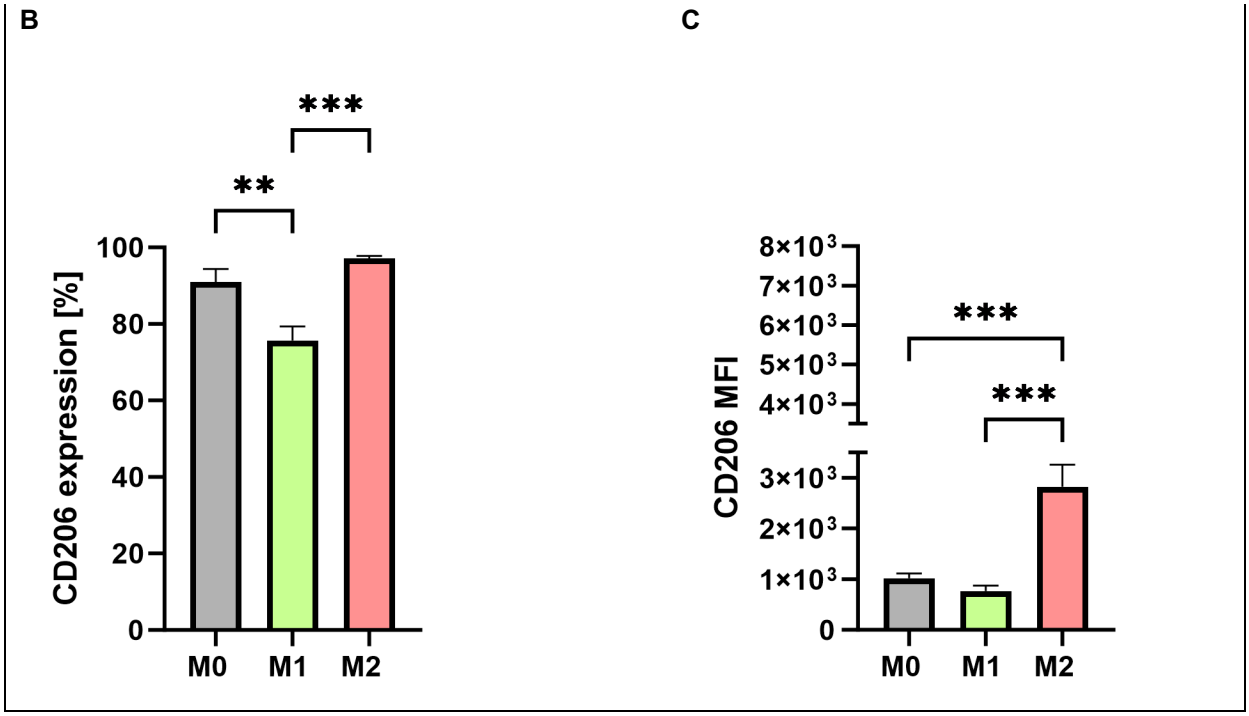

Figure 21: MdM expression and MFI of CD206 subsequent to polarization to M0-, M1- and M2-phenotype*. **A** Representative histogram of PE fluorescence of MdM using flow cytometric assessment following their polarization to M0- (grey area), M1- (green area), and M2- (red area) phenotype for 2 days. Referentially, autofluorescence of unstained MdM is depicted for M0- (grey line), M1- (green line) and M2- (red line) phenotype. **B** Arithmetic means ± SEM (n = 5) of MdM CD206 expression [%] following their polarization to M0- (grey), M1- (green), and M2- (red) phenotype for 2 days. **p ≤ 0,01, ***p ≤ 0,0003 indicates significant difference (one-way ANOVA). **C** Arithmetic means ± SEM (n=5) of MdM CD206 MFI following their polarization to M0- (grey), M1-(green), and M2- (red) phenotype for 2 days. **p ≤ 0.01 and ***p ≤ 0.0003 indicate significant difference (one-way ANOVA).*

3.3.9 Expression of CD209

The surface marker CD209 is generally considered to be another marker verifying M2-polarization. For the purpose of characterization of the polarized MdM, the CD209 expression was hence analyzed. Subsequent to the polarization of the MdM for 2 days using complete medium without any polarizing agents, complete medium with addition of 50 ng/ml IFNγ and 10 ng/ml LPS and complete medium with addition of 20 ng/ml IL4 and 20 ng/ml IL13 for the M0-, M1- and M2-phenotype, respectively, flow cytometry was done. ***Fig. 22*** shows a significant as well as specific increase of the CD209 expression of M2-MdM compared to the M0- and M1-phenotype. The representative histogram demonstrates a distinct and specific increase of FITC fluorescence of M2-MdM. The arithmetic means ± SEM of the percentage of CD209 expression for n = 3 repeats were 9.67 ± 3.85 %, 3.72 ± 2.03 % and 75.70 ± 3.84 % for the M0-, M1- and M2-MdM, respectively.

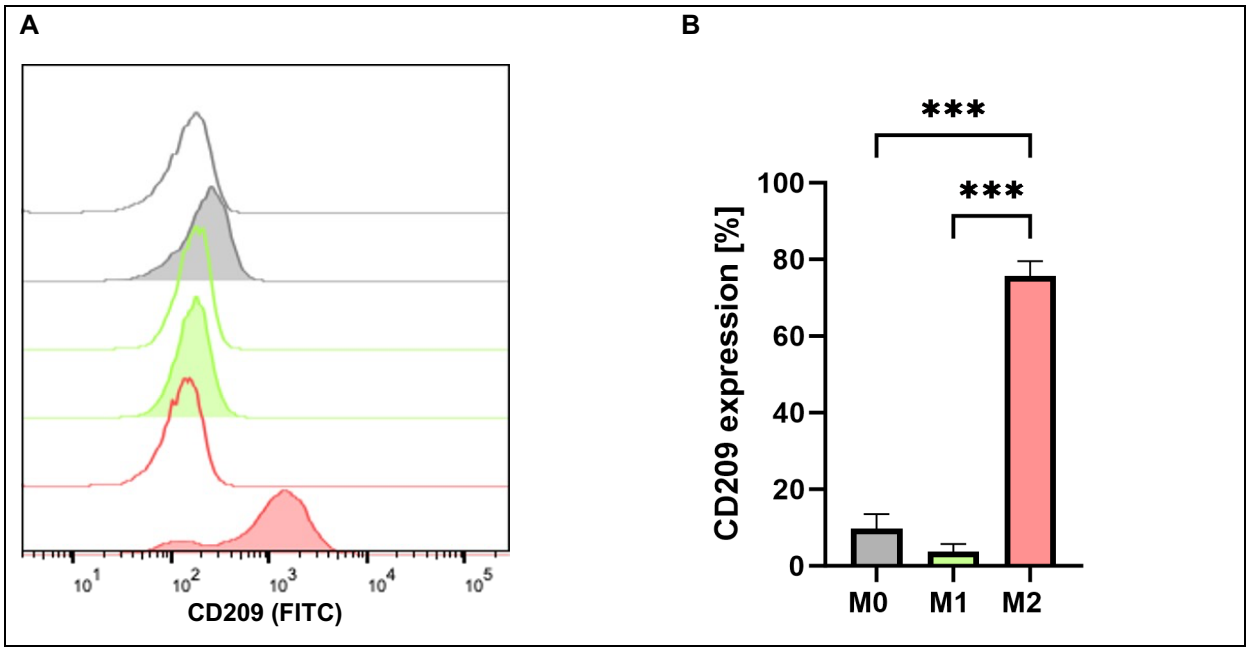

Figure 22: MdM expression of CD209 subsequent to polarization to M0-, M1- and M2-phenotype*. **A** Representative histogram of FITC fluorescence of MdM using flow cytometric assessment following their polarization to M0- (grey area), M1- (green area), and M2- (red area) phenotype for 2 days. Referentially, autofluorescence of unstained MdM is depicted for M0- (grey line), M1- (green line) and M2- (red line) phenotype. **B** Arithmetic means ± SEM (n = 3) of MdM CD209 expression [%] following their polarization to M0- (grey), M1-(green), and M2- (red) phenotype for 2 days. ***p ≤ 0.0003 indicates significant difference (one-way ANOVA).*

3.3.10 Expression of Arg1

Eventually, the intracellular marker Arg1 is also considered to indicate M2-polarization. We therefore studied the Arg1 expression of the MdM so as to their characterization. To this, the MdM were either treated for 2 days with complete medium without any polarization agents, complete medium with 50 ng/ml IFNγ and 10 ng/ml LPS or complete medium with 20 ng/ml IL4 and 20 ng/ml IL13 to allow for polarization to the M0-, M1 or M2-phenotype, respectively, before measurement by means of FACS. As illustrated in **Fig. 23**, neither of the MdM express the intracellular marker Arg1, irrespective of their polarization. The representative histogram shows no increased PerCP fluorescence for all MdM-phenotypes. The arithmetic means ± SEM of the percentage of Arg1 expression for n = 3 repeats are 0.1863 ± 0.08, 0.32 ± 0.12 and 0.16 ± 0.04 for the M0-, M1- and M2-MdM, respectively.

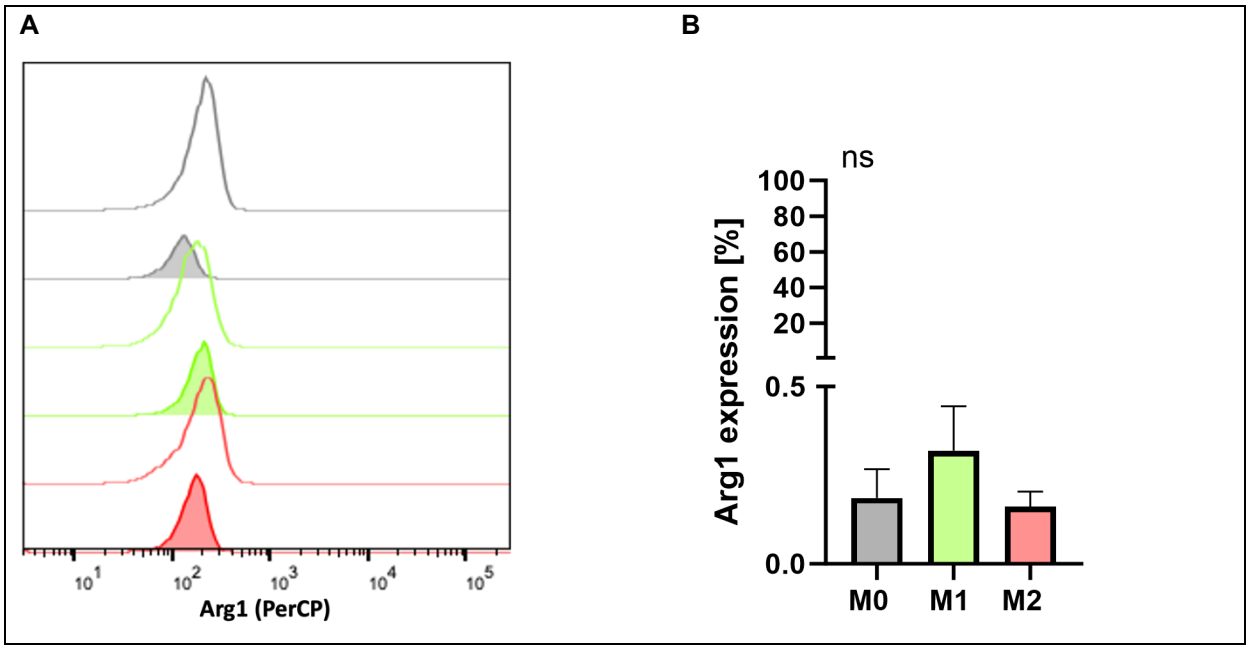

***Figure 23: MdM expression of Arg1 subsequent to polarization to M0-, M1- and M2-phenotype**. **A** Representative histogram of PerCP fluorescence of MdM using flow cytometric assessment following their polarization to M0- (grey area), M1- (green area), and M2- (red area) phenotype for 2 days. Referentially, autofluorescence of unstained MdM is depicted for M0- (grey line), M1- (green line) and M2- (red line) phenotype. **B** Arithmetic means ± SEM (n = 3) of MdM Arg1 expression [%] following their polarization to M0- (grey), M1-(green), and M2- (red) phenotype for 2 days. ns indicated non-significancy (one-way ANOVA).*

3.4 Characterization of MdM using CLSM

At last, the M0-, M1- and M2-MdM were assessed concerning their morphology as well as their surface marker expression using CLSM. Based on our preliminary studies (*data not shown*) and as deducible from the flow cytometric investigations presented afore ***(Chap. 3.3)***, the surface markers CCR7 as well as CD209 were presumed to be specific regarding the M1- or the M2-phenotype, respectively, and were thus deployed as surrogates for the correspondent polarization status hereinafter. Hence, to the MdM characterization by means of CLSM, cytoskeletal staining was performed using phalloidin and surface markers CCR7 and CD209 were examined using specific primary and fluorescently labelled secondary antibodies. Nuclei were counterstained deploying DRAQ5 in the context of both, cytoskeletal as well as surface marker staining [77].

3.4.1 Cytoskeletal morphology

In order to evaluate the morphology of the M0-, as well as the polarized M1- and M2-MdM, we stained the cells' cytoskeletons using phalloidin as well as the nuclei

employing DRAQ5. To this, the MdM were seeded onto coverslips following to their differentiation. Treatment with complete medium without any polarization agents, complete medium with 50 ng/ml IFNγ and 10 ng/ml LPS or complete medium with 20 ng/ml IL4 and 20 ng/ml IL13 for 2 days was undertaken to allow for polarization to the M0-, M1- or M2-phenotype, respectively, before the assessment using CLSM. As depicted in ***Fig. 24***, M0-MdM featured a round morphology with a rather undefined structure of their cytoskeleton. Similarly, M1-MdM also showed a round appearance. Yet, the cytoskeleton of these cells exhibited spiculae effectuating a star-shaped aspect. M2-MdM, on the contrary, featured both, round as well as elongated cells with their cytoskeleton showing filopodia-like elongations to some extent.

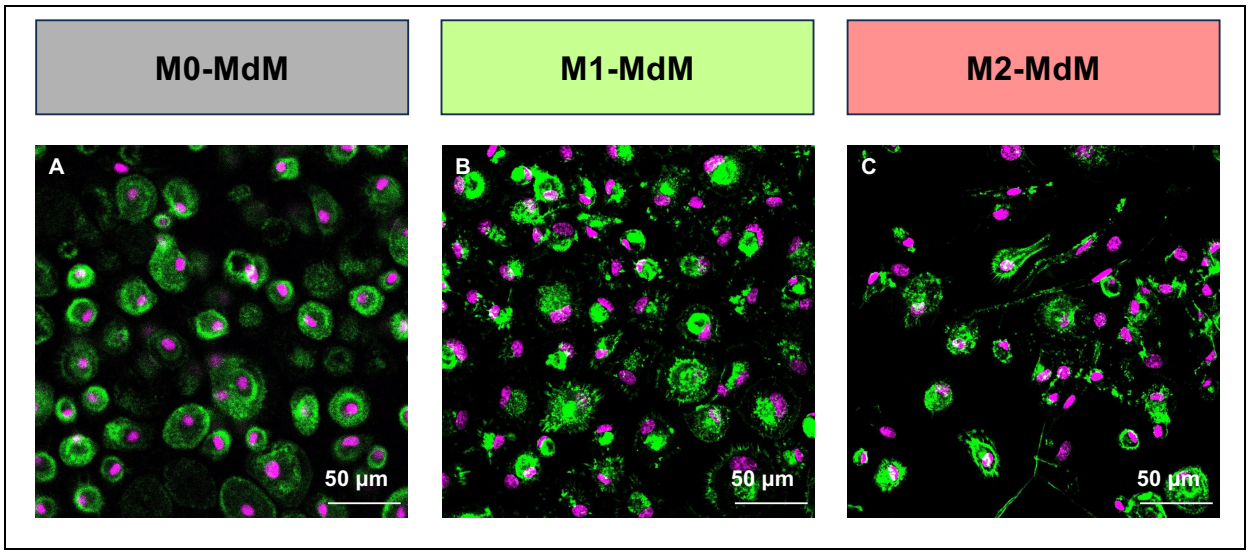

Figure 24: MdM cytoskeletal morphology subsequent to polarization to M0-, M1- and M2-phenotype*. Representative cytoskeletal MdM morphology using CLSM with phalloidin as well as DRAQ5 staining following incubation with complete medium without addition of polarizing agents, complete medium with 50 ng/ml IFNγ and 10 ng/ml LPS or complete medium with 20 ng/ml IL4 and 20 ng/ml IL13 for 2 days to induce M0-, M1- or M2-polarization, respectively. Polarization was undertaken adjacent to seeding differentiated MdM onto coverslips. Green = phalloidin staining, pink = DRAQ5 staining.* ***A*** *M0-MdM, 25X magnification, 2.5 X zoom,* ***B*** *M1-MdM, 25X magnification, 2.5X zoom,* ***C*** *M2-MdM, 25X magnification, 2.5 X zoom.*

3.4.2 Expression of CCR7 and CD209

Regarding the characterization of the polarized MdM, we lastly examined the expression of CCR7 and CD209 using CLSM. To this, differentiated MdM were seeded onto coverslips and incubated with complete medium without any polarization agents, complete medium with 50 ng/ml IFNγ and 10 ng/ml LPS or complete medium with 20 ng/ml IL4 and 20 ng/ml IL13 for 2 days to induce M0-, M1- or M2-polarization, respectively.

Counterstaining of the nuclei was done utilizing DRAQ5 and cells were analyzed via CLSM. ***Fig. 25*** illustrates a strong and specific CCR7 expression of M1-MdM, whereas M0- and M2-MdM exhibited only minor CCR7-related fluorescence. Contrarily, CD209 was distinctly and specifically expressed in M2-MdM. Neither M0-, nor M1-MdM featured relevant CD209 expression [77]. At this point, no fluorescence intensity was determined, as quantity of CCR7 and CD209 was measured before using flow cytometry ***(Chap. 2.6.7, Chap. 3.3)*** resulting in more precise results than deploying semi-quantitative CLSM analysis.

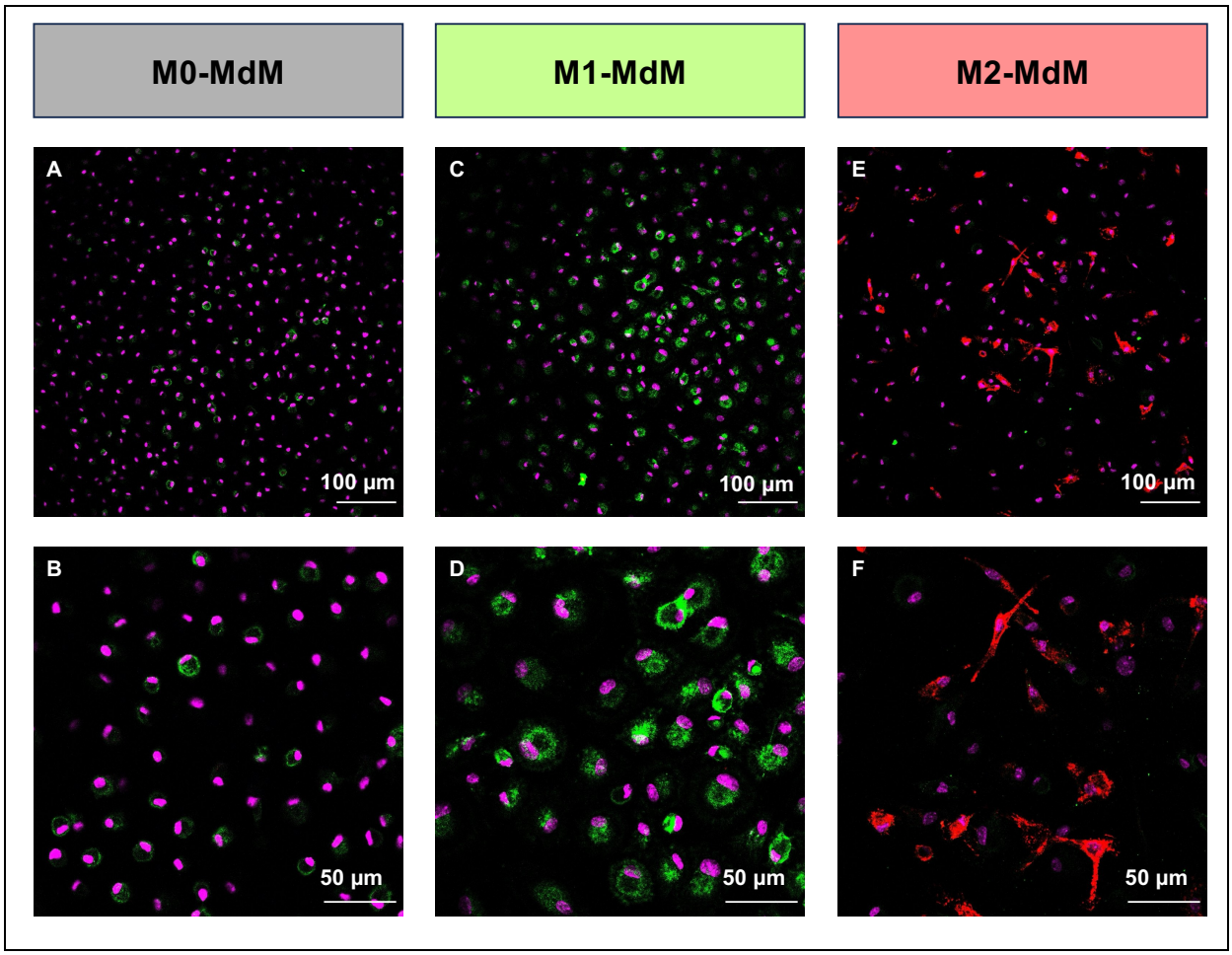

Figure 25: MdM expression of CCR7 and CD209 subsequent to polarization to M0-, M1- and M2-phenotype *modified according to [77]. Representative expression of CCR7 and CD209 of MdM using CLSM and antibody staining of the surface markers as well as DRAQ5 staining following incubation with complete medium without addition of polarizing agents, complete medium with 50 ng/ml IFNγ and 10 ng/ml LPS or complete medium with 20 ng/ml IL4 and 20 ng/ml IL13 for 2 days to induce M0-, M1- or M2-polarization, respectively. Polarization was undertaken adjacent to seeding differentiated MdM onto coverslips. Green = CCR7 staining, red = CD209 staining, pink = DRAQ5 staining.* ***A*** *M0-MdM, 25X magnification, 1X zoom,* ***B*** *M0-MdM, 25X magnification, 2.5X zoom,* ***C*** *M1-MdM, 25X magnification, 1X zoom,* ***D*** *M1-MdM, 25X magnification, 2.5X zoom,* ***E*** *M2-MdM, 25X magnification, 1X zoom,* ***F*** *M2-MdM, 25X magnification, 2.5X zoom.*

In summary, the results presented afore ***(Chap. 3.1, Chap. 3.2, Chap. 3.3, Chap. 3.4)*** document the successful establishment of a protocol for the isolation of monocytes, their differentiation to MdM and eventually the polarization as well as the characterization of the M1- and M2-phenotype. As to their morphology, M1-MdM were marked by a round appearance, whereas M2-MdM were elongated with stellate-like branching. ***Tab. 16*** provides a résumé of the markers studied using ELISA, flow cytometry and CLSM. Due to their specificity, secretion of TNFα as well as CCL13 and expression of the surface markers CCR7 as well as CD209 were used as M1- and M2-markers, respectively, for the subsequent implementation of the protocol.

Table 16: Markers studied for the characterization of M0-, M1- and M2-MdM using ELISA, FACS and CLSM

Marker	Polarization	M0-MdM	M1-MdM	M2-MdM
ELISA				
TNFα	**M1**	-	+	-
CCL13	**M2-marker**	-	-	+
CCL17	**M2-marker**	-	-	+
FACS				
CD14	**Pan-marker**	+	+	+
CD68	**Pan-marker**	-	-	-
CD80	**M1-marker**	-	+	+/-
CD86	**M1-marker**	+	+	+
CCR7	**M1-marker**	-	+	-
CD1A	**M2-marker**	-	-	+
CD163	**M2-marker**	+	+	+/-
CD206	**M2-marker**	+	-	+
CD209	**M2-marker**	-	-	+
Arg1	**M2-marker**	-	-	-
CLSM				
CCR7	**M1-marker**	-	+	-
CD209	**M2-marker**	-	-	+

In order to implement the protocol established afore, differentiated MdM were cultivated on titanium surfaces in the second part of this study to test for immunomodulatory influences of different biomaterial surfaces. To this, either Ti-SLA discs or Ti-Ana discs were deployed as modified titanium surfaces and Ti-ma discs as well as tissue culture plastic coverslips were utilized as control surfaces. Incubation on all surfaces was done using complete medium without any polarization agents, complete medium with 50 ng/ml IFNγ and 10 ng/ml LPS or complete medium with 20 ng/ml IL4 and 20 ng/ml IL13 for 2 days to allow for polarization to the M0-, M1 or M2-phenotype, respectively.

Following, the polarized MdM were investigated using CCK8 cell proliferation assay, ELISA as well as BCA protein assay and CLSM in order to assess potential immunomodulatory effects of the diverse biomaterial surfaces.

3.5 Evaluation of immunomodulatory effects using CCK8 cell proliferation assay

CCK8 cell proliferation assay was conducted to control for direct adverse effects of the titanium surfaces on the cultivated cells. At this juncture, metabolic activity was assessed being a surrogate of MdM viability and cell number, thus enabling to determine the relative proliferation of the cells. Prior to the measurement, MdM were cultivated on the diverse titanium discs as well as on coverslips and polarization was induced each using complete medium without any polarizing agents, complete medium with addition of 50 ng/ml IFNγ and 10 ng/ml LPS as well as complete medium with addition of 20 ng/ml IL4 and 20 ng/ml IL13 for 2 days for the M0-, M1- and M2-phenotype, respectively. As shown in ***Fig. 26***, metabolic activity and thus relative proliferation is high for all MdM, irrespective of their polarization. Moreover, MdM on all surfaces tested showed a relative proliferation rate of similar extent. Neither polarization nor biomaterial surface resulted in any significant difference of MdM metabolic activity. Thus, regarding compatibility, Ti-SLA discs and Ti-Ana discs are assimilable to Ti-ma discs and none of the surfaces tested has a significant, direct adverse effect on the cultivated MdM. The arithmetic means ± SEM of relative proliferation for n = 5 repeats (for M0 coverslip, M0 Ti-ma, M0 Ti-SLA, M0 Ti-Ana, M1 coverslip, M1 Ti-ma, M2 coverslip, M2 Ti-ma) or for n = 3 (for M1 Ti-SLA, M1 Ti-Ana, M2 Ti-SLA, M2 Ti-Ana) were 99.99 ± 10.93 %, 91.41 ± 12.28 % and 105.0 ± 15.15 % for M0-, M1-, and M2-MdM on coverslips, 102.4 ± 18.42 %, 86.72 ± 12.32 % and 100.5 ± 14.91 % for M0-, M1- and M2-MdM on Ti-ma discs, 85.97 ± 10.59 %, 94.08 ± 20.22 % and 102.4 ± 20.60 % for M0-, M1- and M2-MdM on Ti-SLA discs as well as 90.92 ± 15.72 %, 99.93 ± 13.23 % and 113.2 ± 16.28 % for M0-, M1- and M2-MdM on Ti-Ana discs.

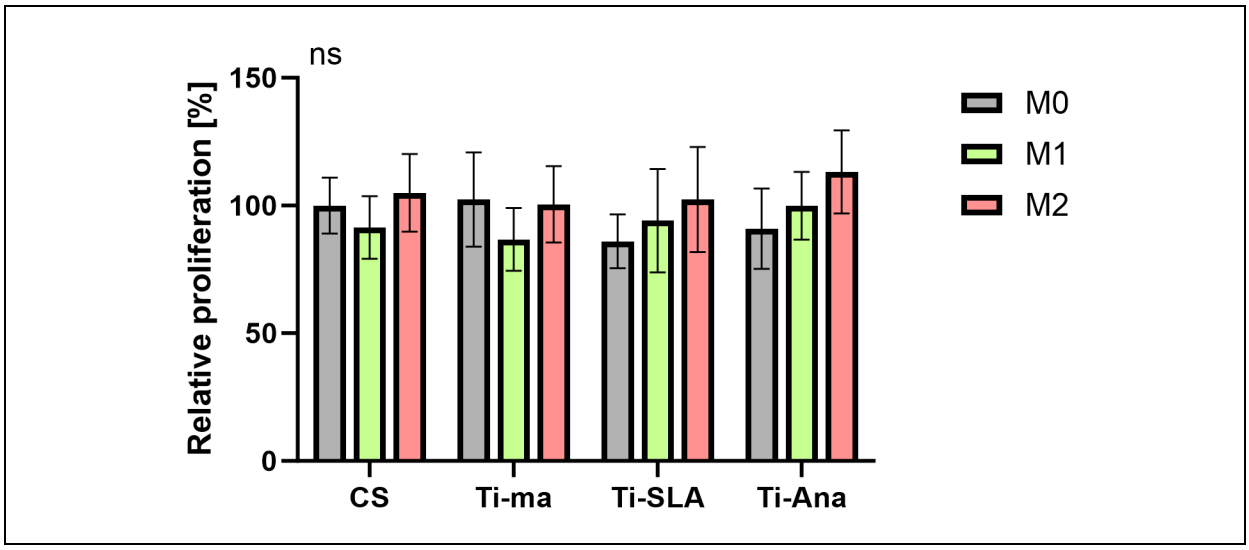

Figure 26: MdM relative proliferation on tissue culture plastic coverslips, Ti-ma discs, Ti-SLA discs and Ti-Ana discs subsequent to polarization to M0-, M1- and M2-phenotype*. Arithmetic means ± SEM (n = 5 for M0 coverslip, M0 Ti-ma, M0 Ti-SLA, M0 Ti-Ana, M1 coverslip, M1 Ti-ma, M2 coverslip, M2 Ti-ma; n = 3 for M1 Ti-SLA, M1 Ti-Ana, M2 Ti-SLA, M2 Ti-Ana) of MdM relative proliferation [%] on coverslips, Ti-ma discs, Ti-SLA dics and Ti-Ana discs following their polarization to M0- (grey), M1- (green), and M2- (red) phenotype for 2 days. ns indicated non-significancy (Kruskal-Wallis test).*

3.6 Evaluation of immunomodulatory effects using ELISA and BCA protein assay

In order to assess potential immunomodulatory effects of the diverse titanium surfaces on the cultivated MdM, ELISA was conducted regarding the secretion of cytokines. As determined afore ***(Chap. 3.2)***, TNFα as well as CCL13 were chosen as markers regarding M1- and M2-polarization, respectively, due to their specificity and their accented secretion. Moreover, BCA protein assay was complemented to normalize the cytokine concentration to the amount of total protein secreted. Prior to the measurement, the MdM were cultivated on the diverse titanium discs as well as on coverslips and polarization was induced each using complete medium without any polarizing agents, complete medium with addition of 50 ng/ml IFNγ and 10 ng/ml LPS as well as complete medium with addition of 20 ng/ml IL4 and 20 ng/ml IL13 for 2 days for the M0-, M1- and M2-phenotype, respectively. ***Fig. 27*** depicts TNFα secretion of M0-MdM as well as of M1-MdM. As depicted, regarding both polarization states, neither of the surfaces tested induced increased secretion of TNFα as compared to coverslips and Ti-ma discs and thus Ti-SLA discs and Ti-Ana discs did not exert proinflammatory effects. The arithmetic means ± SEM of the TNFα concentration for n = 5 repeats were 36.69 ± 17.91 pg/ml/mg of total protein, 47.07 ± 11.00 pg/ml/mg of total protein, 37.30 ± 10.79

pg/ml/mg of total protein and 56.57 ± 20.86 pg/ml/mg of total protein for the M0-MdM on coverslips, Ti-ma discs, Ti-SLA discs and Ti-Ana discs, respectively. The arithmetic means ± SEM of the TNFα concentration for n = 5 (M1 coverslip, M1 Ti-ma) or n = 3 (M1 Ti-SLA, M1 Ti-Ana) repeats were 807.60 ± 96.46 pg/ml/mg of total protein, 781.10 ± 102.90 pg/ml/mg of total protein, 849.40 ± 162.40 pg/ml/mg of total protein and 1024.00 ± 427.10 pg/ml/mg of total protein for the M1-MdM on coverslips, Ti-ma discs, Ti-SLA discs and Ti-Ana discs, respectively.

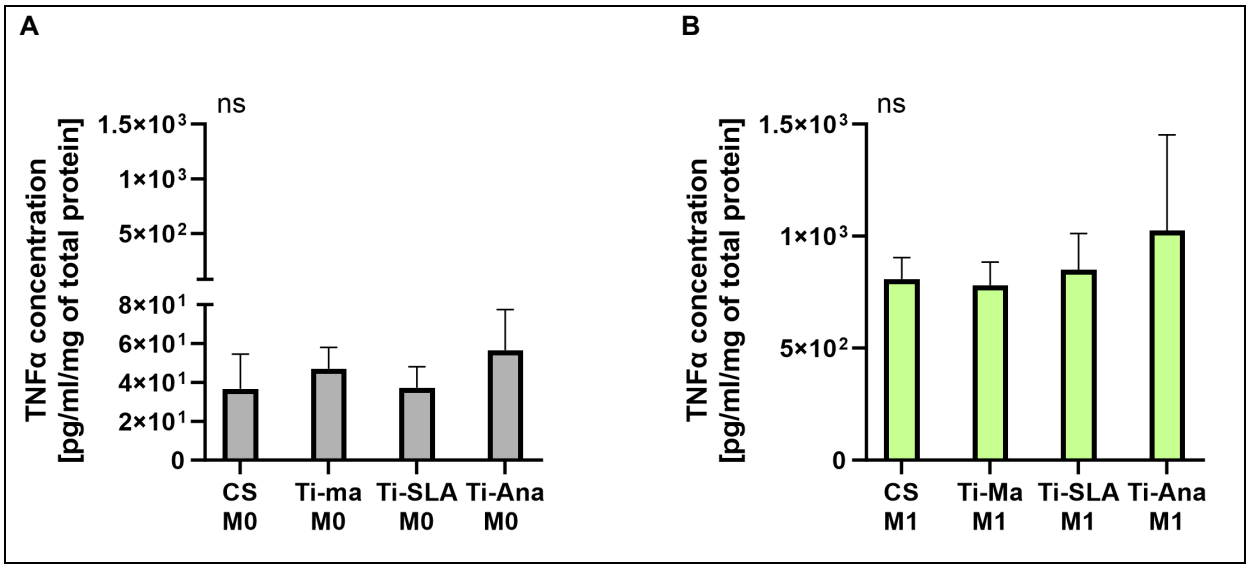

Figure 27: MdM secretion of TNFα subsequent to polarization to M0- and M1-phenotype on coverslips, Ti-ma discs, Ti-SLA discs and Ti-Ana discs*. **A** Arithmetic means ± SEM (n = 5) of TNFα concentration [pg/ml/mg of total protein] in the cell culture supernatant after polarization to M0-MdM for 2 days using ELISA. ns indicates non-significancy (Friedmann test). **B** Arithmetic means ± SEM (n = 5 for M1 coverslip, M1 Ti-ma; n = 3 for M1 Ti-SLA, M1 Ti-Ana) of TNFα concentration [pg/ml/mg of total protein] in the cell culture supernatant after polarization to M1-MdM for 2 days using ELISA. ns indicated non-significancy (one-way ANOVA).*

Fig. 28 depicts CCL13 secretion of M0-MdM as well as of M2-MdM. As illustrated, concerning the M0-phenotype, CCL13 secretion of MdM cultivated on Ti-Ana discs was significantly lower compared to Ti-ma discs. Besides, no other significant differences of CCL13 concentration existed as to M0-MdM. Regarding the M2-phenotype, CCL13 secretion of MdM cultivated on Ti-Ana discs was significantly decreased compared to M2-MdM cultivated on coverslips. No other significant differences of CCL13 concentration existed as to M2-MdM. Both findings suggest a diminished anti-inflammatory influence of Ti-Ana discs. The arithmetic means ± SEM of the CCL13 concentration for n = 5 repeats were 21.15 ± 5.49 pg/ml/mg of total protein, 38.55 ± 4.04 pg/ml/mg of

total protein, 30.97 ± 5.63 pg/ml/mg of total protein and 11.22 ± 0.70 pg/ml/mg of total protein for the M0-MdM on coverslips, Ti-ma discs, Ti-SLA discs and Ti-Ana discs, respectively. The arithmetic means ± SEM of the CCL13 concentration for n = 5 (M2 coverslip, M2 Ti-ma) or n = 3 (M2 Ti-SLA, M2 Ti-Ana) repeats were 571.10 ± 71.31 pg/ml/mg of total protein, 334.90 ± 61.91 pg/ml/mg of total protein, 422.50 ± 60.47 pg/ml/mg of total protein and 1510 ± 32.58 pg/ml/mg of total protein for the M2-MdM on coverslips, Ti-ma discs, Ti-SLA discs and Ti-Ana discs, respectively.

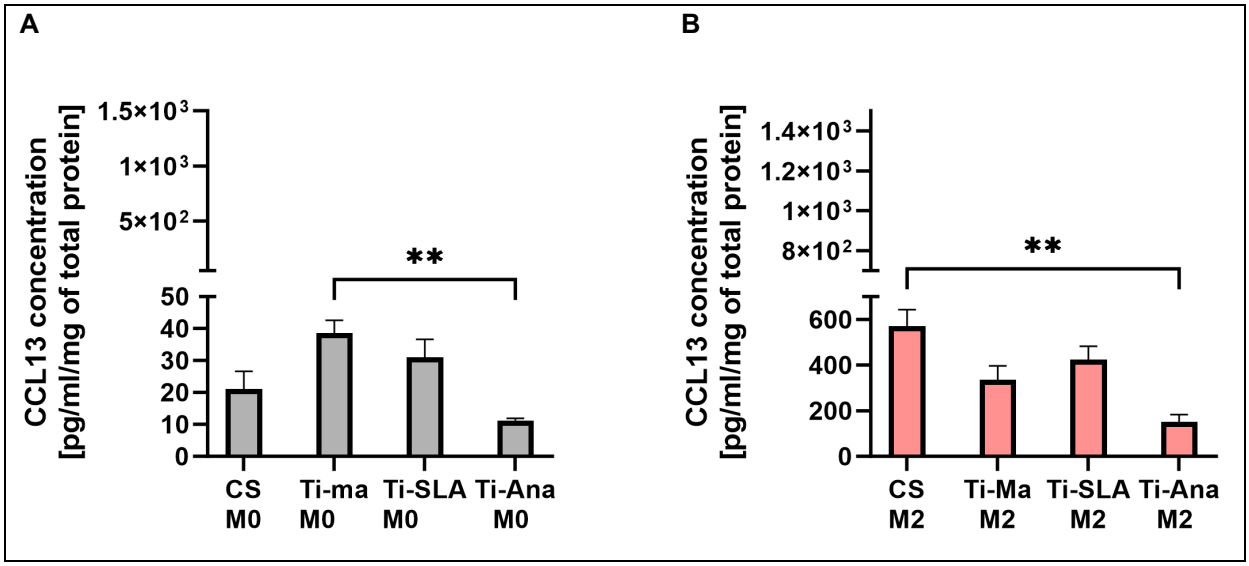

Figure 28: MdM secretion of CCL13 subsequent to polarization to M0- and M2-phenotype on coverslips, Ti-ma discs, Ti-SLA discs and Ti-Ana discs*. **A** Arithmetic means ± SEM (n = 5) of CCL13 concentration [pg/ml/mg of total protein] in the cell culture supernatant after polarization to M0-MdM for 2 days using ELISA. (one-way ANOVA). **B** Arithmetic means ± SEM (n = 5 for M2 coverslip, M2 Ti-ma; n = 3 for M2 Ti-SLA, M2 Ti-Ana) of CCL13 concentration [pg/ml/mg of total protein] in the cell culture supernatant after polarization to M2-MdM for 2 days using ELISA. ** p ≤ 0.01 indicates significant difference (one-way ANOVA).*

3.7 Evaluation of immunomodulatory effects using CLSM

Eventually, potential immunomodulatory effects of the diverse titanium surfaces on the cultivated MdM were tested using CLSM. Morphology of the M0-, M1- and M2-MdM was evaluated as a start deploying phalloidin for cytoskeleton staining and DRAQ5 as staining of the nuclei. To this, the MdM were seeded on coverslips following to their differentiation. Treatment with complete medium without any polarizing agents, complete medium with 50 ng/ml IFNγ and 10 ng/ml LPS or complete medium with 20 ng/ml IL4 and 20 ng/ml IL13 for 2 days was undertaken to allow for polarization to the M0-, M1 or M2-phenotype, respectively, before the assessment using CLSM. As illustrated

in ***Fig. 29***, no major morphologic differences between the MdM cultivated on the different surfaces could be determined. As stated afore ***(Chap. 3.4.1)***, independent of the respective surface M0-MdM featured a round morphology, M1-MdM exhibited a round shape with some star-shaped spiculae and M2-MdM were hallmarked by elongation.

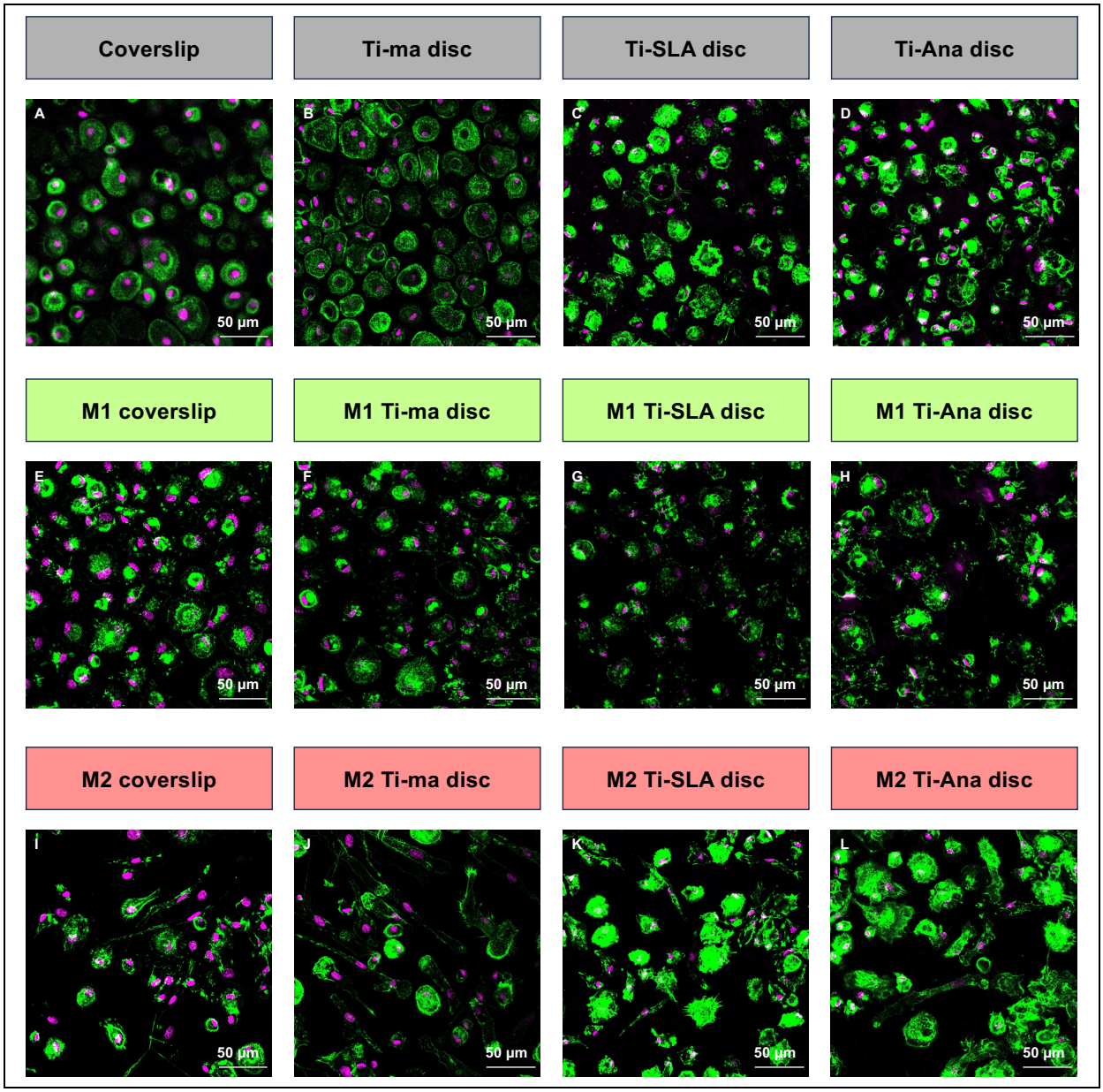

Figure 29: MdM cytoskeletal morphology subsequent to polarization to M0-, M1- and M2-phenotype on coverslips, Ti-ma discs, Ti-SLA discs and Ti-Ana discs*. Representative cytoskeletal MdM morphology using CLSM with phalloidin as well as DRAQ5 staining following incubation with complete medium without addition of polarizing agents, complete medium with 50 ng/ml IFNγ and 10 ng/ml LPS or complete medium with 20 ng/ml IL4 and 20 ng/ml IL13 for 2 days to induce M0-, M1- or M2-polarization, respectively. Polarization was undertaken adjacent to seeding differentiated MdM onto coverslis, Ti-ma discs, Ti-SLA discs and Ti-Ana discs. Green = phalloidin staining, pink = DRAQ5 staining.* ***A*** *M0-MdM on coverslip, 25X magnification, 2.5X zoom,* ***B*** *M0-MdM on Ti-ma disc, 25X magnification, 2.5X zoom,* ***C*** *M0-MdM on Ti-SLA disc, 25X magnification, 2.5X zoom,* ***D*** *M0-MdM on Ti-Ana disc, 25X magnification, 2.5X zoom,* ***E*** *M1-MdM on coverslip, 25X magnification, 2.5X zoom,* ***F*** *M1-MdM on Ti-ma*

disc, 25X magnification, 2.5X zoom, ***G*** *M1-MdM on Ti-SLA disc, 25X magnification, 2.5X zoom,* ***H*** *M1-MdM on Ti-Ana disc, 25X magnification, 2.5X zoom,* ***I*** *M2-MdM on coverslip, 25X magnification, 2.5X zoom,* ***J*** *M2-MdM on Ti-ma disc, 25X magnification, 2.5X zoom,* ***K*** *M2-MdM on Ti-SLA disc, 25X magnification, 2.5X zoom,* ***L*** *M2-MdM on Ti-Ana disc, 25X magnification, 2.5X zoom.*

Finally, CCR7 as well as CD209 expression of the polarized MdM cultivated on the different surfaces was assessed using CLSM. The latter markers were stained deploying specific primary and fluorescently labelled secondary antibodies. Furthermore, nuclei staining was done utilizing DRAQ5. Prior to staining, the MdM were seeded on coverslips following to their differentiation. Treatment with complete medium without any polarization agents, complete medium with 50 ng/ml IFNγ and 10 ng/ml LPS or complete medium with 20 ng/ml IL4 and 20 ng/ml IL13 for 2 days was undertaken to allow for polarization to the M0-, M1 or M2-phenotype, respectively, before the assessment using CLSM. ***Fig. 30*** shows a specific CCR7 expression of M1-MdM rather independent of the respective surfaces tested whereas M0- and M2-MdM exhibit only minor CCR7-related fluorescence. There were no significant differences in CCR7 fluorescence intensity regarding each, M0- or M1-MdM. Therefore, neither Ti-SLA discs, nor Ti-Ana discs exerted proinflammatory effect distinct from the control surfaces. The arithmetic means ± SEM of the CCR7 fluorescence intensity for n = 4 repeats were 0.53 ± 0.22, 0.50 ± 0.24, 0.46 ± 0.10 and 0.33 ± 0.06 for the M0-MdM on coverslips, Ti-ma discs, Ti-SLA discs and Ti-Ana discs, respectively. The arithmetic means ± SEM of the CCR7 fluorescence intensity for n = 2 repeats were 1.16 ± 0.26, 1.06 ± 0.36, 2.51 ± 1.36 and 1.24 ± 0.63 for the M1-MdM on coverslips, Ti-ma discs, Ti-SLA discs and Ti-Ana discs, respectively. Contrarily, CD209 was specifically expressed in M2-MdM. Likewise, expression was rather independent of the respective surface utilized for cultivation. Neither M0-, nor M1-MdM feature relevant CD209 expression. There were no significant differences in CD209 fluorescence intensity regarding each, M0- or M2-MdM. Neither Ti-SLA discs, nor Ti-Ana discs significantly reduced anti-inflammatory effects as compared to the deployed control surfaces. The arithmetic means ± SEM of the CCR7 fluorescence intensity for n = 4 repeats were 0.11 ± 0.05, 0.40 ± 0.19, 0.06 ± 0.03 and 0.16 ± 0.11 for the M0-MdM on coverslips, Ti-ma discs, Ti-SLA discs and Ti-Ana discs, respectively. The arithmetic means ± SEM of the CCR7 fluorescence intensity for n = 2 repeats were 2.42 ± 0.67, 1.43 ± 0.30, 3.47 ± 2.34 and 1.00 ± 0.24 for the M2-MdM on coverslips, Ti-ma discs, Ti-SLA discs and Ti-Ana discs, respectively.

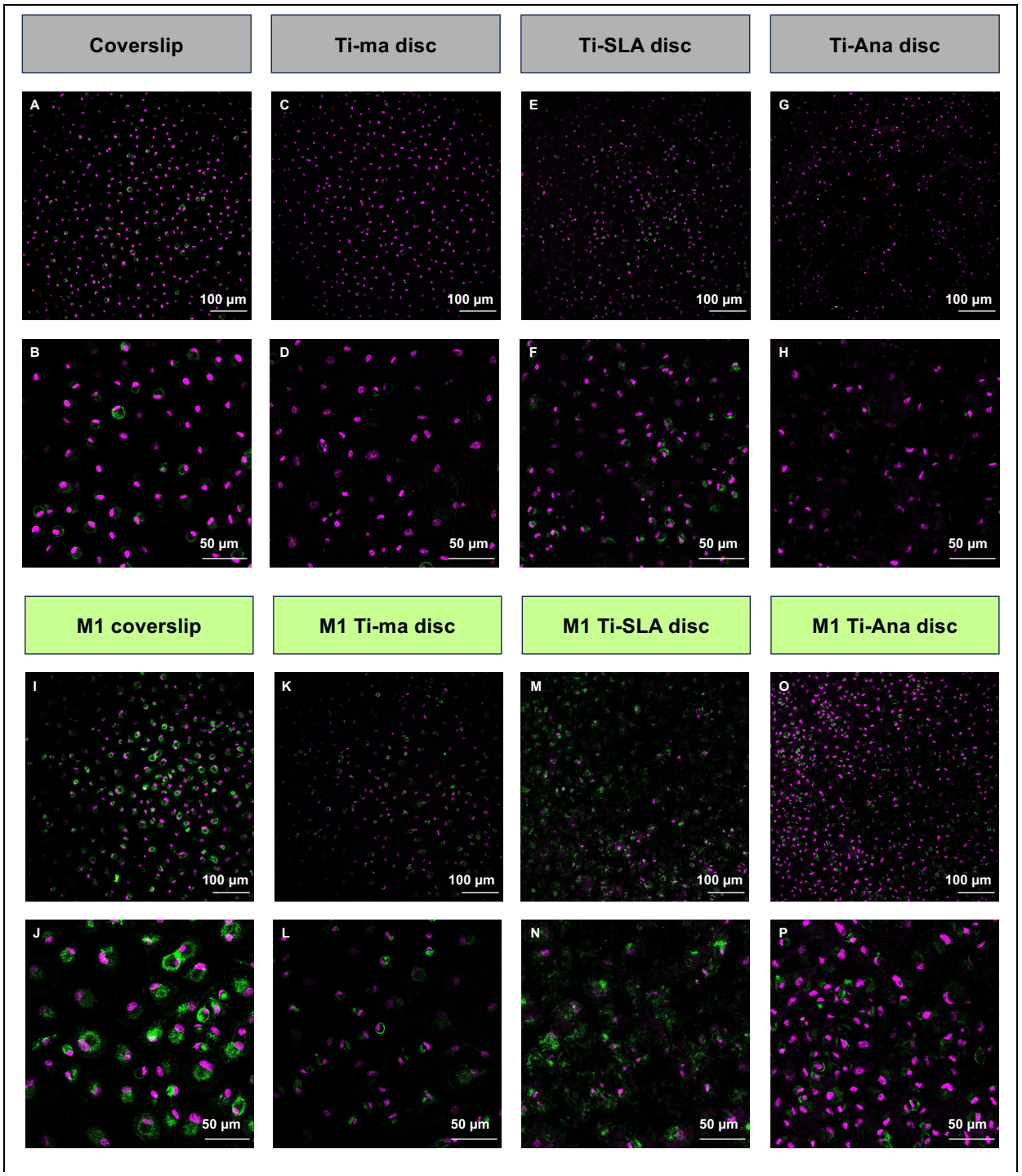
Coverslip
Ti-ma disc
Ti-SLA disc
Ti-Ana disc
A
C
E
G
100 µm
B
D
F
H
50 µm
M1 coverslip
M1 Ti-ma disc
M1 Ti-SLA disc
M1 Ti-Ana disc
I
K
M
O
J
L
N
P

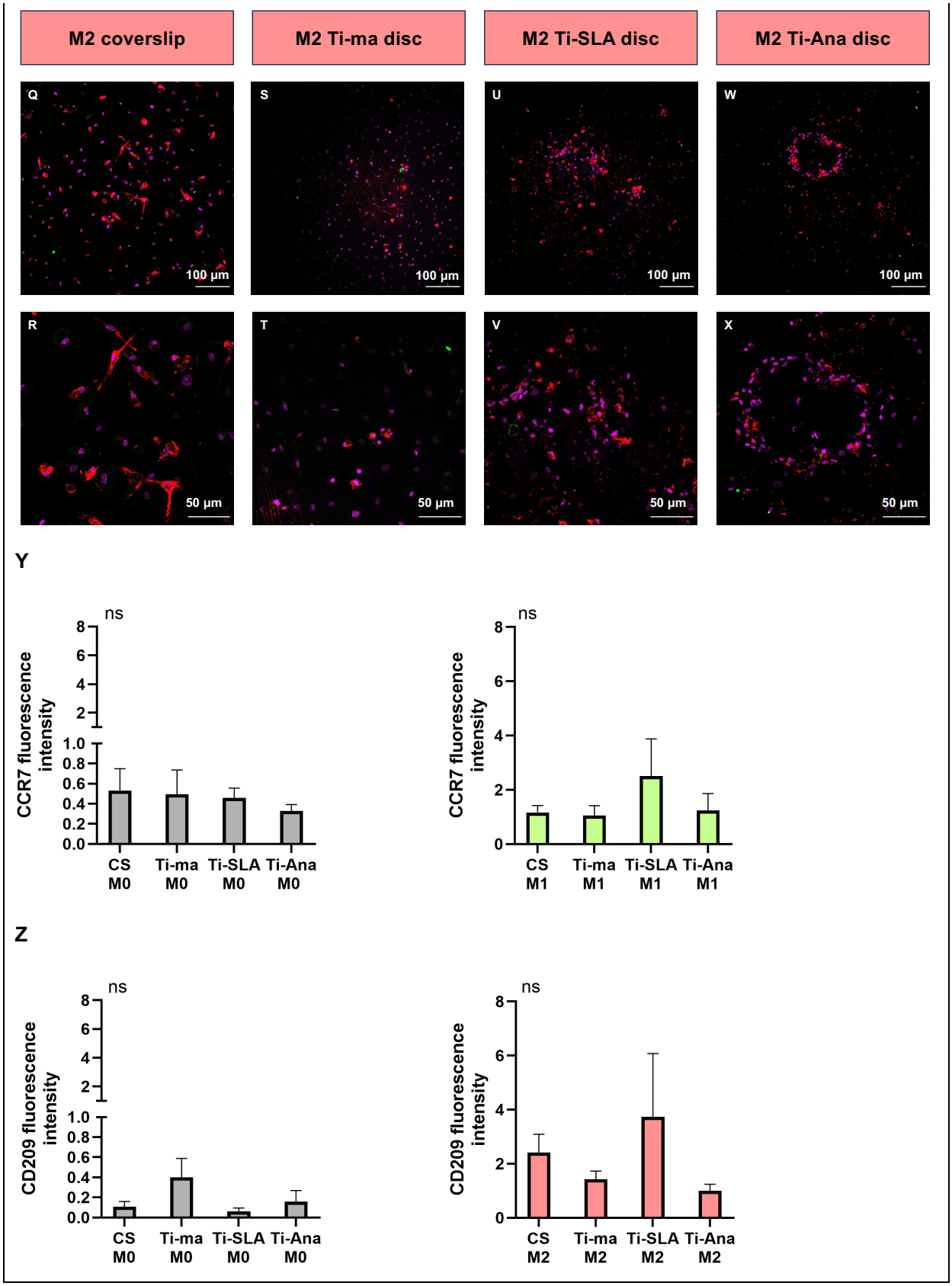

Figure 30: MdM expression of CCR7 and CD209 subsequent to polarization to M0-, M1- and M2-phenotype on coverslips, Ti-ma discs, Ti-SLA discs and Ti-Ana discs *modified according to [77]. Representative expression of CCR7 and CD209 of MdM using CLSM and antibody staining of the surface markers as well as DRAQ5 staining following incubation with complete medium without addition of polarizing agents, complete medium with 50 ng/ml IFNγ and 10 ng/ml LPS or complete medium with 20 ng/ml IL4 and 20 ng/ml IL13 for 2 days to induce M0-, M1- or M2-polarization, respectively. Polarization*

was undertaken adjacent to seeding differentiated MdM onto coverslips, Ti-ma discs, Ti-SLA discs and Ti-Ana discs. Green = CCR7 staining, red = CD209 staining, pink = DRAQ5 staining. ***A*** *M0-MdM on coverslip, 25X magnification, 1X zoom,* ***B*** *M0-MdM on coverslip, 25X magnification, 2.5X zoom,* ***C*** *M0-MdM on Ti-ma discs, 25X magnification, 1X zoom,* ***D*** *M0-MdM on Ti-ma disc, 25X magnification, 2.5X zoom,* ***E*** *M0-MdM on Ti-SLA discs, 25X magnification 1X zoom,* ***F*** *M0-MdM on Ti-SLA disc, 25X magnification, 2.5X zoom,* ***G*** *M0-MdM on Ti-Ana discs, 25X magnification 1X zoom,* ***H*** *M0-MdM on Ti-Ana disc, 25X magnification, 2.5X zoom,* ***I*** *M1-MdM on coverslip, 25X magnification, 1X zoom,* ***J*** *M1-MdM on coverslip, 25X magnification, 2.5X zoom,* ***K*** *M1-MdM on Ti-ma discs, 25X magnification, 1X zoom,* ***L*** *M1-MdM on Ti-ma disc, 25X magnification, 2.5X zoom,* ***M*** *M1-MdM on Ti-SLA discs, 25X magnification 1X zoom,* ***N*** *M1-MdM on Ti-SLA disc, 25X magnification, 2.5X zoom,* ***O*** *M1-MdM on Ti-Ana discs, 25X magnification 1X zoom,* ***P*** *M1-MdM on Ti-Ana disc, 25X magnification, 2.5X zoom,* ***Q*** *M2-MdM on coverslip, 25X magnification, 1X zoom,* ***R*** *M2-MdM on coverslip, 25X magnification, 2.5X zoom,* ***S*** *M2-MdM on Ti-ma discs, 25X magnification, 1X zoom,* ***T*** *M2-MdM on Ti-ma disc, 25X magnification, 2.5X zoom,* ***U*** *M2-MdM on Ti-SLA discs, 25X magnification 1X zoom,* ***V*** *M2-MdM on Ti-SLA disc, 25X magnification, 2.5X zoom,* ***W*** *M2-MdM on Ti-Ana discs, 25X magnification 1X zoom,* ***X*** *M2-MdM on Ti-Ana disc, 25X magnification, 2.5X zoom.* ***Y*** *Arithmetic means ± SEM (n = 4 for M0-MdM; n = 2 for M1-MdM) of MdM CCR7 fluorescence intensity following their polarization to M0- (grey) or M1- (green) phenotype for 2 days. ns indicates non-significancy (one-way ANOVA for M0-MdM; Friedmann test for M1-MdM).* ***Z*** *Arithmetic means ± SEM (n = 4 for M0-MdM; n = 2 for M2-MdM) of MdM CD209 fluorescence intensity following their polarization to M0- (grey) or M2- (red) phenotype for 2 days. ns indicates non-significancy (one-way ANOVA for M0-MdM; Friedmann test for M2-MdM).*

4 Discussion

Tooth loss up to total edentulism is a frequent and globally existent issue [56, 102]. To the concerned patients, this affliction is of particular importance, as it is not only concomitant with limitations concerning mastication and phonetics but also results in constricted aesthetics and psychosocial discomfort [3, 41, 102, 107, 113]. Therapeutically, prosthetic restorations, such as bridges or removable dentures, are deployed as to the substitution of missing teeth [56]. Yet, the latter treatment options oftentimes require the preparation of adjacent teeth and furthermore, especially removable dentures may be functionally and aesthetically unfavorable [38, 56]. Dental implants on the other hand allow for the avoidance of these detriments and therefore have evolved into a major alternative within the rehabilitation of tooth loss [25, 38, 41, 56, 85, 110, 112]. Moreover, the latter therapeutic option allows for high survival rates as well as longevity and is therefore considered to be reliable [3, 6, 25, 42, 56, 110, 133].

However, malfunction redounding to as far as implant failure can occur and particularly encompasses progressive peri-implant bone loss [8, 37, 42, 65, 78, 110]. Due to the considerable number of placed dental implants, this malfunction constitutes a rising problem and consistent solution approaches have been owing [93, 123]. On a molecular level, marginal bone loss is based upon aggravated immune processes in terms of a continuing or a recurrent FBR correspondent to a failed establishment or the loss of an FBE ***(Chap. 1.3.1)*** [93, 123, 133].

An FBR is set off in the context of an implant insertion successional to the surgically provoked trauma and the contact between the foreign body as well as the host's tissue and blood [8, 10-12, 44, 71, 145]. To begin with, interstitial and blood proteins adsorb to the biomaterial surface [1, 12, 22, 32, 44, 51, 63, 118, 131, 142, 145] and the coagulation as well as the complement cascade are commenced [10, 11, 44, 145]. Immune cells, particularly comprising neutrophilic granulocytes and MΦ, migrate due to chemotaxis and bind to the biomaterial's surface [10-12, 32, 44, 51, 145]. There, the latter cells engulf intruded pathogens as well as debris and secrete proteolytic enzymes and ROS [10, 44, 145]. These defense mechanisms might concomitantly damage the implant [8, 123]. As the FBR proceeds, MΦ soon predominate [10-12, 44, 145] and, conditional upon the prevalent micro-environment, sequentially adjust their polarization

state from a pro-inflammatory M1-phenotype to a regulatory and wound-healing M2-polarization [1, 32, 44, 145]. Furthermore, the residing MΦ partially fuse forming FBGC [10, 24, 44, 145]. In terms of these different phenotypes, MΦ are present on the biomaterial's surface throughout its *in vivo* lifetime [11, 22, 24, 106, 123]. In case at this point anti-inflammatory influences markedly excel the pro-inflammatory immune activation, tantamount to an FBE, osseointegration as to bone ensues [8, 10, 12, 37, 123]. Contrarily, if pro-inflammatory stimuli persist, equivalent to a lasting FBR, reinforced MΦ fusion results provoking biomaterial damage and marginal bone loss due to exacting degradative capacity as well as extensive fibrous encapsulation of the implant [1, 12, 23, 31, 44, 145].

As can be derived from the aforementioned considerations, MΦ critically control major phases of the FBR and the FBE [11, 22, 24, 106, 123]. On this account, solution statements concerning peri-implant bone loss should aim at disclosing cellular and molecular mechanisms of the FBR and the FBE bringing MΦ into focus [123].

Antecedently, MΦ have manifoldly been investigated and characterized bearing heterogenous markers using diverse cell models as well as protocols [2, 60, 62, 77, 119, 130]. In order to enhance reliability and enable comparability of MΦ research, an appropriate cell model, corresponding consensus markers as well as standardized and verified protocols as to the preparation as well as to the analysis of MΦ are precondition [77]. Accordingly, the conducted study strived for the establishment of a protocol to isolate and differentiate human peripheral blood monocytes towards polarized MdM in the first section to subsequently deepen knowledge on osseointegration and investigate potential immunomodulatory effects of biomaterials on the latter cells *in vitro* in the second part [77].

Regarding the MΦ cell model, cells emanating from diverse sources have been deployed for the purpose of research [77, 82, 83, 101, 119, 130, 132, 145]. From a biological and scientific contemplation, human primary MΦ may be most representative and reliable concerning the *in vivo* situation [77, 82, 83]. However, the latter cells are differentiated and thus limitedly proliferating, impeding their sufficient quantitative availability [13, 34, 52, 53, 67, 82, 83, 96, 105, 144]. Furthermore, human primary MΦ are

tissue-resident cells necessitating intricate isolation processes concomitant with a disproportional and ethically discerning impairment of their donor [13, 34, 52, 53, 67, 83, 96, 105, 144]. Lastly, due to the heterogeneity of primary cells, validity as well as reproducibility of research results may be restricted [29]. Hence, either murine MΦ, appropriate human cell lines or MdM are commonly utilized instead [81, 119, 145].

Murine MΦ for *in vitro* research are either attained from the red bone marrow as BMdM or are isolated from murine tissue in terms of readily differentiated, tissue-resident cells ***(Chap. 1.4.1)*** [88, 101]. However, these MΦ differ from human cells regarding several facets, thus findings cannot unrestrictedly be transferred to the *in vivo* situation [61, 62, 82, 88, 119].

Cell lines on the other hand encompass immortalized cells hallmarked by unrestricted proliferation upon cultivation [26, 77, 83]. As to MΦ, several human cell lines of varying degree of differentiation are available ***(Chap. 1.4.1)*** [13, 29, 30, 34, 96]. Due to their similarity to primary cells regarding morphology, function and their ability to be polarized, THP1 cells are oftentimes employed with reference to *in vitro* research [13, 28-30, 96, 105, 119, 145]. Advantageously, cell lines are cost-effective, modest as to their cultivation and proliferate up to a high passage constituting an infinite source of barely senescent cells [13, 29, 30, 77, 83, 105, 145]. Furthermore, these cells feature a homogenous geno- as well as phenotype facilitating consistency and reproducibility [13, 29, 30, 83, 105, 145]. However, cell lines are commonly derived from malignant neoplasms, thus characteristics, especially regarding gene expression, may be clearly distinct from primary cells [29, 30, 77, 88, 119]. Correspondingly, THP1 cells were shown to be contorted towards the M1-polarization and its associated characteristics whereas U937 cells are rather prone to the M2-phenotype [77, 83]. Moreover, commonly, pharmacological treatment deploying unphysiological stimuli, like phorbol-12-myristate-13-acetate (PMA), is needed as to the differentiation towards MΦ [88]. Altogether, findings deduced from cell lines may thus be biased [29, 30, 34, 96, 105, 119].

By reason of the above-quoted limitations of the preceding cell models, human primary monocytes oftentimes are utilized for *in vitro* research instead [88, 119, 144]. The latter cells constitute the precursors to a subset of the human MΦ ***(Chap. 1.2.1)*** [40, 53, 54, 57, 80]. Advantageously, human primary monocytes can be accessed straightforwardly as well as ethically more reasonably in sufficient quantity in terms of whole blood or buffy coat via peripheral venipuncture [67, 68, 84]. Adjacent to their isolation,

these cells can be differentiated towards MdM as well as polarized *in vitro* [67, 68, 84]. On the basis of these considerations, MdM were chosen as cell model for the present study [77].

Following to the determination of the cell model, an adequate protocol as to the preparation of polarized MdM was to be established. To the isolation of monocytes, the differentiation to MdM and the eventual polarization, a multiplicity of protocols are delineated ***(Chap. 1.4.2)*** [18, 55, 59, 61, 62, 67, 68, 84, 98-100, 119, 130]. Generally, PBMC are separated from whole blood or buffy coat at first using density gradient centrifugation on the basis of varying density of the blood components [18, 33, 55, 59, 61, 67, 68, 84, 98-100, 119, 130, 144]. Subsequently, monocytes can be partitioned from lymphocytes by means of reapplication of density gradient centrifugation [17, 33, 35, 50, 98], CD14+ or negative immunoselection [18, 33, 55, 59, 67, 84, 100, 119, 130] or monocyte adhesion [55, 61, 84, 100, 144]. Following, differentiation to MdM is attained incubating the former cells with growth factors such as GM-CSF or M-CSF for 3 to 7 days [18, 59, 61, 62, 84, 100, 119, 130]. The resulting MdM can eventually be polarized by means of another stimulation using cytokines, LPS, immune complexes as well as glucocorticoids for 24 hours up to 3 days [18, 55, 61, 62, 84, 100, 119, 130]. Regarding the techniques of monocyte isolation and MΦ differentiation as well as polarization delineated afore, various considerations have to be taken heed of [33, 84, 98].

Density gradient centrifugation of whole blood or buffy coat allows for a rough separation of different cell populations [33]. Yet, cell loss due to the isolation procedure has to be taken into account [33]. Concerning PBMC, a considerable fraction of granulocytes and furthermore nonviable cells and debris can be eliminated effectuating a concentration of monocytes and facilitating their further isolation [33].

As to the separation of monocytes from lymphocytes, the existing protocols, irrespective of the particular method deployed, for the most part are rather laborious as well as time-consuming [98]. Both, density gradient centrifugation and monocyte adhesion are feasible, dependable and cost-effective techniques [98]. Yet, regarding density gradient centrifugation, a separation medium is deployed [98]. As the cells are directly exposed during the isolation process, monocytes might be affected, particularly in case of persisting contact [98]. Favorably, monocyte adhesion only depends on a plastic or glass surface as well as cell culture or adhesion medium [98]. However, if loose

monocytes are sought, cell detachment, either enzymatically or mechanically, is required subsequent to the isolation, potentially impairing the cells' integrity [43, 88, 98]. Immunoselection on the other hand necessitates elaborate appliances and is rather costly [98]. Furthermore, cell yield, purity, viability and the resulting phenotype of the successive MdM are contingent on the method utilized [84, 98]. Due to an overlap of monocyte as well as lymphocyte density, density gradient centrifugation is hindered and yields considerable contamination [19, 98]. Utilizing a separation medium with modified osmolarity can enhance partition depending on a more distinct susceptibility of lymphocytes to heightened osmolarity [19, 98]. An increase in purity simultaneously involves diminution in the cell number of isolated monocytes, though, whereas cell viability remains unaffected [19, 98]. Additionally, another centrifugation with iso-osmotic separation medium may furthermore effectuate the depletion of contaminating platelets [98]. Immunoselection, both CD14+ immunoselection as well as negative immunoselection, was shown to amount to an elevated monocyte yield as well as to high viability [84]. Regarding purity however, negative immunoselection resulted in increased platelet contamination, whereas CD14+ immunoselection was highly specific [84]. Using monocyte adhesion, platelet as well as lymphocyte contamination was observed to be considerably increased [35, 84, 98] and viability was found to be lessened compared to immunoselection [84]. On the other hand, however, neither monocyte adhesion nor density gradient centrifugation skew the monocytic subpopulation as might follow from CD14+ immunoselection [84]. In due consideration of these potential influences on the isolated monocytes and the resulting MdM, the employed method of isolation has to be taken account of and adjusted to the intended research purpose, if necessary [84].

In terms of the differentiation of isolated human blood monocytes towards MdM, it was shown, that sole cell culture medium is not sufficient for sustained cell survival [15, 144]. Instead, growth factors, such as GM-CSF or M-CSF, cytokines, like IL3, or normal human serum (NHS) are required to effectuate differentiation [130, 144]. At this juncture, the growth factors GM-CSF and M-CSF were shown to already influence polarization as well as MdM morphology [74, 130, 144]. While a slight M1-polarization is attributed to GM-CSF, M-CSF was revealed to foster the M2-phenotype [64, 81, 117, 128, 130]. NHS on the other hand was detected to least result in polarization as characterized by marker expression [130]. Regarding the morphology, several studies link GM-CSF with a round phenotype and M-CSF with stellate-like elongation [126, 130, 144].

Regarding a distinct polarization of the MdM, amongst others, cytokines are utilized [18, 55, 61, 62, 84, 100, 119, 130]. In this context, multiple agents have been deployed at various concentrations as well as conflations for varying periods [18, 55, 59, 61, 84, 100, 119, 130]. Furthermore, diverse subtypes of polarization, particularly concerning the M2-polarization, are distinguished [18, 55, 59, 61, 84, 100, 103, 119, 130].

With reference to the objective of establishing a protocol for the preparation of polarized MdM, within this study whole blood was deployed as to the isolation of monocytes [77]. Firstly, density gradient centrifugation was conducted for the isolation of PBMC and the blood suspension was carefully laid over the Lymphocyte Separation Medium to perpetuate an interface and prevent monocytes from subsiding. Following to the centrifugation, plasm was carefully but completely as possible removed to expose the fraction of PBMC and to obviate platelet contamination. The former cells were then collected into new tubes to elude remaining debris and sufficient washing was done to circumvent negative influences of the Lymphocyte Separation Medium on the PBMC. In order to deplete contaminating erythrocytes more distinctly, lysis was conducted using erythrocyte lysis buffer. This buffer osmotically affects erythrocytes without being effective on leukocytes [33]. Again, sufficient washing was performed to avoid prolonged impact of the lysis buffer as well as to remove debris and the isolated PBMC were collected. Monocytes were partitioned from lymphocytes using monocyte adhesion. To this, the PBMC were resuspended in pre-warmed Monocyte Attachment Medium and seeded into T75-flasks at a given cell density. Incubation was done for 90 minutes at 37° C and 5 % CO_2 to allow for the monocytes to adhere. Adjacently, the cells were carefully rinsed once using complete medium in order to remove residual suspended cells from the adherend monocytes [88]. Against the manufacturer's specific instructions, this washing step was done tentatively, as previously and repeatedly monocytes got lost in large part when washing vigorously as well as 3 times as demanded within the manufacturer's protocol (*data not shown*). Following to the isolation, monocytes were incubated with complete medium supplemented with 10 ng/ml M-CSF at 37° C and 5 % CO_2 in order to induce differentiation to MdM. M-CSF was chosen at a concentration of 10 ng/ml, as this growth factor has been predominantly employed within prior studies and as M-CSF was shown to enable M1- as well as M2-polarization of the resultant MdM [61, 62, 88, 119]. Treatment was done for 6 days and medium was exchanged every other day, discarding loose cells to possibly enhance purity.

Lastly, the differentiated MdM were polarized using either 50 ng/ml IFNγ and 10 ng/ml LPS as to the M1-phenotype or 20 ng/ml IL4 and 20 ng/ml IL13 in terms of the M2-polarization. MdM were incubated for 2 days at 37° C and 5 % CO_2.

Subsequent to the establishment of the protocol regarding the MdM preparation delineated afore, adequate consensus markers were determined as to a consistent and reliable characterization of the resultant cells. Within multiple studies, MΦ have been distinguished regarding their morphology, cytokine secretion, surface as well as intracellular marker expression and gene expression [18, 55, 59, 61, 62, 91, 108, 119, 126, 130]. However, characterization has been inconsistent and partly conflicting [2, 60, 62, 77, 119, 130, 132]. In the context of the present study, an index of multiple MdM markers was therefore determined [77]. Adjacent verification by means of assessment using light microscopy, ELISA, FACS and CLSM, all being frequently as well as routinely utilized methods, was deployed [77].

As to their morphology, the MdM prepared within this study were routinely evaluated during their differentiation and polarization using light microscopy ***(Chap. 3.1)***. At this juncture, M0-MdM were characterized by an irregular and extended constitution with some cells being elongated. M1-MdM predominantly featured a round phenotype effectuating a homogenous morphology. M2-MdM on the other hand were hallmarked by distinct elongation as well as stellate-like branching. These findings parallel results of prior studies [62, 119, 126, 129], although also obverse findings concerning morphology were delineated [130].

Regarding cytokine expression, previous studies reported TNFα to be specific as to the M1-phenotype [62, 130]. On the other hand, amongst others, CCL13 as well as CCL17 were shown to be increased with reference to M2-polarization [62]. For these reasons, the aforementioned cytokines were selected as potential markers of polarized MdM and thus checked within this study [77]. As delineated in ***Chap. 3.2***, TNFα concentration in the supernatant of M1-MdM was significantly as well as specifically heightened as compared to both, M0- and M2-polarization featuring a neglectable secretion [77]. In contrast, M2-MdM distinctly and specifically secreted CCL13 as well as CCL17, whereas concentration of these markers was quite low in the supernatant of M0- and M1-MdM ***(Chap. 3.2)*** [77]. Within this study, we hence confirmed TNFα and CCL13 as

well as CCL17 to be consensus markers of M1- and M2-phenotype, respectively, [77] and these results are in line with previous studies [18, 108, 119, 130].

Particularly concerning marker expression of the MdM, multiple surface as well as intracellular molecules have been investigated and findings are inconsistent to some extent here [18, 55, 59, 61, 62, 91, 108, 119, 126, 130]. Hence, many markers were tested within this study ***(Chap. 3.3)***. Regarding MΦ pan-markers, CD14 was highly expressed by all phenotypes. However, M0-MdM and M1-MdM still exhibited significantly heightened CD14 expression compared to the M2-polarization. CD68 on the other hand did not work as pan-marker for the cells prepared in this study. Regarding M1-polarization, CD80, CD86 and CCR7 were tested. Expression of CD80 was distinctly significant for M1-polarization compared to M0- and M2-MdM. Still, M2-MdM expression of CD80 was significantly higher than expression of M0-MdM, thus not being a fully specific marker. Furthermore, CD86 did not work for the cells prepared in this study, as this surface marker was highly and unselectively present on all MdM phenotypes. CCR7, on the other hand, was selectively expressed by M1-MdM and expression was significantly increased compared to M0- and M2-phenotype, thus constituting specific marker. Within previous studies, CD80 was frequently found to be a marker for M1-polarization [61, 62, 119]. CD86 was described to be specific for the M1-phenotype of MdM differentiated utilizing GM-CSF [18]. Within the present study however, although M-CSF was deployed as growth factor, all phenotypes highly expressed CD86, identifying this molecule to be unspecific at least in case of differentiation utilizing the latter growth factor. As to M2-polarization, CD1A, CD163, CD206, CD209 and Arg1 were investigated in the present study. Expression of CD1A was specific and significant regarding the M2-phenotype, whereas neither M0- nor M1-MdM exhibited distinct CD1A expression. CD163 expression, in contrast, was found in M0-, M1- and M2-phentoype, with M0-MdM expression being significantly heightened compared to M2-MdM. Furthermore, also M1-MdM CD163 expression was increased. Thus, CD163 was not appropriate as a marker for M2-polarization. CD206 was highly expressed by M0-, M1- and M2-MdM and expression of M0- and M2-phenotype was significantly higher compared to M1-MdM. Consequently, regarding marker expression, CD206 was not specific. Considering CD206 MFI, however, abundance of CD206 was significantly increased in M2-MdM and thus selectively marked these cells. Expression of CD209 was distinctly and significantly heightened in M2-MdM, whereas M0- and M1-polaization negligibly expressed this marker. Hence, CD209 constituted a specific

marker. Lastly, Arg1 did not work for the MdM prepared in this study, as neither of the M0-, M1- or M2-phenotype noteworthily expressed this surface marker. Specific M2-MdM expression of CD1A and CD209 was described in previous studies with our results being in line [119]. Regarding CD163, expression plurally was attributed to the M2c-phenotype and thus to IL10 or dexamethasone stimulation [61, 130]. Our M2-MdM, on the contrary, were prepared using IL4 and IL13, correspondent to the M2a-phenotype [77, 84]. Accordantly, CD163 was shown to not be increased following to IL4 stimulation [130]. As to CD206, this marker was ascribed to murine MΦ and expression in human cells is reported to be unspecific [62]. This is commensurate to our findings, however, regarding MFI, CD206 was rather specific in the present study. Arg1 was detected to be specific for murine MΦ and neutrophils [82]. Yet, as to human cells, Arg1 was found in neutrophils only [82]. Hence, our findings concerning this marker are in line with previous results [82].

Finally, the prepared MdM were characterized regarding their marker expression employing CLSM [77]. This examination was conducted, as marker expression constitutes a major and impactful part of MdM characterization [18, 59, 61, 62, 77, 91, 108, 119, 126, 130]. Yet, flow cytometrical analysis as performed afore is dependent on suspended cells, thus requiring MdM detachment [77]. As the MdM within this study should be utilized to test for immunomodulatory effects of biomaterial surfaces subsequent to successfully preparing and characterizing these cells, CLSM was selected to assess marker expression of adherend MdM [77]. In doing so, surface marker expression could at least be examined semi-quantitatively without impacting and damaging the MdM owing to detaching the cells [43, 77, 88]. Furthermore, we were able to reduce the number of seeded MdM as cell loss within the scope of detachment could be avoided [77]. Due to CLSM being semi-quantitative, specificity of markers to be tested is prerequisite, as otherwise analysis is hindered, in case markers are expressed across all MdM-phenotypes [77]. As discussed afore, CCR7 and CD209 flow cytometrically were identified to be specifically expressed by M1- and M2-MdM, respectively. Hence, these markers were selected for CLSM assessment [77]. Referred to ***Chap. 3.4***, MdM surface markers were successfully investigated using CLSM and CCR7 was selectively expressed by M1-MdM, whereas CD209 expression was specific as to the M2-polarization [77].

Compendiously, within the first section of this study, MdM were successfully prepared from human peripheral blood monocytes and polarized to the M1- and M2-phenotype in equal measure, thus constituting a suitable cell model [77]. Moreover, the latter cells were characterized using diverse methods detecting multiple consensus markers [77]. While M1-MdM were specifically marked by a round phenotype, the expression of the surface markers CCR7 as well as the secretion of TNFα, M2-MdM particularly featured an elongated phenotype, the expression of the surface makers CD1A and CD209 as well as the secretion of CCL13 and CCL17 [77]. However, as can also be deduced from these results, regarding polarization, there is no sole specific marker in terms of characterization, as markers to some extents were expressed consistently in spite of obverse polarization [77, 119, 130]. Thus, polarization is characterized most precisely if a synopsis of markers is considered. This finding is in line with the findings of previous studies [62, 119, 130].

Within the second part of this study, the protocol relating to the MdM preparation established afore should be implemented and thus utilized to investigate biomaterial-related immunomodulatory effects. To this, monocytes were isolated as delineated before using density gradient centrifugation and monocyte adhesion. The latter cells were then differentiated by means of incubation with 10 ng/ml M-CSF for 6 days as aforementioned. Following to their differentiation, the resultant MdM were detached chemically using Accutase as well as mechanically employing a cell scraper. Cells were then seeded onto diverse surfaces, encompassing Ti-SLA discs or Ti-Ana discs as modified titanium surfaces as well as Ti-ma discs and tissue culture coverslips as control surfaces [77]. Polarization to the M0-, M1- or M2-phenotype was accomplished adjoining complete medium without any polarizing agents, complete medium with addition of 50 ng/ml IFNγ and 10 ng/ml LPS or complete medium with addition of 20 ng/ml IL4 and 20 ng/ml IL13, respectively, for 2 days [77]. In order to assess immunomodulatory effects, the resultant polarized MdM adjacently were analyzed using CCK8 cell proliferation assay, furthermore the markers determined afore were examined deploying ELISA and BCA protein assay as well as CLSM [77].

Regarding the CCK8 cell proliferation assay, metabolic activity of the cultivated cells was investigated being surrogate of MdM viability and cell number. As disclosed in ***Chap. 3.5***, neither of the surfaces tested had significant direct adverse effects on the

cultivated cells. Following, ELISA was conducted in order to assess cytokine secretion of the MdM seeded on the titanium surfaces. Since TNFα and CCL13 were identified to be specific before ***(Chap.3.2)***, these markers were selected and investigated. As the cultivated cells were tightly adherent to the titanium discs and could not be detached as to counting, normalization could not be done to the cell number. Instead, total amount of protein was determined using BCA protein assay to normalize cytokine concentration. Neither of the surfaces examined effectuated increased level of TNFα, thus, foreclosing significant pro-inflammatory influences of the titanium discs ***(Chap. 3.6)***. CCL13, on the other hand, was significantly reduced for M0-MdM or M2-MdM seeded on Ti-Ana discs as compared to coverslips or Ti-ma discs, respectively ***(Chap. 3.6)***. Both findings suggest a diminished anti-inflammatory influence of Ti-Ana discs. Lastly, cytoskeletal morphology as well as surface marker expression of the MdM cultivated on Ti-ma discs, Ti-SLA discs and Ti-Ana discs was assessed using CLSM. As identified in ***Chap. 3.7***, neither of the surfaces tested induced distinct morphologic discrepancies nor elicited significant differences in CCR7 and CD209 expression. Accordingly, none of the surfaces investigated exerted significantly more pronounced pro- or anti-inflammatory effects as compared to the residual surfaces.

Taken together, within the second part of this study, MdM were successfully cultivated on diverse titanium surfaces as well as subsequently analyzed to investigate potential immunomodulatory effects of biomaterials [77]. At this juncture, despite their tight adhesion to surfaces, monocyte differentiation to MdM prior to seeding these cells on titanium discs was critical to imitate the *in vivo* conditions [88]. Monocyte differentiation *in vitro* as well as *in vivo* takes time, thus seeding the latter cells could affect and skew the resultant MdM prematurely confounding experimental results [88]. As can be deduced from the results discussed afore, regarding cytokine secretion, Ti-Ana discs featured a diminished anti-inflammatory effect on the MdM, whereas pro-inflammatory effects were similar in all surfaces tested. Concerning morphology and marker expression, none of the titanium surfaces nor the coverslips effectuated significantly increased pro- or anti-inflammatory effects.

Regarding the conducted study, several limitations have to be considered.

As a start, in spite of the conveniences of primary human monocytes as source of MdM disclosed afore, some detriments as to their availability, preparation and characteristics exist [77, 83]. Venipuncture from healthy volunteers, although being markedly less invasive than isolation of tissue-resident primary MΦ, has to be assessed ethically [83]. Within whole blood, monocytes constitute a variable fraction of cells accounting for about 10 to 20 % of the PBMC [68]. Thus, monocyte yield is clearly diverging between diverse donors and cell number is rather poorly forecastable as well as limited [83]. Isolation of monocytes from the drawn whole blood is elaborate and long-standing [83]. Furthermore, human primary monocytes exhibit intra- as well as inter-individual discrepancy and variability [83]. Monocytes of various donors might differ and respond aberrantly to impacting stimuli [83]. The conducted investigations were thus multiply repeated using monocytes of several individuals. Within each repetition a control group was employed [77].

The established protocol encompasses *in vitro* investigations [77]. Neither animal experiments nor *in vivo* research have been undertaken [77]. Accordingly, the experimental setup, despite its utility, cannot entirely reflect the intricate as well as dynamic conditions within a living human organism and has to be construed conditionally [65, 77, 123, 130]. Thus, the obtained findings may not unrestrainedly be transferred to the *in vivo* situation nor to potential clinical circumstances and applications [77]. Nevertheless, within this study, experimental conditions were sought to be as physiological as possible. To this, blood was obtained immediately before monocyte isolation and it was utilized at room temperature [33]. Venipuncture was done complying with the general procedures in order to reflect the *in vivo* situation at best and to avoid unphysiological changes to the cells resulting in, amongst others, diminished viability or altered expression of cell markers [33]. Buffers necessary in the context of PBMC and monocyte isolation were pre-warmed to +37° C, except from Lymphocyte Separation Medium which was to be utilized at room temperature according to the manufacturer's specific instructions. Furthermore, incubation of the cells was done with complete medium at +37° C under protection from light to be similar to the *in vivo* conditions. Still, monocytes as well as the resulting MdM were unphysiologically concentrated in the context of their isolation. Consequently, potential impact of this enrichment on the cells' characteristics and function has to be minded as to functional studies [33].

Whole blood drawn from healthy donors was utilized for the isolation of monocytes [77]. Effects of pre-existing illnesses as well as pharmaceuticals hence were not considered. However, surgical implant insertion is typically accompanied with analgesia oftentimes deploying antiphlogistics. A modulation of monocyte and MΦ characteristics and function is conceivable, furthermore MΦ polarization might be altered due to the anti-inflammatory influences concerning the local micro-environment. Moreover, implants are increasingly applied in clinically compromised situations including elderly patients exhibiting pre-existing conditions and requiring medication [65]. The established protocol obtained within this study serves as a starting point as to the investigation of the FBR and does not include these circumstances. Further enhancement of the *in vitro* research as well as subsequent *in vivo* studies will be necessary to prospectively take account of these considerations.

Within the present study, MdM were used as MΦ model [77], thereby considering MΦ derived from the hematopoietic system. Tissue-resident MΦ resulting from the embryological development hence were not portrayed at this juncture [1], although it is not clear to which extent MdM resemble tissue-resident MΦ [144]. Monocytes were differentiated to MdM deploying M-CSF as growth factor [77]. GM-CSF was not tested, notwithstanding that distinctions in the resulting MdM were found in previous studies [64, 81, 117, 128, 130]. Furthermore, M1- as well as M2-polarization were considered compendiously and simplified [77]. Existing subtypes of polarized MdM, especially regarding the M2-polarization, amongst others comprising the M2a-, M2b and M2c-phenotype, were not factored [77]. Additionally, well defined stimuli as to the M1- and M2-polarization have been deployed separately for a steady duration [77]. The utilized cytokines were not varied during the incubation period and moreover, the working concentration was kept constant [77]. Regarding the *in vivo* situation however, a plethora of, occasionally contrary, stimuli operate simultaneously and the micro-environment may promptly alter, complicating MΦ polarization [119, 130]. These considerations are particularly consequential, as MΦ are hallmarked by high plasticity ***(Chap. 1.2.2)*** [72, 80, 94, 108, 109, 119]. At this point, future investigations refining the present protocol going into detail and effectuating more diverse models *in vitro* as well as eventually *in vivo* studies should be sought.

Lastly, regarding monocyte adhesion, loose cells were discarded each time cell culture medium was replaced. This approach was undertaken to enrich the adherend

monocytes and MdM as floating cells were assumed to potentially be contaminating lymphocytes. Within earlier studies, however, it has been reported, that loose cells also comprise MdM [130, 144], although their marker expression was lessened and differed from the expression of adherend MdM to some extent [130]. At this point, deepening investigations will be needed prospectively to further characterize MdM respecting floating cells.

Taken together, despite its limitations discussed afore, this *in vitro* protocol, along with ample previous research [61, 62, 88, 130], aimed at the advancement of MdM characterization and allowed for essential and important cognition on MΦ [77]. Concomitantly, the complexity of the cell model selection as well as the deployed activation markers were revealed [77]. Investigating MΦ in the context of biomaterials facilitates the understanding of mechanisms underlying the FBR as well as consequentially the systematic study of immunomodulation [77].

Prospectively, in order to enhance the established protocol concerning the MdM preparation and characterization as well as to further expedite knowledge on the FBR and immunomodulation, continuing establishment is essential [77].

To this, firstly, the subtypes of polarization, amongst others comprising the M2a-, M2b- and M2c-phenotypes, should be considered [77]. Thereby, the complex and dynamic *in vivo* conditions would be reflected more precisely in the *in vitro* experimental setup. Concomitantly, characterization of the MdM should be broadened to include and distinguish the aforementioned subtypes. Accordingly, a multitude of further cytokines regarding ELISA, such as IL1, IL6, IL12 as well as chemokine C-X-C motif ligand (CXCL10) as to the M1-polarization and IL10, CCL22 as well as TGFβ as to the M2-polarization and its subtypes are delineated in the literature [62, 130], but were not investigated within the present study. Similarly, concerning flow cytometry, more markers, amongst others CD40 and CD64 as to the M1-phenotype and CD200R as to the M2-polarization [62, 130], are described and should be evaluated in the scope of future studies. Moreover, besides extending characterization markers utilizing the methods deployed within this study, also further methods, such as assessment of gene expression by means of qRT-PCR or of functionality by means of phagocytosis assay, should be and partly have been adopted *(data not shown)* [62, 77, 119]. In this context, qRT-PCR allows for quantitative insights into the MdM enabling a specific correlation of their

polarization state [77]. Beneficially, both methods do not require suspended cells and can thus be conducted utilizing MdM cultivated on diverse titanium surfaces [77]. By means of applying diverse methods investigating as many markers as possible, polarization states of the MdM, comprising potential subtypes, are characterized at the best resulting in findings most likely to be reliable [77].

As to the experimental setup, the present study controled the cellular interaction with biomaterial surfaces. Henceforth, however, also the interaction of blood and interstitial proteins with biomaterials should be considered [88]. Immediately after an implant is inserted, present proteins adsorb to its surface [1, 12, 22, 32, 44, 51, 63, 118, 131, 142, 145]. Thereby, the biomaterial is opsonized and conditioned, so that MdM rather interact with autologous blood and interstitial proteins instead of the actual biomaterial surface [88, 89, 122]. Based on this consideration, blood as well as preferably interstitial proteins should be included in future studies.

Furthermore, within the present study, readily differentiated and partially polarized MdM were cultivated on the titanium discs [77]. Within the *in vivo* setting, however, presumably, also monocytes interact with the surface of an implanted biomaterial and differentiate towards MΦ while residing on the biomaterial [88]. Accordingly, in the context of future studies, this consideration should be preconceived, consequentially seeding MdM as well as monocytes simultaneously, for instance, on biomaterial surfaces [88]. Additionally, even further enhancement of the present protocol could be accomplished by implementation of co-cultures [123, 145]. By this means, not only MdM but also other cells, such as further immune cells, osteoblasts and osteoclasts, could be examined and most notably, their mutual interaction could be investigated [123, 145]. Still, despite the considerable and enhancing *in vitro* models as well as the latter considerations of establishing and employing co-cultures, auxiliary animal and *in vivo* studies will be needful as to reliably deepen the understanding and dependability of the FBR and the bone response to inserted implants [65].

Lastly, in order to systematically and constructively advance research on immunomodulatory effects of biomaterials, prospectively also characterization of the biomaterial surfaces should be included into the protocol [1, 2]. Consequentially, amongst others, specifications on the surface topography by means of scanning electron microscopy, on the surface roughness using confocal microscopy as well as on the hydrophilicity

via sessile drop contact angle goniometry will be beneficial to characterize to biomaterials investigated and to consolidate and contextualize all findings attained [1, 2].

Deductively, as to prospective MΦ research, further establishment, careful study design as well as consideration of the experimental objective is required in order to engross insights into MΦ, the FBR and FBE as well as immunomodulation [77, 83]. Utilizing the presented *in vitro* protocol established within this study can allow for meaningful insight into immunomodulation of biomaterials as well as facilitate the development of novel immunomodulatory features [77]. The study hence may contribute to improve healing processes subsequent to implant insertion [77]. Furthermore, continuing inflammatory processes due to both aggravated FBR and abrogated FBE might be prevented to allow for effective and lasting osseointegration [77]. Still, marginal bone loss occurs and due to the increasing number of dental implants inserted, this issue marks a rising problem without reliable and exhaustive solution approaches being available [123]. Yet aggravating, insertion of dental implants is increasingly conducted within compromised and challenging clinical circumstances, such as reduced bone quality and osteoporosis, preceding radiotherapy as well as restricted wound healing due to diabetes and other metabolic constraints, oftentimes concerning elderly patients [65]. Thus, a continuous advancement in terms of immunomodulation of dental implants is of major importance to approach and eventually reliably overcome proceeding peri-implant bone loss and implant failure [65].

Moreover, the findings obtained within this study not only apply to dental implants but may also be transferred to any other implantable medical device. Biomaterials are manifoldly as well as increasingly appropriated for various diagnostic as well as therapeutic uses [79, 116]. Within all scopes of application, aggravated FBR consecutively lead to malfunction and damage as far implant failure [79, 116]. Accordingly, as to orthopedic implants, aseptic implant loosening is ascribed to the latter immune reaction [49]. Contrariwise, successful osseointegration resulting from a subtly balanced FBR and FBE might render possible to pass on cement with regard to joint replacement [5, 49]. Concerning cardiology, cardiac pacemakers as well as implantable cardioverter defibrillators are vulnerable to stress cracking of their leads caused by the inflammatory reaction directed against the implant [116, 118]. Besides, stents as well as valvular transplants are prone and may occlude. In terms of the latter cardiologic implants, a

severe FBR impairs the indispensable function and thus might seriously threaten the concerned patient. As regards endocrinology, implantable sensors, such as glucose sensors, are used amongst others relating to diabetes [79, 139]. Enduring FBR can lead to fortified fibrous encapsulation of the sensor averting its destined function [79, 139]. Likewise, within pharmacology the intended purpose of drug delivery systems may be delimited due to encapsulation. Lastly, as to plastic surgery implants concerning soft tissue, such as mammary implants, are also embedded as a consequence of the FBR [118]. In case of an aggravated immune reaction, the resultant amplified fibrous encapsulation can redound to painful hardening of the implant, furthermore degradation to the point of implant rupture is possible [118].

As pointed out afore, with regard to both dental implants as well as to any other implantable medical device a profound comprehension and engrossed knowledge on the FBR are essential as to project the interaction of a biomaterial and its receiving host [79, 116]. Within all ambits, a thorough biomaterial selection adjusted to its intended use is prerequisite to a favorable outcome [79, 116]. Given deepened insights into the FBR, immunomodulatory effects of biomaterials can be taken into consideration as well as sought aiming at circumventing abiding inflammation and enhancing the implant's functionality as well as longevity [79, 116].

Altogether, the conducted study provides an established protocol to reproducibly as well as reliably isolate and differentiate human peripheral blood monocytes towards – if necessary, polarized – MdM [77]. Using these findings, knowledge on the FBR, the FBE as well as on osseointegration can be engrossed prospectively and potential immunomodulatory effects of biomaterials on MΦ may be studied *in vitro* [77]. Consecutively, the design and development of immunomodulatory biomaterials can be expedited in order to facilitate healing and osseointegration as well as to circumvent marginal bone loss and subsequent implant failure [77].

5 Abstract

The loss of teeth is a remarkable issue predominantly resulting from caries-related decay, severe periodontitis and trauma concomitant with, amongst others, limitations upon mastication and phonetics. By reason of their beneficial function and aesthetics along with promising long-term results, dental implants have evolved into a major therapeutic option. However, peri-implant bone loss constitutes an increasing problem and can lead up to implant failure, as reliable solution approaches are currently lacking. Marginal bone loss is ascribed to immune processes in terms of a continuing or recurrent foreign body reaction (FBR) in which macrophages (MΦ) prevail. Efforts to overcome peri-implant bone loss should therefore strive for the disclosure of the FBR focusing on MΦ. Accordingly, this study aimed at the establishment of a protocol to reliably and reproducibly isolate and differentiate human peripheral blood monocytes to polarized monocyte-derived MΦ (MdM) to subsequently engross insights into the FBR and investigate immunomodulatory effects of biomaterials *in vitro*.

To this, monocytes were isolated from peripheral whole blood of healthy donors by density gradient centrifugation and subsequent monocyte adhesion. These cells were then differentiated to MdM using10 ng/ml MΦ colony stimulating factor (M-CSF) for 6 days. Subsequently, for M1 polarization, MdM were incubated with 50 ng/ml interferon γ (IFNγ) and 10 ng/ml lipopolysaccharide (LPS), whereas M2 phenotype was induced using 20 ng/ml interleukin (IL) 4 and 20 ng/ml IL13 for 2 days. MdM were then light microscopically characterized as to their morphology. Furthermore, cytokine secretion using enzyme-linked immunosorbent assay (ELISA), marker expression deploying flow cytometry and cytoskeletal morphology as well as surface marker expression utilizing confocal laser scanning microscopy (CLSM) were assessed. As to the implementation of the established protocol, differentiated MdM adjacently were cultured and polarized on diverse titanium (Ti) surfaces including Ti-machined (Ti-ma), sandblasted with large grits and acid-etched titanium (Ti-SLA) as well as Ti-anatase (Ti-Ana) discs and immunomodulatory effects were evaluated via cell counting kit (CCK) 8 cell proliferation assay, ELISA, bicinchoninic acid assay (BCA protein assay) and CLSM.

Resultantly, M1-MdM morphologically exhibit a round phenotype and are reliably characterized by secretion of proinflammatory tumor necrosis factor (TNF) α as well as expression of chemokine C-C motif receptor (CCR) 7. M2-MdM, in contrast, are rather

elongated, specifically secrete chemokine C-C motif ligand (CCL) 13 and CCL17 and exhibit significantly increased levels of cluster of differentiation (CD) 1A and CD209. As to immunomodulatory effects of diverse titanium surfaces, CCK8 cell proliferation assay was conducted at first to preclude direct adverse effects of Ti-ma discs, Ti-SLA discs and Ti-Ana discs on the cultivated MdM. Concerning cytokine secretion, neither of the surfaces investigated effectuated increased level of TNFα secretion, thus, foreclosing significant pro-inflammatory influences. CCL13 concentration as marker of the M2-polarization, on the other hand, was significantly reduced for M0-MdM or M2-MdM seeded on Ti-Ana discs as compared to coverslips or Ti-ma discs, respectively. Lastly, cytoskeletal morphology as well as surface marker expression of the MdM cultivated on Ti-ma discs, Ti-SLA discs and Ti-Ana discs was assessed, neither disclosing distinct morphologic discrepancies nor revealing significant differences of CCR7 and CD209 expression. Hence, none of the surfaces investigated exert significantly more pronounced pro- or anti-inflammatory effects as compared to the residual surfaces.

Accordingly, the established protocol allows for a reproducible preparation and characterization of differentiated and polarized MdM. These cells subsequently render possible to further delve into the FBR and investigate immunomodulatory effects of biomaterials *in vitro*.

6 Zusammenfassung

Zahnverlust stellt ein erhebliches Problem dar, das vor allem durch Karies, schwere Parodontitis und Traumata verursacht wird und unter anderem zu Einschränkungen des Kauens und des Sprechens führt. Aufgrund ihrer vorteilhaften Funktion und Ästhetik sowie ihrer vielversprechenden Langzeitergebnisse haben sich Zahnimplantate hier zu einer wichtigen Therapieoption entwickelt. Periimplantärer Knochenverlust stellt jedoch ein zunehmendes Problem dar und kann bis hin zu Implantatversagen führen, weil derzeit zuverlässige Lösungsansätze fehlen. Marginaler Knochenverlust wird auf Immunprozesse im Sinne einer anhaltenden oder wiederkehrenden Fremdkörperreaktion (FRB) zurückgeführt, bei der auf zellulärer Ebene Makrophagen (MΦ) vorherrschen. Bemühungen zur Überwindung des periimplantären Knochenverlusts sollten sich daher auf die FBR mit Schwerpunkt auf MΦ konzentrieren. Dementsprechend strebte diese Studie die Etablierung eines Protokolls zur zuverlässigen und reproduzierbaren Isolierung und Differenzierung humaner peripherer Blutmonozyten mit anschließender Polarisation hin zu aus Monozyten gewonnenen MΦ (MdM) an, um anschließend die Kenntnisse über die FBR zu vertiefen und immunmodulatorische Einflüsse von Biomaterialien *in vitro* zu untersuchen.

Zu diesem Zweck wurden Monozyten aus dem peripheren Vollblut gesunder Spender mittels Dichtegradientenzentrifugation und anschließender Monozytenadhäsion isoliert. Die letzteren Zellen wurden sodann mittels 10 ng/ml MΦ koloniestimulierendem Faktor (M-CSF) für 6 Tage zu MdM differenziert. Für die M1-Polarisation wurden die MdM anschließend mit 50 ng/ml Interferon γ (IFNγ) und 10 ng/ml Lipopolysaccharid (LPS) inkubiert, wohingegen die M2-Polarisation mittels 20 ng/ml Interleukin (IL) 4 und 20 ng/ml IL13 hervorgerufen wurde. Die MdM wurden anschließend lichtmikroskopisch bezüglich ihrer Morphologie charakterisiert. Des Weiteren wurden die Zytokinsekretion mittels Enzyme-linked immunosorbent assay (ELISA), die Markerexpression mittels Durchflusszytometrie sowie die Morphologie des Zytoskeletts und die Oberflächenmarkerexpression mittels konfokaler Laser-Scanning Mikroskopie (CLSM) untersucht. Zur Implementierung des etablierten Protokolls wurden anschließend differenzierte MdM auf verschiedenen Oberflächen, darunter machiniertes Titan (Ti-ma Disks), sandgestrahltes und säuregeätztes Titan (Ti-SLA Disks) und Titan Anatas (Ti-Ana Disks), ausgesät und polarisiert. Mögliche immunmodulatorische Wirkungen wurden mittels

Cell Counting Kit (CCK) 8 Zellproliferationsassay, ELISA, Bicinchoninsäure (BCA) Assay und CLSM überprüft.

Bezüglich der Charakterisierung zeigen M1-MdM morphologisch einen runden Phänotyp und sind zuverlässig durch die Sekretion des proinflammatorischen Tumornekrosefaktors (TNF) α sowie durch die Expression des Chemokin C-C Motiv Rezeptors (CCR) 7 gekennzeichnet. M2-MdM hingegen weisen einen eher elongierten Phänotyp auf, sezernieren spezifisch den Chemokin C-C Motiv Liganden (CCL) 13 und CCL17 und exprimieren Cluster of Differentiation (CD) 1A sowie CD209. Hinsichtlich immunmodulatorischer Effekte der untersuchten Titanoberflächen wurde zunächst eine direkte negative Auswirkung der Ti-ma Disks, der Ti-SLA Disks sowie der Ti-Ana Disks auf die ausgesäten MdM mittels CCK8 Zellproliferationsassay ausgeschlossen. Bezüglich der Zytokinsekretion bewirkte keine der untersuchten Oberflächen eine Erhöhung von TNFα, so dass ein signifikanter proinflammatorischer Einfluss ausgeschlossen werden konnte. Die CCL13 Konzentration als Marker der M2-Polarisation war hingegen bei den M0-MdM und den M2-MdM, welche auf Ti-Ana Disks ausgesät wurden, im Vergleich zu den Coverslips beziehungsweise den Ti-ma Disks signifikant reduziert. Schließlich wurden die Morphologie des Zytoskeletts sowie die Expression von Oberflächenmarkern der MdM untersucht. Hierbei ergaben sich weder deutliche morphologische Abweichungen noch signifikante Unterschiede in der Expression von CCR7 und CD209 zwischen den Ti-ma Disks, den Ti-SLA Disks und den Ti-Ana Disks, sodass keine der untersuchten Oberflächen eine signifikant erhöhte pro- oder antiinflammatorische Wirkung aufweist.

Das etablierte Protokoll ermöglicht folglich die reproduzierbare Gewinnung und Charakterisierung von differenzierten und polarisierten MdM. Mittels der letzteren Zellen können sodann die Erkenntnisse über die FBR vertieft und immunmodulatorische Effekte von Biomaterialien *in vitro* untersucht werden.

References

1. Abaricia, J.O., Farzad, N., Heath, T.J., Simmons, J., Morandini, L., and Olivares-Navarrete, R., *Control of innate immune response by biomaterial surface topography, energy, and stiffness.* Acta Biomaterialia, 2021. **133**: p. 58-73.
2. Abaricia, J.O., Shah, A.H., Ruzga, M.N., and Olivares-Navarrete, R., *Surface characteristics on commercial dental implants differentially activate macrophages in vitro and in vivo.* Clinical Oral Implants Research, 2021. **32**(4): p. 487-497.
3. Adell, R., Lekholm, U., Rockler, B., and Brånemark, P.-I., *A 15-year study of osseointegrated implants in the treatment of the edentulous jaw.* International journal of oral surgery, 1981. **10**(6): p. 387-416.
4. Albrektsson, T., *Are Oral Implants the Same As Teeth?* 2019, MDPI. p. 1501.
5. Albrektsson, T., Brånemark, P.-I., Hansson, H.-A., and Lindström, J., *Osseointegrated titanium implants: requirements for ensuring a long-lasting, direct bone-to-implant anchorage in man.* Acta Orthopaedica Scandinavica, 1981. **52**(2): p. 155-170.
6. Albrektsson, T., Canullo, L., Cochran, D., and De Bruyn, H., *"Peri-implantitis": a complication of a foreign body or a man-made "disease". Facts and fiction.* Clinical implant dentistry and related research, 2016. **18**(4): p. 840-849.
7. Albrektsson, T., Chrcanovic, B., Jacobsson, M., and Wennerberg, A., *Osseointegration of implants: a biological and clinical overview.* JSM Dental Surgery, 2017. **2**(3).
8. Albrektsson, T., Dahlin, C., Jemt, T., Sennerby, L., Turri, A., and Wennerberg, A., *Is marginal bone loss around oral implants the result of a provoked foreign body reaction?* Clinical implant dentistry and related research, 2014. **16**(2): p. 155-165.
9. Albrektsson, T. and Wennerberg, A., *Oral implant surfaces: Part 1--review focusing on topographic and chemical properties of different surfaces and in vivo responses to them.* International Journal of Prosthodontics, 2004. **17**(5).
10. Anderson, J.M., *Mechanisms of inflammation and infection with implanted devices.* Cardiovascular Pathology, 1993. **2**(3): p. 33-41.
11. Anderson, J.M., *Biological responses to materials.* Annual review of materials research, 2001. **31**(1): p. 81-110.
12. Anderson, J.M., Rodriguez, A., and Chang, D.T. *Foreign body reaction to biomaterials*. in *Seminars in immunology*. 2008. Elsevier.
13. Auwerx, J., *The human leukemia cell line, THP-1: a multifacetted model for the study of monocyte-macrophage differentiation.* Experientia, 1991. **47**(1): p. 22-31.
14. Bauer, S., Schmuki, P., Von Der Mark, K., and Park, J., *Engineering biocompatible implant surfaces: Part I: Materials and surfaces.* Progress in Materials Science, 2013. **58**(3): p. 261-326.
15. Becker, S., Warren, M., and Haskill, S., *Colony-stimulating factor-induced monocyte survival and differentiation into macrophages in serum-free cultures.* Journal of immunology (Baltimore, Md.: 1950), 1987. **139**(11): p. 3703-3709.
16. Becker, W., *Osseointegration: have we tinkered with the process too much??* 2012, Wiley Online Library. p. 779-780.
17. Berthold, F., *Isolation of human monocytes by Ficoll density gradient centrifugation.* Blut, 1981. **43**(6): p. 367-371.
18. Beyer, M., Mallmann, M.R., Xue, J., Staratschek-Jox, A., Vorholt, D., Krebs, W., Sommer, D., Sander, J., Mertens, C., and Nino-Castro, A., *High-resolution transcriptome of human macrophages.* 2012.
19. Bøyum, A., *Isolation of Human Blood Monocytes with Nycodenz, a New Non-Ionic Iodinated Gradient Medium.* Scandinavian Journal of Immunology, 1983. **17**(5): p. 429-436.
20. Braga, T.T., Agudelo, J.S.H., and Camara, N.O.S., *Macrophages during the fibrotic process: M2 as friend and foe.* Frontiers in immunology, 2015. **6**: p. 602.
21. Brånemark, P.-I., Breine, U., Adell, R., Hansson, B., Lindström, J., and Ohlsson, Å., *Intra-osseous anchorage of dental prostheses: I. Experimental studies.* Scandinavian journal of plastic and reconstructive surgery, 1969. **3**(2): p. 81-100.
22. Brodbeck, W., Nakayama, Y., Matsuda, T., Colton, E., Ziats, N., and Anderson, J., *Biomaterial surface chemistry dictates adherent monocyte/macrophage cytokine expression in vitro.* Cytokine, 2002. **18**(6): p. 311-319.
23. Brodbeck, W.G., Patel, J., Voskerician, G., Christenson, E., Shive, M.S., Nakayama, Y., Matsuda, T., Ziats, N.P., and Anderson, J.M., *Biomaterial adherent macrophage apoptosis is increased by hydrophilic and anionic substrates in vivo.* Proceedings of the National Academy of Sciences, 2002. **99**(16): p. 10287-10292.

24. Brodbeck, W.G., Shive, M.S., Colton, E., Nakayama, Y., Matsuda, T., and Anderson, J.M., *Influence of biomaterial surface chemistry on the apoptosis of adherent cells.* Journal of Biomedical Materials Research: An Official Journal of The Society for Biomaterials, The Japanese Society for Biomaterials, and The Australian Society for Biomaterials and the Korean Society for Biomaterials, 2001. **55**(4): p. 661-668.
25. Buser, D., Janner, S.F., Wittneben, J.G., Brägger, U., Ramseier, C.A., and Salvi, G.E., *10-year survival and success rates of 511 titanium implants with a sandblasted and acid-etched surface: a retrospective study in 303 partially edentulous patients.* Clinical implant dentistry and related research, 2012. **14**(6): p. 839-851.
26. Capes-Davis, A., *Cell Line Detective Work: Basic Principles and Molecular Applications.* Advances in Molecular Pathology, 2018. **1**(1): p. 229-238.
27. Cavaillon, J.-M., *The historical milestones in the understanding of leukocyte biology initiated by Elie Metchnikoff.* Journal of leukocyte biology, 2011. **90**(3): p. 413-424.
28. Chanput, W., Mes, J.J., Savelkoul, H.F., and Wichers, H.J., *Characterization of polarized THP-1 macrophages and polarizing ability of LPS and food compounds.* Food & function, 2013. **4**(2): p. 266-276.
29. Chanput, W., Mes, J.J., and Wichers, H.J., *THP-1 cell line: an in vitro cell model for immune modulation approach.* International immunopharmacology, 2014. **23**(1): p. 37-45.
30. Chanput, W., Peters, V., and Wichers, H., *THP-1 and U937 Cells.* The Impact of Food Bioactives on Health: in vitro and ex vivo models, 2015: p. 147-159.
31. Chen, S., Jones, J.A., Xu, Y., Low, H.-Y., Anderson, J.M., and Leong, K.W., *Characterization of topographical effects on macrophage behavior in a foreign body response model.* Biomaterials, 2010. **31**(13): p. 3479-3491.
32. Christo, S.N., Diener, K.R., Bachhuka, A., Vasilev, K., and Hayball, J.D., *Innate immunity and biomaterials at the nexus: friends or foes.* BioMed research international, 2015. **2015**(1): p. 342304.
33. Dagur, P.K. and McCoy Jr, J.P., *Collection, storage, and preparation of human blood cells.* Current protocols in cytometry, 2015. **73**(1): p. 5.1. 1-5.1. 16.
34. Daigneault, M., Preston, J.A., Marriott, H.M., Whyte, M.K., and Dockrell, D.H., *The identification of markers of macrophage differentiation in PMA-stimulated THP-1 cells and monocyte-derived macrophages.* PloS one, 2010. **5**(1): p. e8668.
35. De Almeida, M.C., Silva, A.C., Barral, A., and Barral Netto, M., *A simple method for human peripheral blood monocyte isolation.* Memorias do Instituto Oswaldo Cruz, 2000. **95**: p. 221-223.
36. Delves, P.J. and Roitt, I.M., *The immune system.* New England journal of medicine, 2000. **343**(1): p. 37-49.
37. Donath, K., Laaß, M., and Günzl, H.-J., *The histopathology of different foreign-body reactions in oral soft tissue and bone tissue.* Virchows Archiv A, 1992. **420**: p. 131-137.
38. Duraccio, D., Mussano, F., and Faga, M.G., *Biomaterials for dental implants: current and future trends.* Journal of Materials Science, 2015. **50**: p. 4779-4812.
39. Ehrenfest, D.M.D., Coelho, P.G., Kang, B.-S., Sul, Y.-T., and Albrektsson, T., *Classification of osseointegrated implant surfaces: materials, chemistry and topography.* Trends in biotechnology, 2010. **28**(4): p. 198-206.
40. Epelman, S., Lavine, K.J., and Randolph, G.J., *Origin and functions of tissue macrophages.* Immunity, 2014. **41**(1): p. 21-35.
41. Esposito, M., Ardebili, Y., and Worthington, H.V., *Interventions for replacing missing teeth: different types of dental implants.* Cochrane database of systematic reviews, 2014(7).
42. Esposito, M., Hirsch, J., Lekholm, U., and Thomsen, P., *Biological factors contributing.* Eur J Oral Sci, 1998. **106**(1): p. 527-51.
43. Feuerer, N., Morschl, J., Daum, R., Weiss, M., Hinderer, S., Schenke-Layland, K., and Shipp, C., *Macrophage retrieval from 3D biomaterials: A detailed comparison of common dissociation methods.* Journal of Immunology and Regenerative Medicine, 2021. **11**: p. 100035.
44. Franz, S., Rammelt, S., Scharnweber, D., and Simon, J.C., *Immune responses to implants–a review of the implications for the design of immunomodulatory biomaterials.* Biomaterials, 2011. **32**(28): p. 6692-6709.
45. Fujiwara, Y., Hizukuri, Y., Yamashiro, K., Makita, N., Ohnishi, K., Takeya, M., Komohara, Y., and Hayashi, Y., *Guanylate-binding protein 5 is a marker of interferon-γ-induced classically activated macrophages.* Clinical & translational immunology, 2016. **5**(11): p. e111.
46. Fuss, I.J., Kanof, M.E., Smith, P.D., and Zola, H., *Isolation of whole mononuclear cells from peripheral blood and cord blood.* Current protocols in immunology, 2009. **85**(1): p. 7.1. 1-7.1. 8.

47. García, A., Serrano, A., Abril, E., Jimenez, P., Real, L.M., Cantón, J., Garrido, F., and Ruiz-Cabello, F., *Differential effect on U937 cell differentiation by targeting transcriptional factors implicated in tissue-or stage-specific induced integrin expression.* Experimental hematology, 1999. **27**(2): p. 353-364.
48. Gasperini, S., Calzetti, F., Bazzoni, F., and Cassatella, M.A., *The neutrophil as a cellular source of chemokines.* Immunol Rev, 2000. **177**: p. 195-203.
49. Gibon, E., Takakubo, Y., Zwingenberger, S., Gallo, J., Takagi, M., and Goodman, S.B., *Friend or foe? Inflammation and the foreign body response to orthopedic biomaterials.* Journal of Biomedical Materials Research Part A, 2024. **112**(8): p. 1172-1187.
50. Gmelig-Meyling, F. and Waldmann, T.A., *Separation of human blood monocytes and lymphocytes on a continuous Percoll gradient.* Journal of immunological methods, 1980. **33**(1): p. 1-9.
51. Gorbet, M.B. and Sefton, M.V., *Biomaterial-associated thrombosis: roles of coagulation factors, complement, platelets and leukocytes.* The Biomaterials: Silver Jubilee Compendium, 2004: p. 219-241.
52. Gordon, S., *The macrophage.* Bioessays, 1995. **17**(11): p. 977-986.
53. Gordon, S. and Plüddemann, A., *Tissue macrophages: heterogeneity and functions.* BMC biology, 2017. **15**(1): p. 53.
54. Gordon, S. and Taylor, P.R., *Monocyte and macrophage heterogeneity.* Nature reviews immunology, 2005. **5**(12): p. 953-964.
55. Graff, J.W., Dickson, A.M., Clay, G., McCaffrey, A.P., and Wilson, M.E., *Identifying functional microRNAs in macrophages with polarized phenotypes.* Journal of Biological Chemistry, 2012. **287**(26): p. 21816-21825.
56. Guillaume, B., *Dental implants: A review.* Morphologie, 2016. **100**(331): p. 189-198.
57. Hashimoto, D., Chow, A., Noizat, C., Teo, P., Beasley, M.B., Leboeuf, M., Becker, C.D., See, P., Price, J., and Lucas, D., *Tissue-resident macrophages self-maintain locally throughout adult life with minimal contribution from circulating monocytes.* Immunity, 2013. **38**(4): p. 792-804.
58. Hetrick, E.M., Prichard, H.L., Klitzman, B., and Schoenfisch, M.H., *Reduced foreign body response at nitric oxide-releasing subcutaneous implants.* Biomaterials, 2007. **28**(31): p. 4571-4580.
59. Hoppstädter, J., Seif, M., Dembek, A., Cavelius, C., Huwer, H., Kraegeloh, A., and Kiemer, A.K., *M2 polarization enhances silica nanoparticle uptake by macrophages.* Frontiers in pharmacology, 2015. **6**: p. 55.
60. Hotchkiss, K.M., Reddy, G.B., Hyzy, S.L., Schwartz, Z., Boyan, B.D., and Olivares-Navarrete, R., *Titanium surface characteristics, including topography and wettability, alter macrophage activation.* Acta biomaterialia, 2016. **31**: p. 425-434.
61. Iqbal, S. and Kumar, A., *Characterization of in vitro generated human polarized macrophages.* J Clin Cell Immunol, 2015. **6**(06): p. 4172.
62. Jaguin, M., Houlbert, N., Fardel, O., and Lecureur, V., *Polarization profiles of human M-CSF-generated macrophages and comparison of M1-markers in classically activated macrophages from GM-CSF and M-CSF origin.* Cellular immunology, 2013. **281**(1): p. 51-61.
63. Jenney, C.R. and Anderson, J.M., *Adsorbed IgG: a potent adhesive substrate for human macrophages.* Journal of Biomedical Materials Research: An Official Journal of The Society for Biomaterials, The Japanese Society for Biomaterials, and The Australian Society for Biomaterials and the Korean Society for Biomaterials, 2000. **50**(3): p. 281-290.
64. Joshi, S., Singh, A.R., Zulcic, M., Bao, L., Messer, K., Ideker, T., Dutkowski, J., and Durden, D.L., *Rac2 controls tumor growth, metastasis and M1-M2 macrophage differentiation in vivo.* PloS one, 2014. **9**(4): p. e95893.
65. Junker, R., Dimakis, A., Thoneick, M., and Jansen, J.A., *Effects of implant surface coatings and composition on bone integration: a systematic review.* Clinical oral implants research, 2009. **20**: p. 185-206.
66. Kao, W.J. and Lee, D., *In vivo modulation of host response and macrophage behavior by polymer networks grafted with fibronectin-derived biomimetic oligopeptides: the role of RGD and PHSRN domains.* Biomaterials, 2001. **22**(21): p. 2901-2909.
67. Kelly, A., Grabiec, A.M., and Travis, M.A., *Culture of human monocyte-derived macrophages*, in *Macrophages: Methods and Protocols*, G. Rousselet, Editor. 2018, Human Press. p. 1-11.
68. Kleiveland, C.R., *Peripheral blood mononuclear cells.* The Impact of Food Bioactives on Health: in vitro and ex vivo models, 2015: p. 161-167.
69. Kobayashi, S.D., Voyich, J.M., Burlak, C., and DeLeo, F.R., *Neutrophils in the innate immune response.* Archivum Immunologiae Et Therapiae Experimentalis-English Edition-, 2005. **53**(6): p. 505.

70. Le Guéhennec, L., Soueidan, A., Layrolle, P., and Amouriq, Y., *Surface treatments of titanium dental implants for rapid osseointegration.* Dental materials, 2007. **23**(7): p. 844-854.
71. Luu, T.U., Gott, S.C., Woo, B.W., Rao, M.P., and Liu, W.F., *Micro-and nanopatterned topographical cues for regulating macrophage cell shape and phenotype.* ACS applied materials & interfaces, 2015. **7**(51): p. 28665-28672.
72. Mantovani, A., Sica, A., Sozzani, S., Allavena, P., Vecchi, A., and Locati, M., *The chemokine system in diverse forms of macrophage activation and polarization.* Trends in immunology, 2004. **25**(12): p. 677-686.
73. Marshall, J.S., Warrington, R., Watson, W., and Kim, H.L., *An introduction to immunology and immunopathology.* Allergy, Asthma & Clinical Immunology, 2018. **14**: p. 1-10.
74. Martinez, F.O., Gordon, S., Locati, M., and Mantovani, A., *Transcriptional profiling of the human monocyte-to-macrophage differentiation and polarization: new molecules and patterns of gene expression.* The Journal of immunology, 2006. **177**(10): p. 7303-7311.
75. McWhorter, F.Y., Wang, T., Nguyen, P., Chung, T., and Liu, W.F., *Modulation of macrophage phenotype by cell shape.* Proceedings of the National Academy of Sciences, 2013. **110**(43): p. 17253-17258.
76. Mills, C., Kincaid, K., Alt, J., Heilman, M., and Hill, A., *M-1/M-2 macrophages and the Th1.* Th2 paradigm, 2000.
77. Mohammadnejad, L., Conrady, H., Mangold, M., Kimmerle-Mueller, E., Hechler, A., von Ohle, C., Rupp, F., and Krajewski, S., *Polarization and Characterization of M1 and M2 Human Monocyte-Derived Macrophages on Implant Surfaces.* Journal of Visualized Experiments (JoVE), 2024(214): p. e67180.
78. Montes, C.C., Pereira, F.A., Thome, G., Alves, E.D.M., Acedo, R.V., de Souza, J.R., Melo, A.C.M., and Trevilatto, P.C., *Failing factors associated with osseointegrated dental implant loss.* Implant dentistry, 2007. **16**(4): p. 404-412.
79. Morais, J.M., Papadimitrakopoulos, F., and Burgess, D.J., *Biomaterials/tissue interactions: possible solutions to overcome foreign body response.* The AAPS journal, 2010. **12**: p. 188-196.
80. Mosser, D.M. and Edwards, J.P., *Exploring the full spectrum of macrophage activation.* Nature reviews immunology, 2008. **8**(12): p. 958-969.
81. Murray, P.J., Allen, J.E., Biswas, S.K., Fisher, E.A., Gilroy, D.W., Goerdt, S., Gordon, S., Hamilton, J.A., Ivashkiv, L.B., and Lawrence, T., *Macrophage activation and polarization: nomenclature and experimental guidelines.* Immunity, 2014. **41**(1): p. 14-20.
82. Murray, P.J. and Wynn, T.A., *Obstacles and opportunities for understanding macrophage polarization.* Journal of leukocyte biology, 2011. **89**(4): p. 557-563.
83. Nascimento, C.R., Fernandes, N.A.R., Maldonado, L.A.G., and Junior, C.R., *Comparison of monocytic cell lines U937 and THP-1 as macrophage models for in vitro studies.* Biochemistry and Biophysics Reports, 2022. **32**: p. 101383.
84. Nielsen, M.C., Andersen, M.N., and Møller, H.J., *Monocyte isolation techniques significantly impact the phenotype of both isolated monocytes and derived macrophages in vitro.* Immunology, 2020. **159**(1): p. 63-74.
85. Nitschke, I. and Stark, H., *13.4 Zahnverlust und prothetische Versorgung.*, in *Fünfte Deutsche Mundgesundheitsstudie*, M.W. Jordan AR, Cholmakow-Bodechtel C (eds), Editor. 2016, Institut der Deutschen Zahnärzte (IDZ): Köln (Deutschland).
86. Nitschke, I. and Stark, H., *15.4 Zahnverlust und prothetische Versorgung.*, in *Fünfte Deutsche Mundgesundheitsstudie*, M.W. Jordan AR, Cholmakow-Bodechtel C (eds), Editor. 2016, Institut der Deutschen Zahnärzte (IDZ): Köln (Deutschland).
87. Norton, L., Koschwanez, H., Wisniewski, N., Klitzman, B., and Reichert, W., *Vascular endothelial growth factor and dexamethasone release from nonfouling sensor coatings affect the foreign body response.* Journal of biomedical materials research Part A, 2007. **81**(4): p. 858-869.
88. Parisi, L., Bianchi, M.G., Ghezzi, B., Maurizi, E., Macaluso, G.M., Bussolati, O., and Lumetti, S., *Preparation of human primary macrophages to study the polarization from monocyte-derived macrophages to pro-or anti-inflammatory macrophages at biomaterial interface in vitro.* Journal of dental sciences, 2023. **18**(4): p. 1630-1637.
89. Parisi, L., Ghezzi, B., Bianchi, M.G., Toffoli, A., Rossi, F., Bussolati, O., and Macaluso, G.M., *Titanium dental implants hydrophilicity promotes preferential serum fibronectin over albumin competitive adsorption modulating early cell response.* Materials Science and Engineering: C, 2020. **117**: p. 111307.
90. Parkin, J. and Cohen, B., *An overview of the immune system.* The Lancet, 2001. **357**(9270): p. 1777-1789.

91. Patel, U., Rajasingh, S., Samanta, S., Cao, T., Dawn, B., and Rajasingh, J., *Macrophage polarization in response to epigenetic modifiers during infection and inflammation.* Drug discovery today, 2017. **22**(1): p. 186-193.
92. Patil, S.D., Papadimitrakopoulos, F., and Burgess, D.J., *Dexamethasone-loaded poly (lactic-co-glycolic) acid microspheres/poly (vinyl alcohol) hydrogel composite coatings for inflammation control.* Diabetes technology & therapeutics, 2004. **6**(6): p. 887-897.
93. Pikner, S.S. and Gröndahl, K., *Radiographic analyses of "advanced" marginal bone loss around Brånemark® Dental implants.* Clinical implant dentistry and related research, 2009. **11**(2): p. 120-133.
94. Porcheray, F., Viaud, S., Rimaniol, A., Leone, C., Samah, B., Dereuddre-Bosquet, N., Dormont, D., and Gras, G., *Macrophage activation switching: an asset for the resolution of inflammation.* Clinical & Experimental Immunology, 2005. **142**(3): p. 481-489.
95. Qian, J., Wennerberg, A., and Albrektsson, T., *Reasons for marginal bone loss around oral implants.* Clinical implant dentistry and related research, 2012. **14**(6): p. 792-807.
96. Qin, Z., *The use of THP-1 cells as a model for mimicking the function and regulation of monocytes and macrophages in the vasculature.* Atherosclerosis, 2012. **221**(1): p. 2-11.
97. Ratner, B.D., *The engineering of biomaterials exhibiting recognition and specificity.* Journal of Molecular Recognition, 1996. **9**(5-6): p. 617-625.
98. Repnik, U., Knezevic, M., and Jeras, M., *Simple and cost-effective isolation of monocytes from buffy coats.* Journal of immunological methods, 2003. **278**(1-2): p. 283-292.
99. Riedhammer, C., Halbritter, D., and Weissert, R., *Peripheral blood mononuclear cells: isolation, freezing, thawing, and culture.* Multiple Sclerosis: Methods and Protocols, 2016: p. 53-61.
100. Rios, F.J., Touyz, R.M., and Montezano, A.C., *Isolation and differentiation of human macrophages*, in *Hypertension: Methods and Protocols*, R.M. Touyz and E.L. Schiffrin, Editors. 2017. p. 311-320.
101. Rios, F.J., Touyz, R.M., and Montezano, A.C., *Isolation and differentiation of murine macrophages*, in *Hypertension: Methods and Protocols*, R.M. Touyz and E.L. Schiffrin, Editors. 2017. p. 297-309.
102. Roberto, L.L., Crespo, T.S., Monteiro-Junior, R.S., Martins, A.M., De Paula, A.M., Ferreira, E.F., and Haikal, D.S., *Sociodemographic determinants of edentulism in the elderly population: A systematic review and meta-analysis.* Gerodontology, 2019. **36**(4): p. 325-337.
103. Rőszer, T., *Understanding the mysterious M2 macrophage through activation markers and effector mechanisms.* Mediators of inflammation, 2015. **2015**(1): p. 816460.
104. Rupp, F., Scheideler, L., Olshanska, N., De Wild, M., Wieland, M., and Geis-Gerstorfer, J., *Enhancing surface free energy and hydrophilicity through chemical modification of microstructured titanium implant surfaces.* Journal of Biomedical Materials Research Part A: An Official Journal of The Society for Biomaterials, The Japanese Society for Biomaterials, and The Australian Society for Biomaterials and the Korean Society for Biomaterials, 2006. **76**(2): p. 323-334.
105. Schildberger, A., Rossmanith, E., Eichhorn, T., Strassl, K., and Weber, V., *Monocytes, peripheral blood mononuclear cells, and THP-1 cells exhibit different cytokine expression patterns following stimulation with lipopolysaccharide.* Mediators of inflammation, 2013. **2013**(1): p. 697972.
106. Schmidt, D.R. and Kao, W.J., *Monocyte activation in response to polyethylene glycol hydrogels grafted with RGD and PHSRN separated by interpositional spacers of various lengths.* Journal of Biomedical Materials Research Part A: An Official Journal of The Society for Biomaterials, The Japanese Society for Biomaterials, and The Australian Society for Biomaterials and the Korean Society for Biomaterials, 2007. **83**(3): p. 617-625.
107. Schwendicke, F., Nitschke, I., Stark, H., Micheelis, W., and Jordan, R.A., *Epidemiological trends, predictive factors, and projection of tooth loss in Germany 1997–2030: Part II. Edentulism in seniors.* Clinical oral investigations, 2020. **24**: p. 3997-4003.
108. Shapouri-Moghaddam, A., Mohammadian, S., Vazini, H., Taghadosi, M., Esmaeili, S.A., Mardani, F., Seifi, B., Mohammadi, A., Afshari, J.T., and Sahebkar, A., *Macrophage plasticity, polarization, and function in health and disease.* Journal of cellular physiology, 2018. **233**(9): p. 6425-6440.
109. Sica, A. and Mantovani, A., *Macrophage plasticity and polarization: in vivo veritas.* The Journal of clinical investigation, 2012. **122**(3): p. 787-795.
110. Smeets, R., Stadlinger, B., Schwarz, F., Beck-Broichsitter, B., Jung, O., Precht, C., Kloss, F., Gröbe, A., Heiland, M., and Ebker, T., *Impact of dental implant surface modifications on osseointegration.* BioMed research international, 2016. **2016**.

111. Sollazzo, V., Pezzetti, F., Scarano, A., Piattelli, A., Massari, L., Brunelli, G., and Carinci, F., *Anatase coating improves implant osseointegration in vivo.* Journal of Craniofacial Surgery, 2007. **18**(4): p. 806-810.
112. Stark, H. and Nitschke, I., *12.4 Zahnverlust und prothetische Versorgung.*, in *Fünfte Deutsche Mundgesundheitsstudie*, M.W. Jordan AR, Cholmakow-Bodechtel C (eds), Editor. 2016, Institut der Deutschen Zahnärzte (IDZ): Köln (Deutschland).
113. Steele, J.G., Sanders, A.E., Slade, G.D., Allen, P.F., Lahti, S., Nuttall, N., and Spencer, A.J., *How do age and tooth loss affect oral health impacts and quality of life? A study comparing two national samples.* Community dentistry and oral epidemiology, 2004. **32**(2): p. 107-114.
114. Stefater, J.A., Ren, S., Lang, R.A., and Duffield, J.S., *Metchnikoff's policemen: macrophages in development, homeostasis and regeneration.* Trends in molecular medicine, 2011. **17**(12): p. 743-752.
115. Steinbach, F. and Thiele, B., *Phenotypic investigation of mononuclear phagocytes by flow cytometry.* Journal of immunological methods, 1994. **174**(1-2): p. 109-122.
116. Sutherland, K., Mahoney, J., Coury, A., and Eaton, J., *Degradation of biomaterials by phagocyte-derived oxidants.* The Journal of clinical investigation, 1993. **92**(5): p. 2360-2367.
117. Svensson, J., Jenmalm, M.C., Matussek, A., Geffers, R., Berg, G., and Ernerudh, J., *Macrophages at the fetal–maternal interface express markers of alternative activation and are induced by M-CSF and IL-10.* The Journal of Immunology, 2011. **187**(7): p. 3671-3682.
118. Tang, L. and Eaton, J. *Adsorbed Fibrinogen Mediates Acute Inflammatory Responses to Biomaterials*. in *ANNUAL MEETING-SOCIETY FOR BIOMATERIALS IN CONJUNCTION WITH THE INTERNATIONAL BIOMATERIALS SYMPOSIUM*. 1994. SOCIETY FOR BIOMATERIALS.
119. Tarique, A.A., Logan, J., Thomas, E., Holt, P.G., Sly, P.D., and Fantino, E., *Phenotypic, functional, and plasticity features of classical and alternatively activated human macrophages.* American journal of respiratory cell and molecular biology, 2015. **53**(5): p. 676-688.
120. Teti, G., Biondo, C., and Beninati, C., *The phagocyte, Metchnikoff, and the foundation of immunology.* Myeloid Cells in Health and Disease: A Synthesis, 2017: p. 17-29.
121. ThermoFisher, *Immune cell guide*. 2020, Thermo Fisher.
122. Toffoli, A., Parisi, L., Bianchi, M.G., Lumetti, S., Bussolati, O., and Macaluso, G.M., *Thermal treatment to increase titanium wettability induces selective proteins adsorption from blood serum thus affecting osteoblasts adhesion.* Materials Science and Engineering: C, 2020. **107**: p. 110250.
123. Trindade, R., Albrektsson, T., Tengvall, P., and Wennerberg, A., *Foreign Body Reaction to Biomaterials: On Mechanisms for Buildup and Breakdown of Osseointegration.* Clinical Implant Dentistry and Related Research, 2016. **18**(1): p. 192-203.
124. Tsuchiya, S., Kobayashi, Y., Goto, Y., Okumura, H., Nakae, S., Konno, T., and Tada, K., *Induction of maturation in cultured human monocytic leukemia cells by a phorbol diester.* Cancer research, 1982. **42**(4): p. 1530-1536.
125. Tsuchiya, S., Yamabe, M., Yamaguchi, Y., Kobayashi, Y., Konno, T., and Tada, K., *Establishment and characterization of a human acute monocytic leukemia cell line (THP-1).* International journal of cancer, 1980. **26**(2): p. 171-176.
126. van Grevenynghe, J., Rion, S., Le Ferrec, E., Le Vee, M., Amiot, L., Fauchet, R., and Fardel, O., *Polycyclic aromatic hydrocarbons inhibit differentiation of human monocytes into macrophages.* The Journal of Immunology, 2003. **170**(5): p. 2374-2381.
127. VandeVondele, S., Vörös, J., and Hubbell, J.A., *RGD-grafted poly-l-lysine-graft-(polyethylene glycol) copolymers block non-specific protein adsorption while promoting cell adhesion.* Biotechnology and bioengineering, 2003. **82**(7): p. 784-790.
128. Verreck, F.A., de Boer, T., Langenberg, D.M., Hoeve, M.A., Kramer, M., Vaisberg, E., Kastelein, R., Kolk, A., de Waal-Malefyt, R., and Ottenhoff, T.H., *Human IL-23-producing type 1 macrophages promote but IL-10-producing type 2 macrophages subvert immunity to (myco) bacteria.* Proceedings of the National Academy of Sciences, 2004. **101**(13): p. 4560-4565.
129. Verreck, F.A., de Boer, T., Langenberg, D.M., van der Zanden, L., and Ottenhoff, T.H., *Phenotypic and functional profiling of human proinflammatory type-1 and anti-inflammatory type-2 macrophages in response to microbial antigens and IFN-γ-and CD40L-mediated costimulation.* Journal of leukocyte biology, 2006. **79**(2): p. 285-293.
130. Vogel, D.Y., Glim, J.E., Stavenuiter, A.W., Breur, M., Heijnen, P., Amor, S., Dijkstra, C.D., and Beelen, R.H., *Human macrophage polarization in vitro: maturation and activation methods compared.* Immunobiology, 2014. **219**(9): p. 695-703.
131. Vroman, L., Adams, A., Fischer, G., and Munoz, P., *Interaction of high molecular weight kininogen, factor XII, and fibrinogen in plasma at interfaces.* 1980.

132. Wang, Y., Zhang, Y., Sculean, A., Bosshardt, D.D., and Miron, R.J., *Macrophage behavior and interplay with gingival fibroblasts cultured on six commercially available titanium, zirconium, and titanium-zirconium dental implants.* Clinical oral investigations, 2019. **23**: p. 3219-3227.
133. Warreth, A., McAleese, E., McDonnell, P., Slami, R., and Guray, S.M., *Dental implants and single implant-supported restorations.* J Ir Dent Assoc, 2013. **59**(1): p. 32-43.
134. Wei, Q., Deng, Y., Yang, Q., Zhan, A., and Wang, L., *The markers to delineate different phenotypes of macrophages related to metabolic disorders.* Frontiers in Immunology, 2023. **14**: p. 1084636.
135. Williams, D., *Implants in dental and maxillofacial surgery.* Biomaterials, 1981. **2**(3): p. 133-146.
136. Williams, D.F., *On the mechanisms of biocompatibility.* Biomaterials, 2008. **29**(20): p. 2941-2953.
137. Williams, D.F., *On the nature of biomaterials.* Biomaterials, 2009. **30**(30): p. 5897-5909.
138. Williams, D.F. and Williams, D.F., *The Williams dictionary of biomaterials*. 1999: Liverpool University Press.
139. Wilson, G.S. and Gifford, R., *Biosensors for real-time in vivo measurements.* Biosensors and Bioelectronics, 2005. **20**(12): p. 2388-2403.
140. Yamashiro, S., Kamohara, H., Wang, J.-M., Yang, D., Gong, W.-H., and Yoshimura, T., *Phenotypic and functional change of cytokine-activated neutrophils: inflammatory neutrophils are heterogeneous and enhance adaptive immune responses.* Journal of leukocyte biology, 2001. **69**(5): p. 698-704.
141. Yao, Y., Xu, X.-H., and Jin, L., *Macrophage polarization in physiological and pathological pregnancy.* Frontiers in immunology, 2019. **10**: p. 792.
142. Yeo, I.-S.L., *Modifications of dental implant surfaces at the micro-and nano-level for enhanced osseointegration.* Materials, 2019. **13**(1): p. 89.
143. Yim, E.K. and Leong, K.W., *Significance of synthetic nanostructures in dictating cellular response.* Nanomedicine in Cancer, 2017: p. 129-158.
144. Young, D.A., Lowe, L.D., and Clark, S.C., *Comparison of the effects of IL-3, granulocyte-macrophage colony-stimulating factor, and macrophage colony-stimulating factor in supporting monocyte differentiation in culture. Analysis of macrophage antibody-dependent cellular cytotoxicity.* Journal of immunology (Baltimore, Md.: 1950), 1990. **145**(2): p. 607-615.
145. Zhou, G. and Groth, T., *Host responses to biomaterials and anti-inflammatory design—a brief review.* Macromolecular bioscience, 2018. **18**(8): p. 1800112.
146. Ziegler-Heitbrock, H.L., Schraut, W., Wendelgaß, P., Ströbel, M., Sternsdorf, T., Weber, C., Aepfelbacher, M., Ehlers, M., Schütt, C., and Haas, J.G., *Distinct patterns of differentiation induced in the monocytic cell line Mono Mac 6.* Journal of leukocyte biology, 1994. **55**(1): p. 73-80.

Declaration of Authorship

The present thesis was conducted at the department Medizinische Werkstoffkunde und Technologie of the Eberhard Karls University Tübingen under the supervision of Prof. Dr. Stefanie Krajewski.

The study was designed by Prof. Dr. Stefanie Krajewski, Dr. Leila Mohammadnejad and Prof. Dr. Frank Rupp.

The experiments *'Isolation of PBMC'* ***(Chap. 2.6.1)***, *'Isolation of monocytes'* ***(Chap. 2.6.2)***, *'Differentiation of monocytes to MdM'* ***(Chap. 2.6.3)***, *'Polarization of MdM'* ***(Chap. 2.6.4)***, *'Characterization of polarized MdM using light microscopy'* ***(Chap. 2.6.5)***, *'Characterization of polarized MdM using ELISA'* ***(Chap. 2.6.6)*** were conducted by myself after training by Jacqueline Thy Walther and Evi Kimmerle-Müller. The experiment *'Characterization of MdM using flow cytometry'* ***(Chap. 2.6.7)*** was conducted by myself with support from Madhis Tajabadi. The experiment *'Characterization of MdM using CLSM'* ***(Chap. 2.6.8)*** was done in collaboration with Hannah Conrady with support from of Annika Hechler and Dr. Christiane von Ohle, the corresponding method was established by Hannah Conrady. The experiment *'Cultivation and polarization of MdM on titanium surfaces'* ***(Chap. 2.6.9)*** was done with support from Hannah Conrady. The experiment *'Evaluation of immunomodulatory effects using CCK8 cell proliferation assay'* ***(Chap. 2.6.10)*** was done in collaboration with Evi Kimmerle-Müller, Hannah Conrady and Dr. Leila Mohammadnejad. The experiment *'Evaluation of immunomodulatory effects using ELISA and BCA protein assay'* **(Chap. 2.6.11)** was done in collaboration with Evi Kimmerle-Müller and Hannah Conrady. The experiment *'Evaluation of immunomodulatory effects using CLSM'* ***(Chap. 2.6.12)*** was done in collaboration with Evi Kimmerle-Müller and Hannah Conrady.

The statistical analysis for all experiments except from *'Evaluation of immunomodulatory effects using CLSM'* ***(Chap. 2.6.12)*** was performed by myself under the guidance of Dr. Leila Mohammadnejad. The statistical analysis for *'Evaluation of immunomodulatory effects using CLSM'* ***(Chap. 2.6.12)*** was performed by Dr. Leila Mohammadnejad.

The manuscript of the original publication *'Mohammadnejad L, Conrady H, Mangold M, Kimmerle-Müller E, Hechler A, von Ohle C, Rupp F, Krajewski S (2024) Polarization and Characterization of M1 and M2 Human Monocyte-Derived Macrophages on Implant Surfaces*.' was written by Dr. Leila Mohammadnejad.

I hereby declare that I have written the manuscript of the present thesis independently and that I have not used any sources other than those cited.

Original Publications

Parts of this thesis have already been published within the publication hereinafter:

Mohammadnejad, L., Conrady, H., Mangold, M., Kimmerle-Mueller, E., Hechler, A., von Ohle, C., Rupp, F., and Krajewski, S., Polarization and Characterization of M1 and M2 Human Monocyte-Derived Macrophages on Implant Surfaces. Journal of Visualized Experiments (JoVE), 2024(214): p. e67180.

The final published version of this article is available at

app.jove.com/t/67180/polarization-characterization-m1-m2-human-monocyte-derived

Acknowledgements

For the dedicated supervision based on her great knowledge and for the careful sight of the written report I am very grateful to my thesis advisor Prof. Dr. Stefanie Krajewski. I highly appreciate the trustful relationship I have experienced throughout dissertation period.

As well, my deepest thanks go to Leila Mohammadnejad, my academic advisor, who masterfully guided me, who patiently answered all my questions, who always lent a helping hand and who was greatly engaged to get the thesis propelled and accomplished.

I also want to express my sincere thanks to Prof. Dr. Frank Rupp, head of the institute and my initial doctorate supervisor. Without his acceptance to include me in his research team and without his support I would not have been able to submit this thesis.

Furthermore, I would like to give thanks to Prof. Dr. Stella Autenrieth for being the second reviewer of the given thesis and for all associated efforts.

Not forgetting Evi Kimmerle-Müller, my reliable and trustworthy lab colleague and contact person, who was always there for me when it came to experimental procedure or when organizational challenges needed to be met.

Last but not least in my academic environment I would like to thank my fellow students Hannah Conrady and Peter Schneider for the cooperative work and for the mutual support in numerous test executions.

Without the love and the backing of my family I would not have been able to proceed to this degree. Thus, I am honestly thankful to my husband Philipp Mangold, my parents Elke and Joachim Fink, my siblings Annalena and Benedict Fink and my grandparents Rosemarie and Gerhard Fink as well as Lore and Alfred Heuwald. I am glad to have them all in my life!